

Nonequilibrium Molecular Dynamics Simulation
of the Thermocapillary Effect

Molekulardynamische Nichtgleichgewichtssimulation
des thermokapillaren Effekts

Figures

Vom Fachbereich Maschinenbau an der Technischen Universität Darmstadt
zur Erlangung des akademischen Grades eines Doktor-Ingenieurs (Dr.-Ing.)
genehmigte DISSERTATION

vorgelegt von
Dipl.-Ing. Holger Andreas Maier
aus Alzenau

Darmstadt 2011

D17

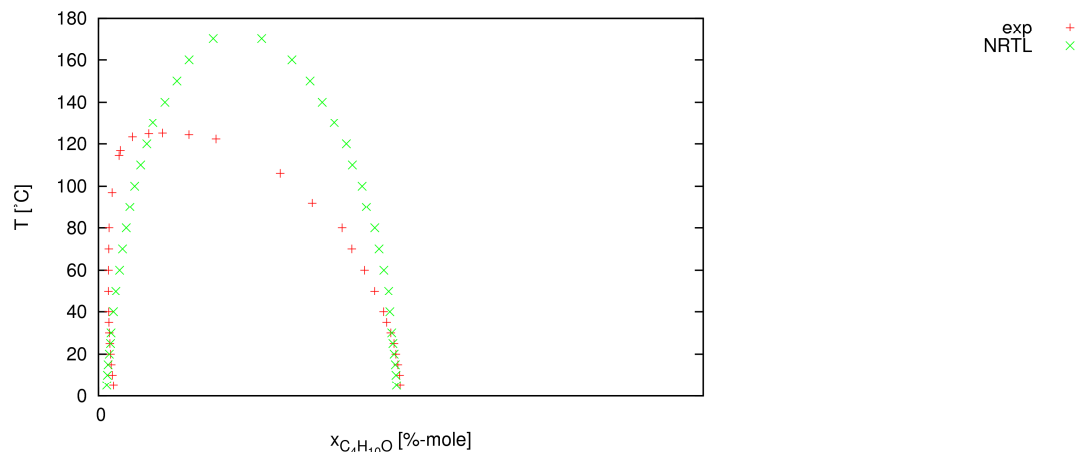
15 Figures

Figure 1	Liquid-liquid phase diagram of a binary water / 1-Butanol mixture at ambient pressure....	15-5
Figure 2	Thermocapillary convection in a physical experiment and its reproduction in a numerical experiment	15-5
Figure 3	Scheme of our procedure to study the thermocapillary effect in a "numerical experiment" instead of the "physical experiment"	15-6
Figure 4	Fundamental approach to study phenomena on the microscopic level in the classical limit.	15-6
Figure 5	Hexagonal convection pattern of the Marangoni-Bénard instability	15-7
Figure 6	Typical experimental setup for the study of thermal creep and molecular gas flows	15-7
Figure 7	Local surface and volume forces on a macroscopically small subvolume ΔV	15-7
Figure 8	Stress tensor elements for three mutually perpendicular and macroscopically small cut surfaces δS_j	15-7
Figure 9	Two different microscopic definitions of the kinetic contribution to the stress vector associated with the cut surface δS_j	15-7
Figure 10	Diffuse and specular reflection at a gas adsorption layer	15-8
Figure 11	Sketch of a typical BD NEMD simulation system with indication of the perturbed "boundary regions"	15-8
Figure 12	Setup of the simulation system with the expected convection roll cells driven by the thermocapillary effect	15-9
Figure 13	Basic sketch of the equilibrium interfacial systems simulated	15-10
Figure 14	Basic sketch of the nonequilibrium interfacial systems simulated	15-10
Figure 15	Dimensionless $T^*\rho^*$ -diagram of the saturation curve of pure one-centre LJ particle substances	15-10
Figure 16	Typical hyperbolic tangent partial density profiles (top) at a liquid-liquid interface in a mixture of the substances ArA and ArB	15-11
Figure 17	Local observables obtained for different spatial resolutions in separate <i>NVT</i> simulations of the first heterophasic equilibrium interfacial system	15-13
Figure 18	Comparison of the local observables obtained by using slabs in the two first nonequilibrium one-phase systems	15-15
Figure 19	Locations and orientations of selected confined cut-surfaces used in the determination of the local stresses	15-15
Figure 20	Sketch of an equilibrium interfacial system together with the subvolumes for which the local observables are computed	15-16
Figure 21	Sketch of a nonequilibrium interfacial system together with the subvolumes for which the local observables are computed	15-16
Figure 22	Production simulations of the different systems in chronological order	15-19
Figure 23	Comparison of selected local observables in different production simulations of the first heterophasic equilibrium interfacial system	15-23

Figure 24	Sequence of the preparational and production simulations of the first systems.....	15-24
Figure 25	Selected snapshots of the demixing in the equilibration simulation e-Ar1Ar2-0.6-1.0-3346-3524-4.74x8.00x9.40-120 (second preparation route).....	15-26
Figure 26	Local densities determined over three 10ns long successive segments of the equilibration simulation e-Ar1Ar2-0.6-1.0-3346-3524-4.74x8.00x9.40-120 (second preparation route)	15-27
Figure 27	Local observables determined over three 10ns long successive segments of the steadying simulation n-Ar1Ar2-0.6-1.0-6795-24-4.74x8.00x9.40-100-140	15-28
Figure 28	Comparison of selected local observables in separate production simulations of the first heterophasic nonequilibrium interfacial system.....	15-32
Figure 29	Preparation of an initial phase point from cut-outs of phase points in Buhn's NPT simulations	15-33
Figure 30	Local observables determined over three 10ns long successive segments of the steadying simulation n-Ar1Ar2-0.6-1.0-3346-3524-4.74x8.00x9.40-100-140 (first preparation route) ..	15-34
Figure 31	Local observables determined over three 10ns long successive segments of the steadying simulation n-Ar1Ar2-0.6-1.0-3346-3524-4.74x8.00x9.40-100-140 (second preparation route)	15-35
Figure 32	Selected snapshots of the demixing in the steadying simulation n-Ar1Ar2-0.6-1.0-3346-3524-4.74x8.00x9.40-100-140 (third preparation route)	15-37
Figure 33	Local observables determined over three 10ns long successive segments of the steadying simulation N-Ar1Ar2-0.6-1.0-3346-3524-4.74x8.00x9.40-100-140 (third preparation route)	15-38
Figure 34	Detailed distributions of the local observables in the first heterophasic nonequilibrium interfacial system and its corresponding ones	15-49
Figure 35	Spatially averaged distributions of the local observables in the first heterophasic nonequilibrium interfacial system and its corresponding ones.....	15-63
Figure 36	Excerpt of the instantaneous heat fluxes coupled into or out of the hot thermostated region and the numbers of the particles residing in it in N-Ar1Ar2-0.6-1.0-6795-24-4.74x8.00x9.40-100-140	15-63
Figure 37	Consistency of the local observables in the first heterophasic nonequilibrium interfacial system.....	15-64
Figure 38	Comparison of the summarised local observables in the corresponding first heterophasic interfacial systems	15-66
Figure 39	Comparison of the summarised local observables in several heterophasic nonequilibrium interfacial systems with different cut-off radii	15-72
Figure 40	Comparison of the summarised local observables in several heterophasic nonequilibrium interfacial systems with different ArB particle masses	15-78
Figure 41	Comparison of the summarised local observables in several heterophasic nonequilibrium interfacial systems with strict and loose thermostats.....	15-82
Figure 42	Comparison of the summarised local observables in the first homo- and heterophasic nonequilibrium interfacial systems.....	15-87
Figure 43	Comparison of the mutual solubilities in the Ar1Ar2 and in the Ar5Ar5 mixture as function of the temperature.....	15-88
Figure 44	Comparison of the thermocapillary convection in Ar5Ar5 systems with different z-dimensions	15-91
Figure 45	Comparison of the thermocapillary convection in Ar5Ar5 systems with different y-dimensions	15-93

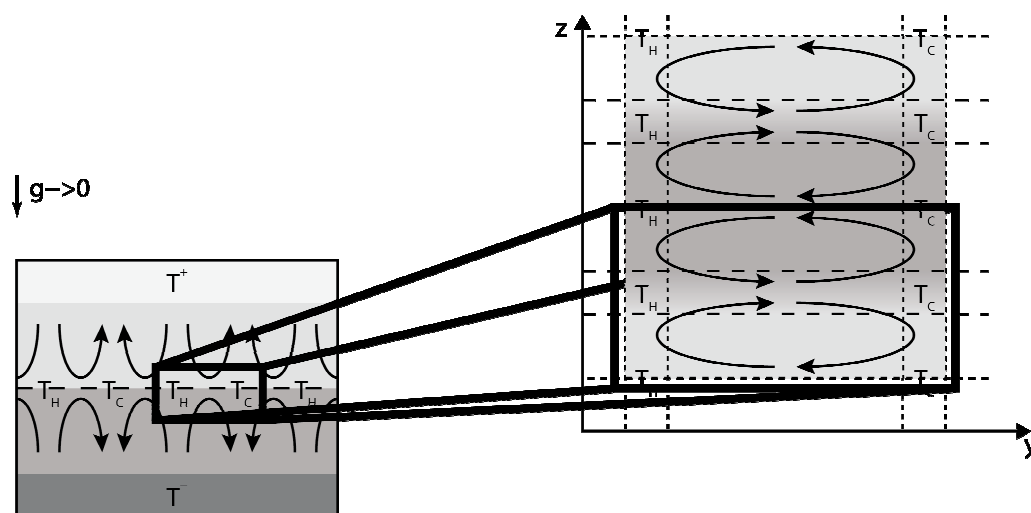
Figure 46	Comparison of the thermocapillary convection in Ar5Ar5 systems with different y- and z-dimensions	15-94
Figure 47	Comparison of the local com velocities in Ar5Ar5 nonequilibrium interfacial systems that differ only in the temperature difference between the thermostated regions	15-95
Figure 48	Section of the Ar5Ar5 pxT diagram at $x_{Ar\oplus}\approx 0.5$ with indication of the global pressures and temperatures in selected systems	15-95
Figure 49	Comparison of the thermocapillary convection in several Ar5Ar5 systems that differ in the global temperatures and pressures.....	15-97
Figure 50	Comparison of the thermocapillary convection in several Ar5Ar5 systems that differ only in the values of the mixing parameter ξ	15-98
Figure 51	Cut of the Ar5Ar5 pxT diagram at $x_{Ar\oplus}\approx 0.5$ with indication of the global pressures and temperatures in the systems with different mixing parameter values ξ	15-98
Figure 52	Comparison of the thermocapillary convection in Ar5Ar5 systems with different particle masses, m_{ArA} and m_{ArB}	15-99
Figure 53	Cut of the Ar5Ar5 pxT diagram at $x_{Ar\oplus}\approx 0.5$ with indication of the global pressures and temperatures in the systems with different particle masses, m_{ArA} and m_{ArB}	15-99
Figure 54	Detailed analysis of the density distribution in the homophasic nonequilibrium interfacial systems	15-101
Figure 55	Equilibrium density distribution to expect in a homophasic nonequilibrium interfacial system;.....	15-102
Figure 56	Example of the density distribution to expect in a nonequilibrium interfacial system based on its related equilibrium interfacial systems;.....	15-104
Figure 57	Phase diagram indicating the global states in several differently composed but otherwise comparable nonequilibrium one-phase systems	15-104
Figure 58	Concentration dependence of the different density y-gradients and of the Soret coefficients in otherwise similar nonequilibrium one-phase systems	15-104
Figure 59	Particle specific com velocities in selected nonequilibrium one-phase and interfacial systems	15-108
Figure 60	Relation between the central particle specific com y-velocities, densities and density y-gradients at the centers between the thermostated regions in a homophasic nonequilibrium interfacial system	15-110
Figure 61	Distributions of selected stress tensor elements using the first homophasic nonequilibrium interfacial system as an example.....	15-111
Figure 62	Comparison of the local volume y-forces obtained from the normal stresses, S_{yy} , and from the shear stresses, S_{yz} , in the first homophasic nonequilibrium interfacial system.....	15-112
Figure 63	Shear stresses, S_{yz} , as function of z in the nonequilibrium interfacial system, N-Ar5Ar5-0.6-1.0-13384-14096-4.74x8.00x37.6-100-140	15-112
Figure 64	Local densities in the unary nonequilibrium liquid-vapour system	15-118
Figure 65	Comparison of the local observables in several unary nonequilibrium liquid-vapour systems with different average system temperatures.....	15-121
Figure 66	Purely repulsive external force field of the type "ff1" in the first solid-liquid interfacial system.....	15-121
Figure 67	Local observables in the first solid-liquid interfacial system with a purely repulsive force field of the type "ff1"	15-127

Figure 68	Intensity of the convection as function of the slope in the first solid-liquid system with an external force field of the type "ff1"	15-128
Figure 69	Repulsive external fore field of the type "ff2" in the unary nonequilibrium interfacial reference system	15-128
Figure 70	Local observables in the unary nonequilibrium interfacial system with a repulsive force field of the type "ff2", N-Ar1-1.0-6870-4.74x8.00x9.40-100-140-ff2~1.0~3.0~1	15-134
Figure 71	Intensity of the thermocapillary convection in several unary nonequilibrium interfacial systems that differ only in the slope of the external force field "ff2"	15-135
Figure 72	Attractive external fore field of the type "ff3" in the unary nonequilibrium interfacial reference system, N-Ar5-1.0-6870-4.74x8.00x9.40-100-140-ff3~1.0~3.0~10	15-135
Figure 73	Local observables in the unary nonequilibrium interfacial system with attractive force field of the type "ff3", N-Ar5-1.0-6870-4.74x8.00x9.40-100-140-ff3	15-141
Figure 74	Intensity of the thermocapillary convection in several unary nonequilibrium interfacial systems that differ only in the slope of the external force field "ff3"	15-142
Figure 75	Attractive-repulsive external fore field of the type "ff4" in the unary nonequilibrium interfacial reference system.....	15-142
Figure 76	Local observables in the unary nonequilibrium interfacial system with an attractive-repulsive force field of the type "ff4", N-Ar1-1.0-6870-4.74x8.00x9.40-100-140-ff4~1.0~3.0~1	15-148
Figure 77	<i>PT</i> -phase diagram of water	15-149
Figure 78	<i>PVT</i> -phase diagram of water.....	15-149
Figure 79	<i>PT</i> -phase diagram of the Ar5Ar5 mixture with equimolar composition.....	15-150
Figure 80	Qualitative <i>PxT</i> -phase diagram of the Ar5Ar5 mixture	15-150
Figure 81	<i>PV</i> -data as obtained in several EMD simulations of an equimolar Ar5Ar5 mixture at different temperatures	15-150
Figure 82	Examples of unusual stable configurations found in the liquid-liquid-vapour region of the Ar5Ar5 mixture.....	15-151
Figure 83	Example of the concentration dependence of different thermodynamic properties related to the mixing behaviour of the Ar5Ar5 mixture.....	15-152
Figure 84	Examples of "butterfly" diagrams of the Ar5Ar5 mixture	15-153
Figure 85	Snap shot of a configuration in the two-dimensional nonequilibrium interfacial system.....	15-153
Figure 86	Local observables in the two-dimensional nonequilibrium interfacial system	15-156



LLE-H2O-C4H10O.eps

Figure 1 Liquid-liquid phase diagram of a binary water / 1-Butanol mixture at ambient pressure
We show the data from experiments and from thermodynamic calculations using the NRTL equation [sorensen1979].



a) **Physical experiment:** Thermocapillary convection in a binary system of two partially miscible liquids (green and yellow) at different bulk phase temperatures T_+ and T_- [oertel2002]; Temperature fluctuations in the interfacial region ignite the thermocapillary convection that self-sustains by dragging new hot liquid from the bulk phases to the interface where the latter gives off the heat to the counterflow in the opposite phase and returns into the hot bulk phase. Under certain system conditions the thermocapillary convection becomes stationary and temperature differences along the interface can be observed between the places where the convection approaches (T_H) and leaves (T_C). Note, gravity is necessary to keep the interface flat but buoyancy driven convection shall be negligible.

b) **Numerical experiment:** reproduction of the physical experiment in MD simulation with simplifications mentioned in the text; The hatching represents the interfacial region. In order to comply with the periodic system boundaries the thermocapillary system is mirrored along the xy - and the xz -plane.

Figure 2 Thermocapillary convection in a physical experiment and its reproduction in a numerical experiment

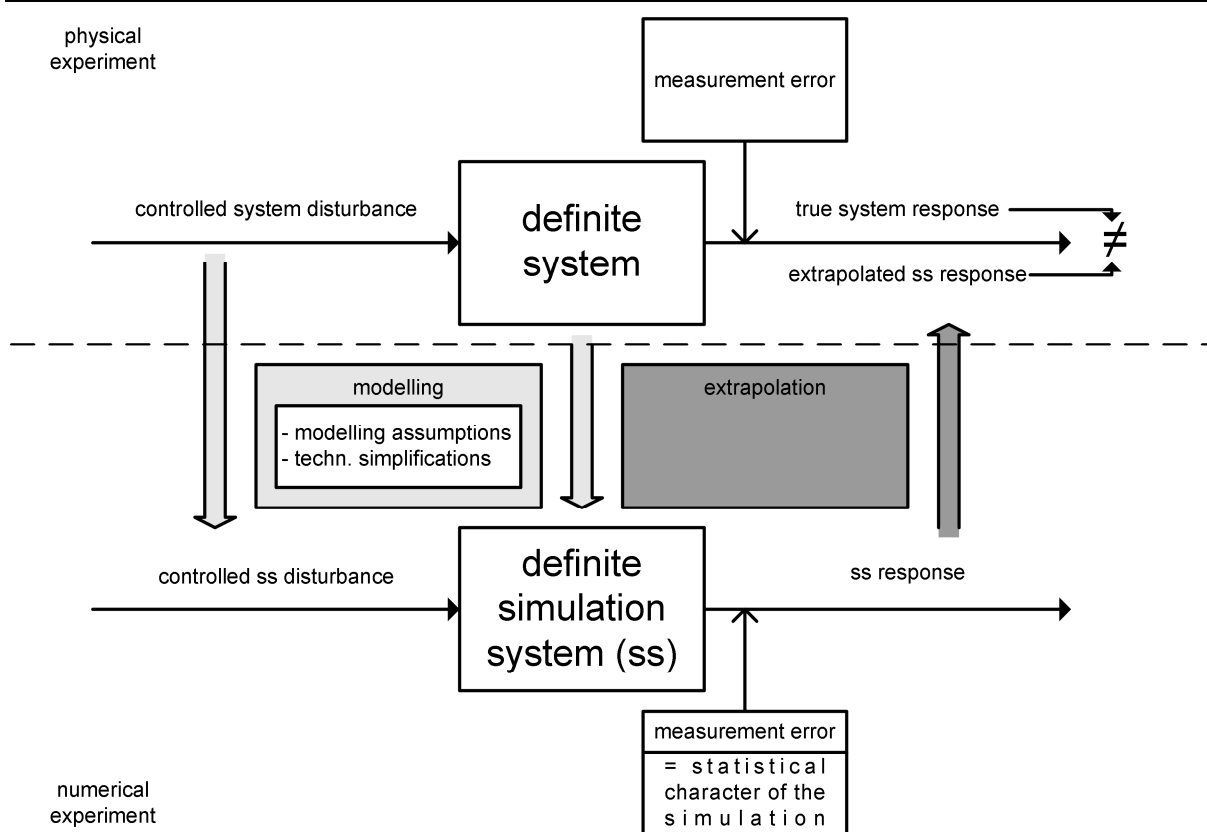


Figure 3 Scheme of our procedure to study the thermocapillary effect in a "numerical experiment" instead of the "physical experiment"

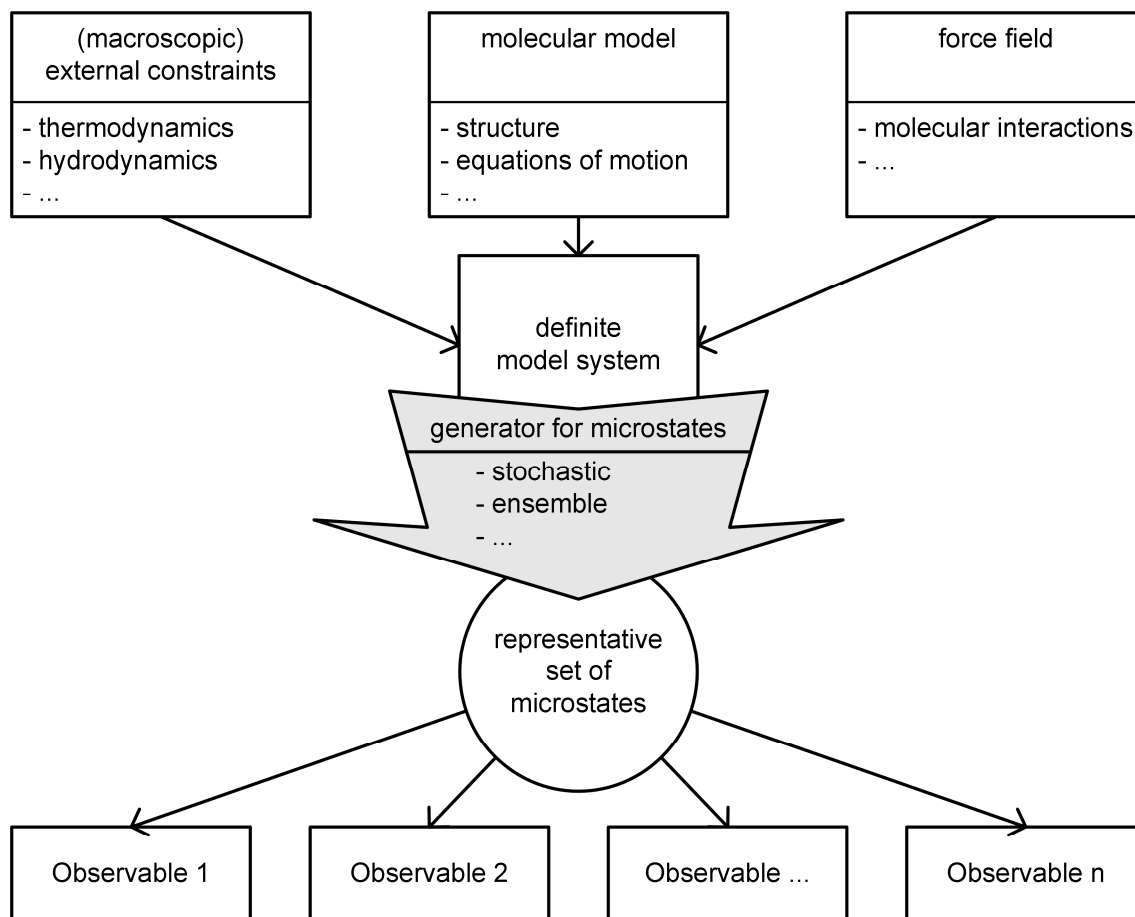


Figure 4 Fundamental approach to study phenomena on the microscopic level in the classical limit

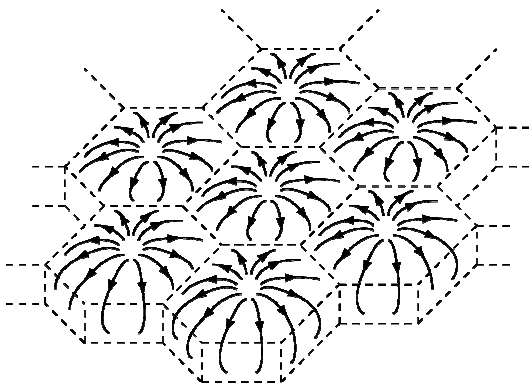


Figure 5 Hexagonal convection pattern of the Marangoni-Bénard instability

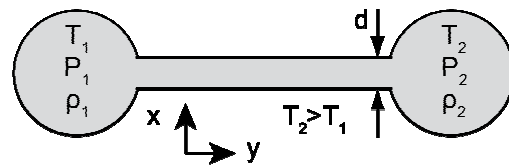


Figure 6 Typical experimental setup for the study of thermal creep and molecular gas flows

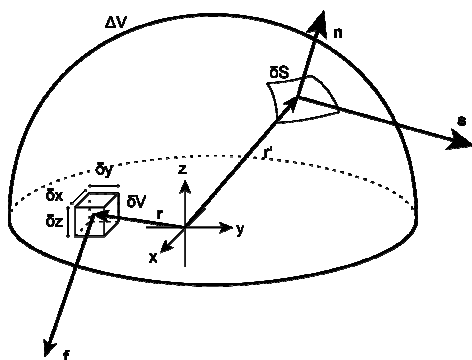


Figure 7 Local surface and volume forces on a macroscopically small subvolume ΔV

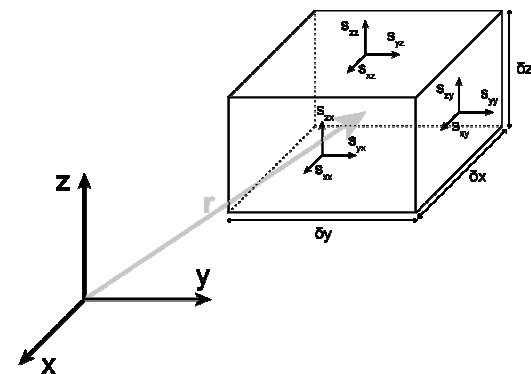
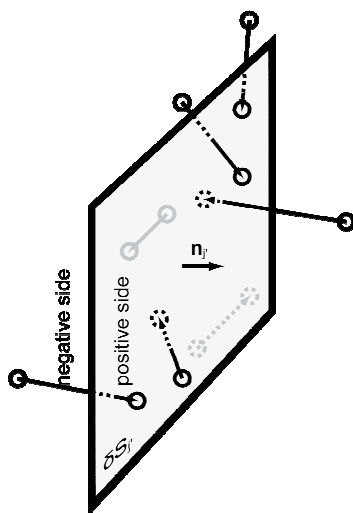
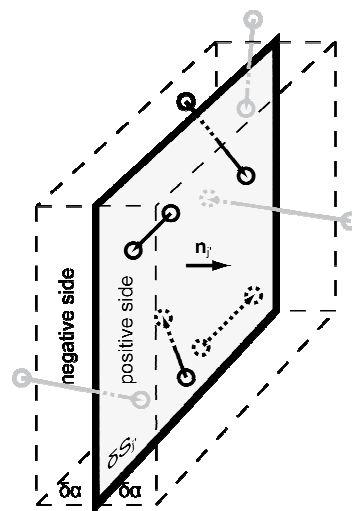


Figure 8 Stress tensor elements for three mutually perpendicular and macroscopically small cut surfaces δS_j



a) definition, that considers only the particles crossing the cut surface



b) definition, that considers all particles in the vicinity of the cut surface

Figure 9 Two different microscopic definitions of the kinetic contribution to the stress vector associated with the cut surface δS_j . Both sketches show the same exemplary particle arrangements at two subsequent time steps. Different particles contribute to the stress vector depending on the definition. We highlight them in black compared to the grey ones.

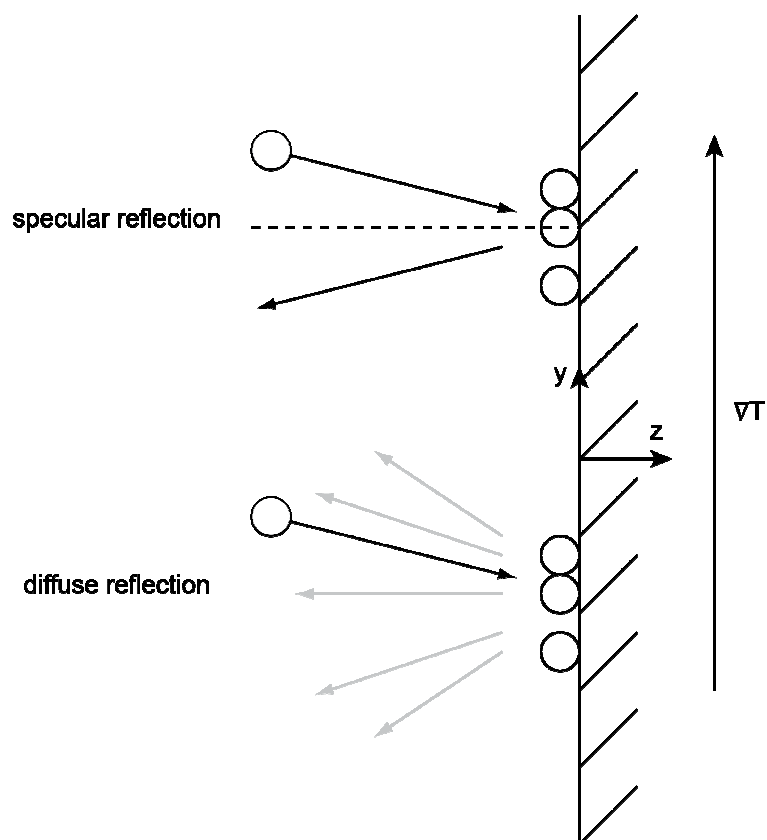


Figure 10 Diffuse and specular reflection at a gas adsorption layer

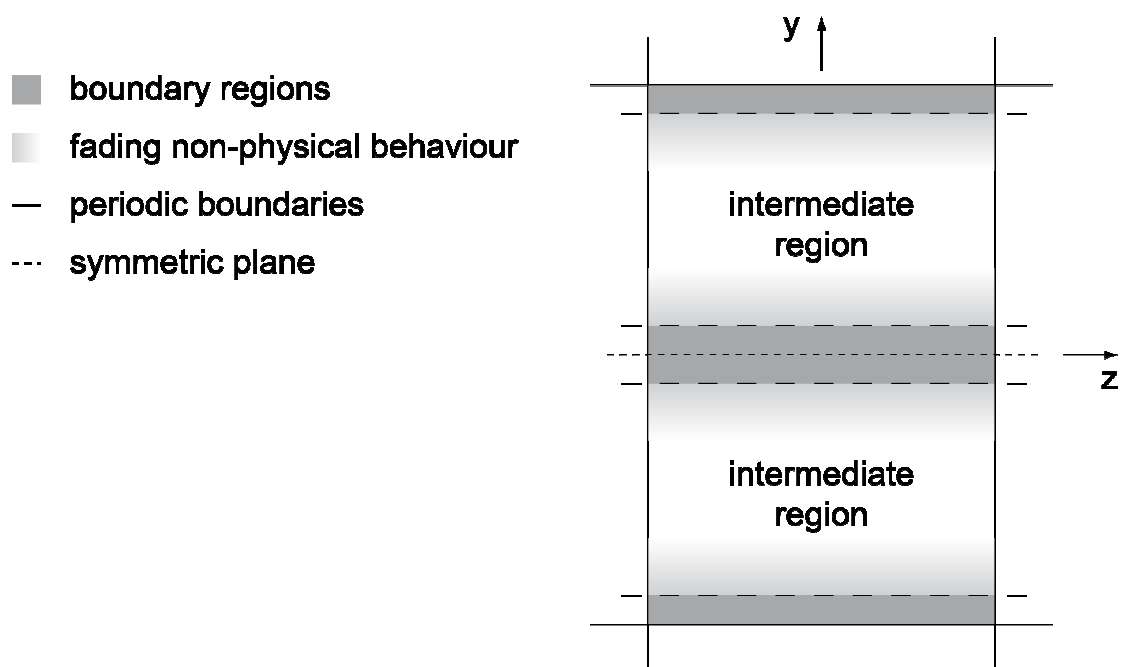


Figure 11 Sketch of a typical BD NEMD simulation system with indication of the perturbed "boundary regions"
In the "intermediate regions" between them, the non-physical behaviour in the perturbation fades

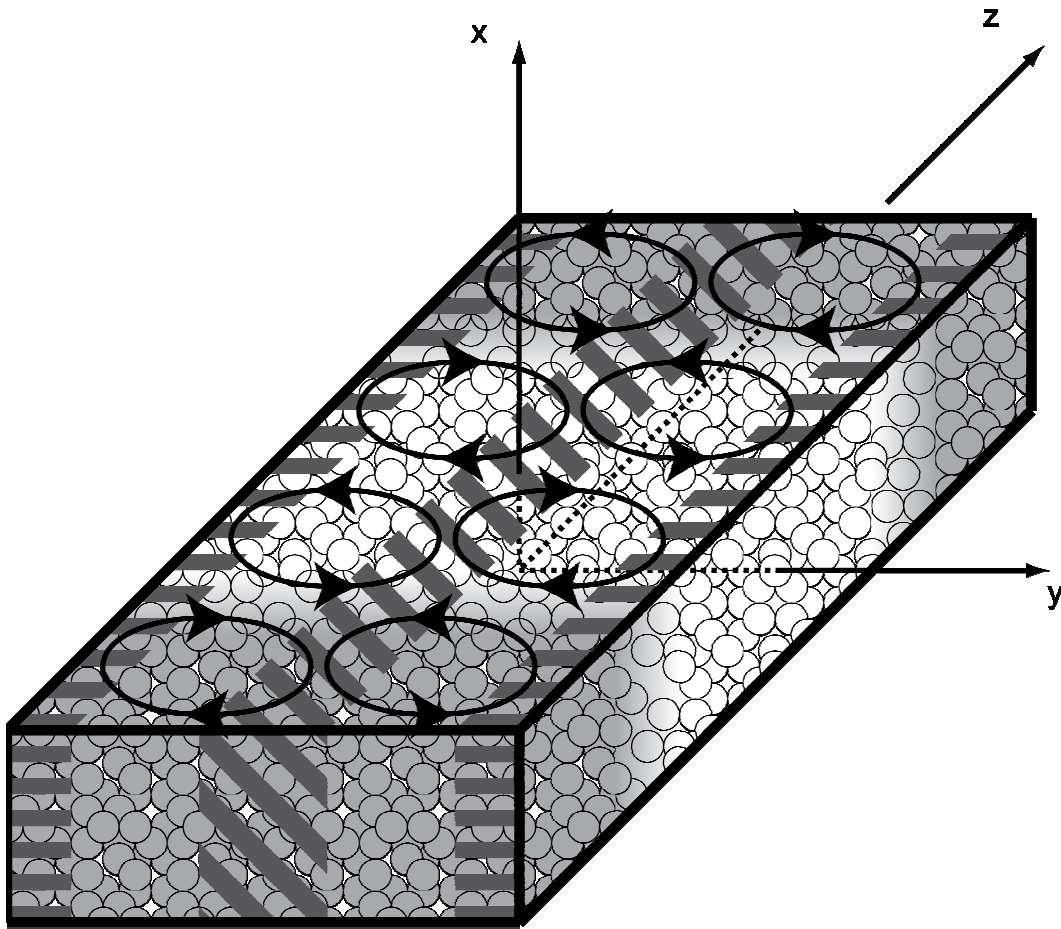


Figure 12 Setup of the simulation system with the expected convection roll cells driven by the thermocapillary effect

The grey and white circles represent the particles of the two species, generally called ArA and ArB here. The liquid-liquid interfaces are oriented parallel to the xy -plane. The regions parallel to the yz -plane represent the "thermostated regions". The hot one carries a horizontal and the cold one a diagonal hatching.

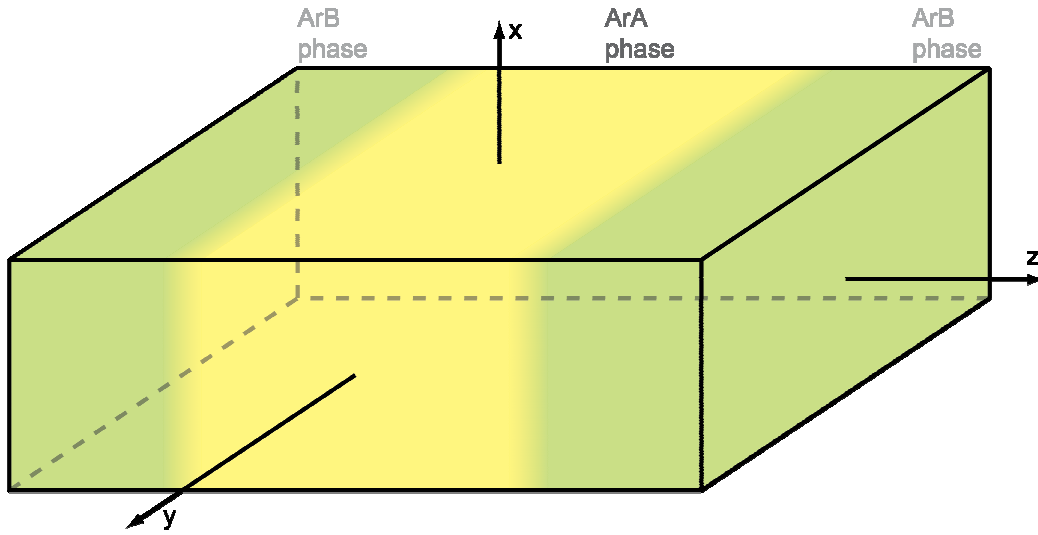


Figure 13 Basic sketch of the equilibrium interfacial systems simulated

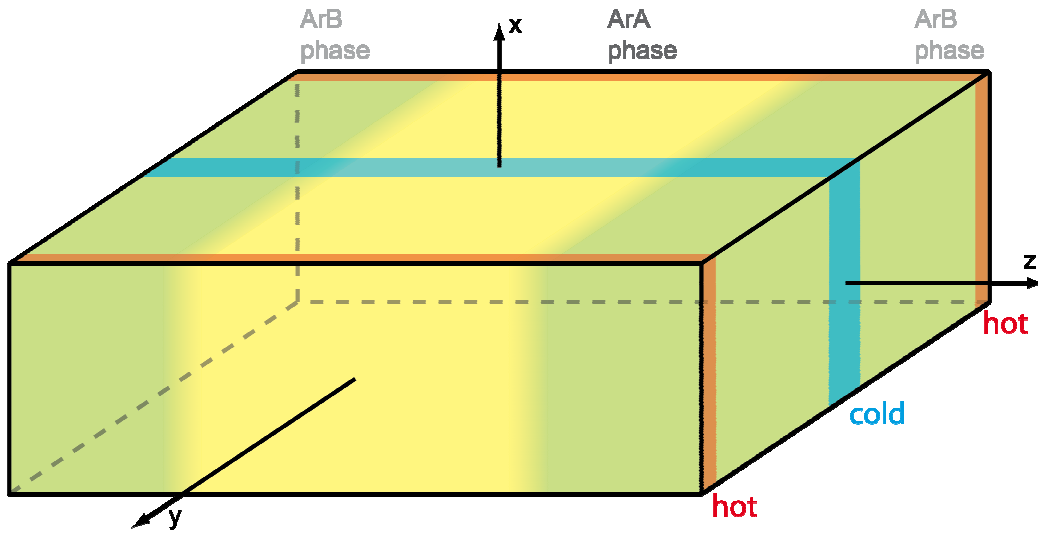
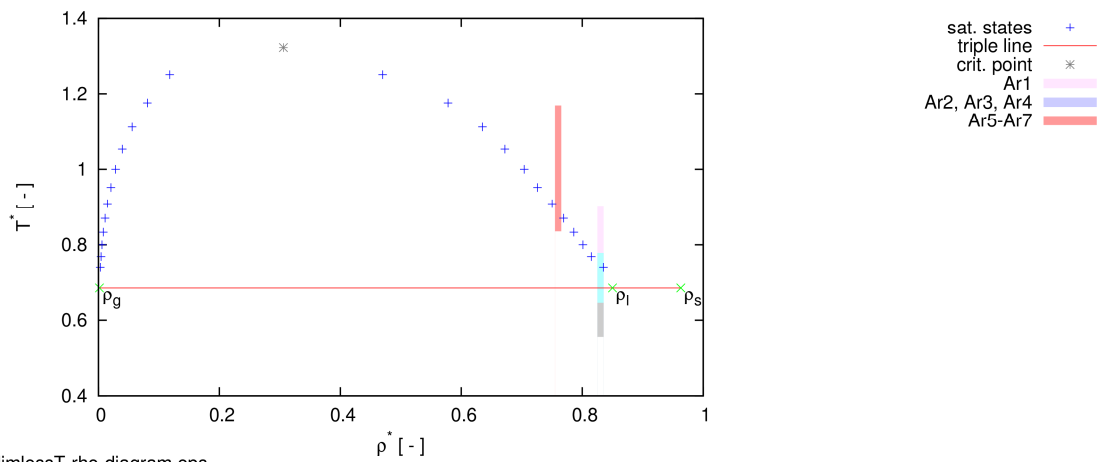
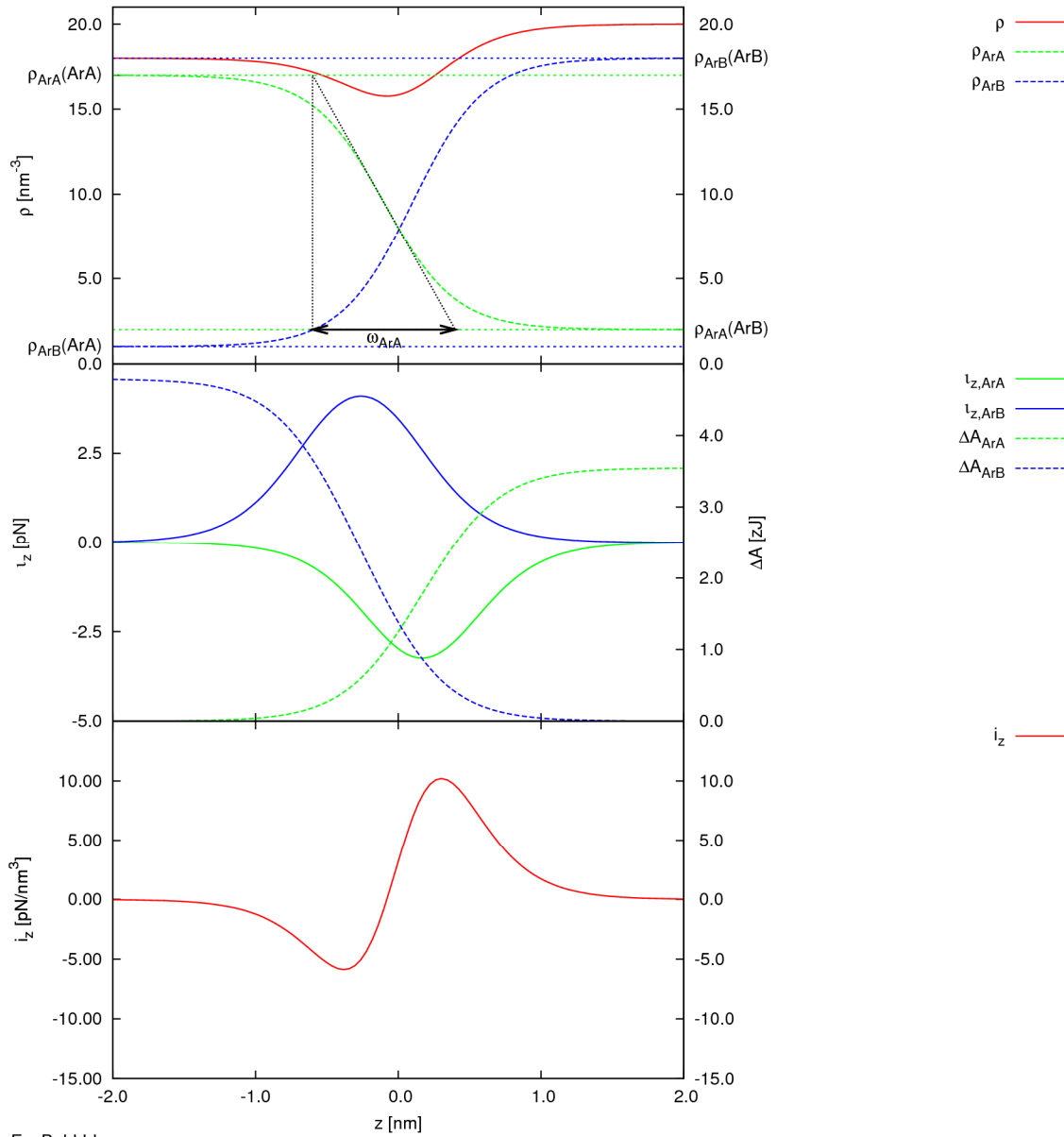


Figure 14 Basic sketch of the nonequilibrium interfacial systems simulated
It indicates additionally the boundary or thermostated regions.



dimlessT-rho-diagram.eps

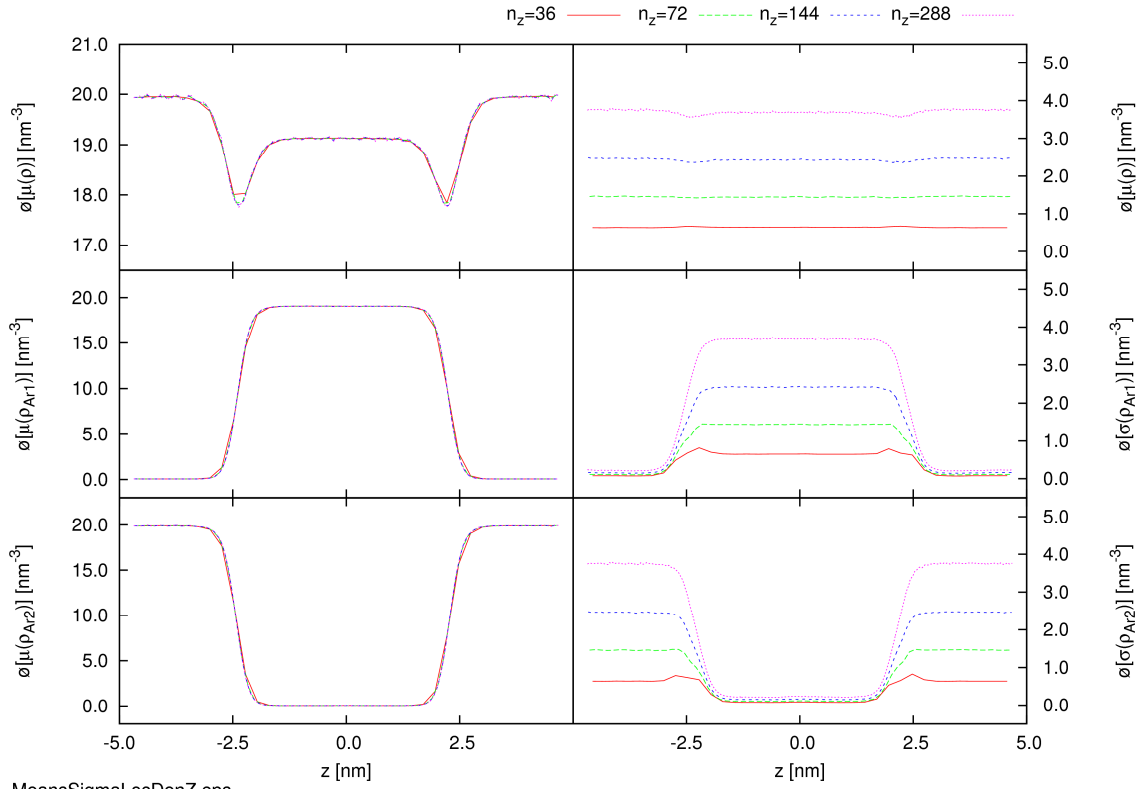
Figure 15 Dimensionless $T^*\rho^*$ -diagram of the saturation curve of pure one-centre LJ particle substances
The diagram shows additionally the reduced temperature-density ranges in the mixtures simulated in this work.



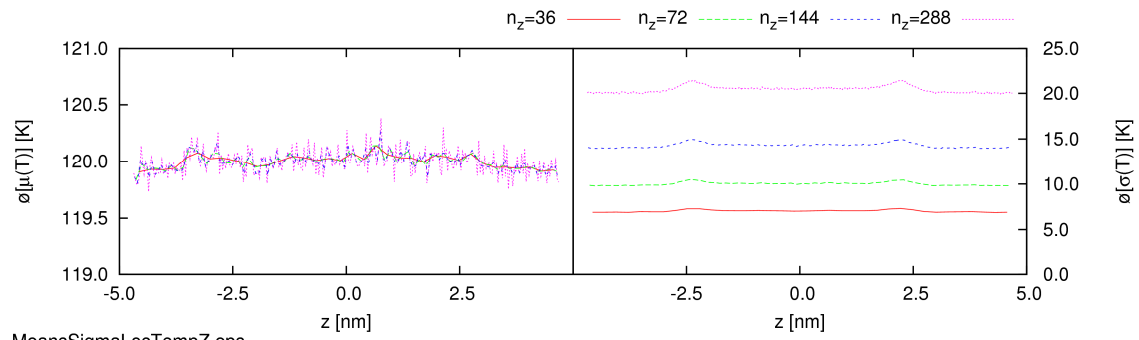
ExpBehLLI.eps

Figure 16 Typical hyperbolic tangent partial density profiles (top) at a liquid-liquid interface in a mixture of the substances ArA and ArB

We show additionally the related interatomic particle force and potential of mean force profiles (middle) as well as the related interatomic volume forces (bottom). The ArA rich phase resides on the left side and the ArB rich phase on the right side. The interfacial width related to the ArA partial density profile ω_{ArA} is indicated by the arrow.

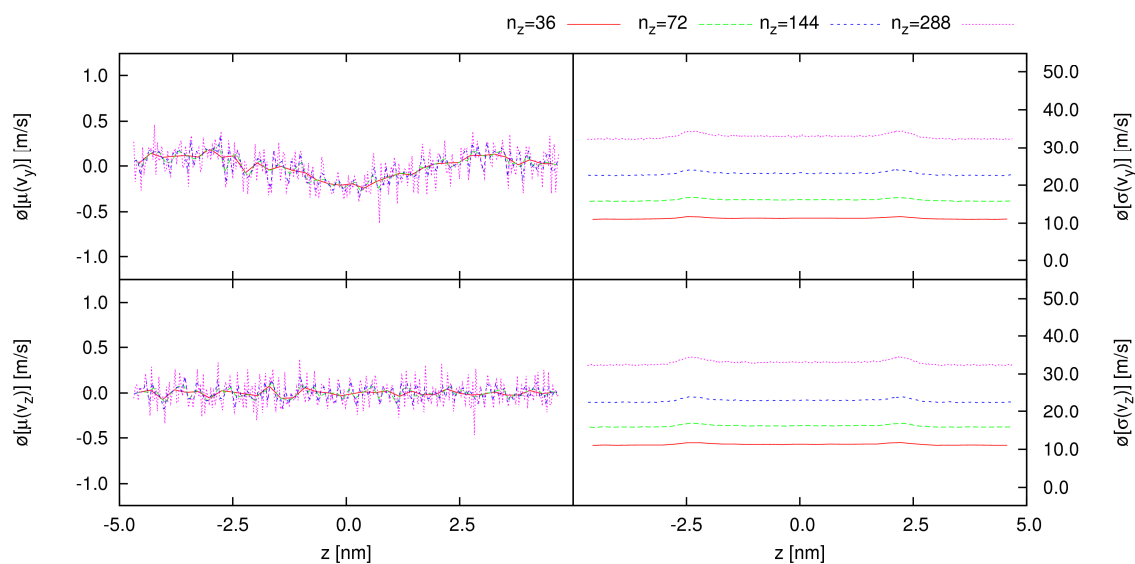


MeansSigmaLocDenZ.eps

a) Densities

MeansSigmaLocTempZ.eps

b) Temperatures



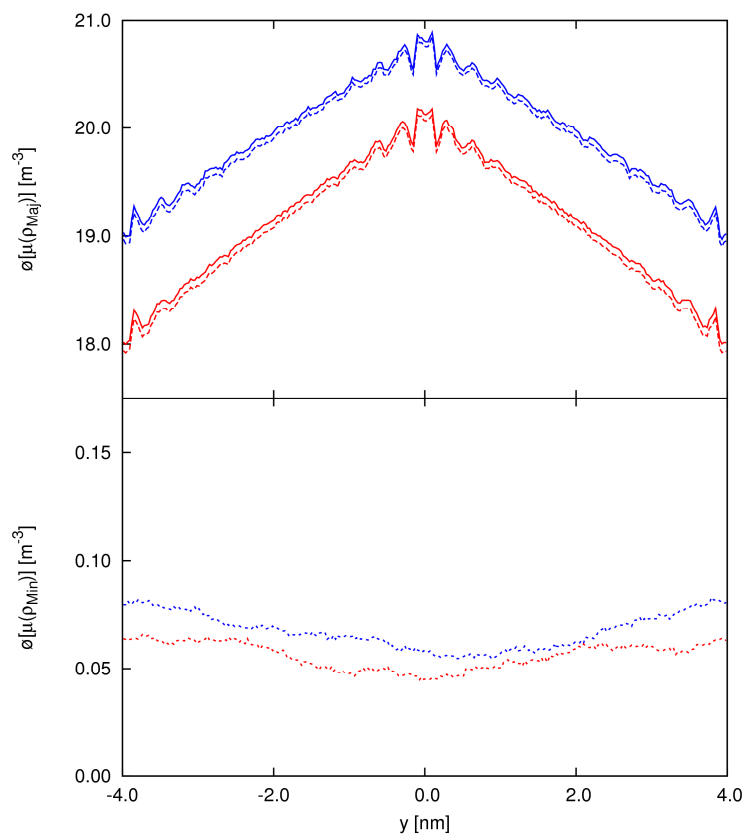
MeansSigmaLocYZComVelZ.eps

c) Com Velocities

Figure 17 Local observables obtained for different spatial resolutions in separate *NVT* simulations of the first heterophasic equilibrium interfacial system

We divide it into different numbers of slab-shaped subvolumes in the analysis. Nondefined results occur for a subdivision into 576 subvolumes since some of them are not populated by particles at every time step.

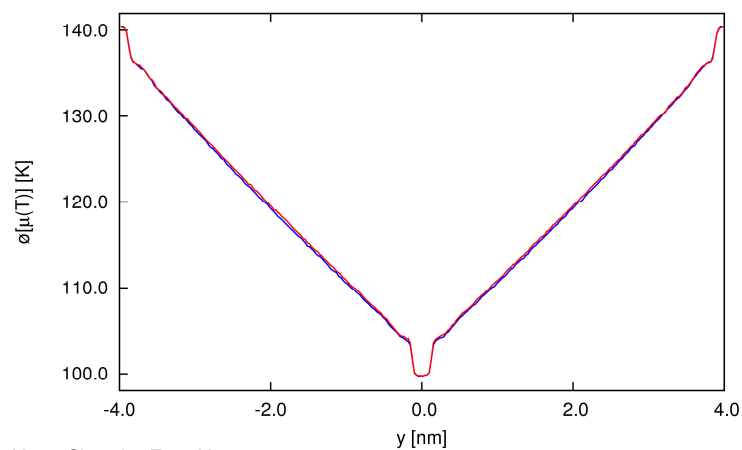
N-Ar1Ar2-0.6-1.0-6795-24-4.74x8.00x9.40-100-140
 N-Ar1Ar2-0.6-1.0-20-7091-4.74x8.00x9.40-100-140



MeansSigmaLocDenY.eps

a) Densities

N-Ar1Ar2-0.6-1.0-6795-24-4.74x8.00x9.40-100-140
 N-Ar1Ar2-0.6-1.0-20-7091-4.74x8.00x9.40-100-140



MeansSigmaLocTempY.eps

b) Temperatures

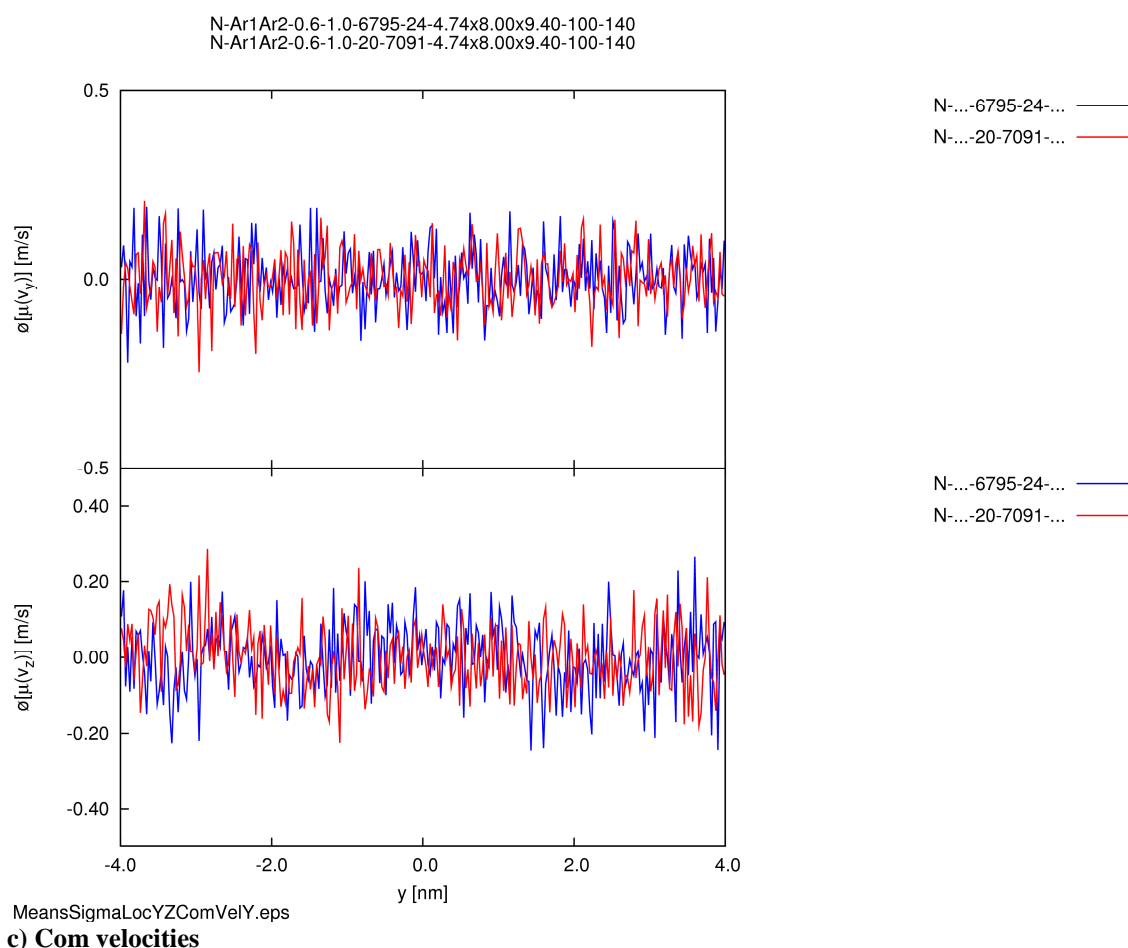


Figure 18 Comparison of the local observables obtained by using slabs in the two first nonequilibrium one-phase systems
N-Ar1Ar2-0.6-1.0-6795-24-4.74x8.00x9.40-100-140
and N-Ar1Ar2-0.6-1.0-20-7091-4.74x8.00x9.40-100-140

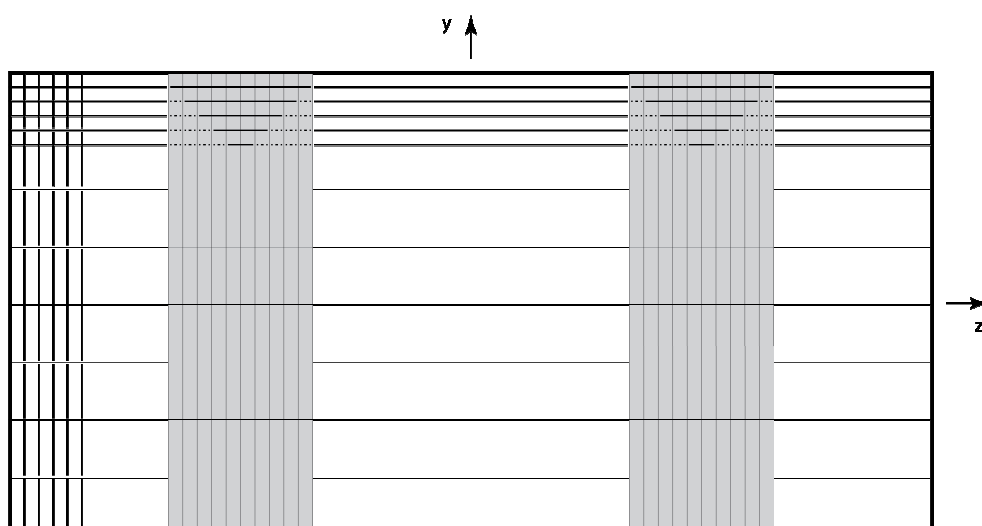


Figure 19 Locations and orientations of selected confined cut-surfaces used in the determination of the local stresses

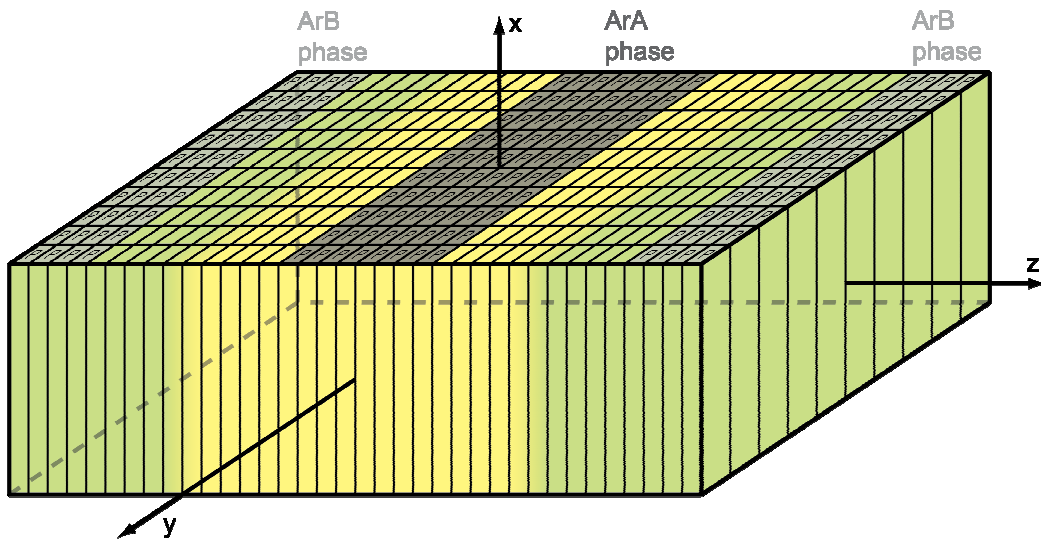


Figure 20 Sketch of an equilibrium interfacial system together with the subvolumes for which the local observables are computed
The subvolumes lumped together into the ArA or ArB phases are indicated in different shades of grey. The subvolumes considered in the calculation of the P-averages in each phase are additionally labelled with the letter "P".

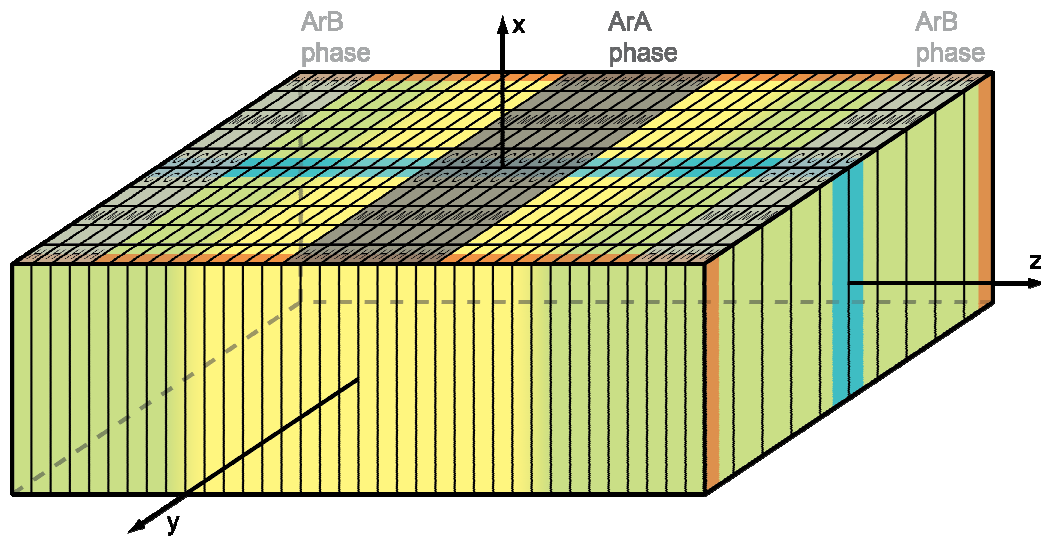
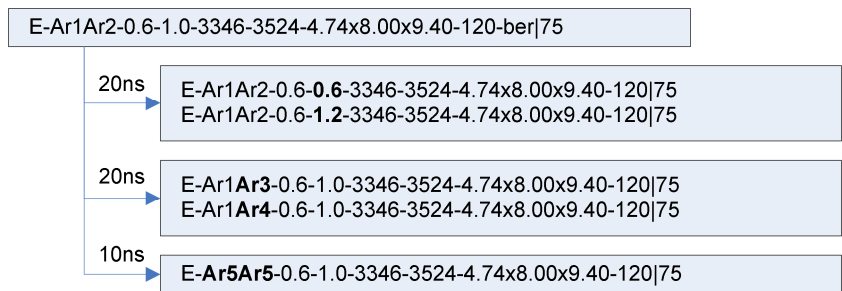
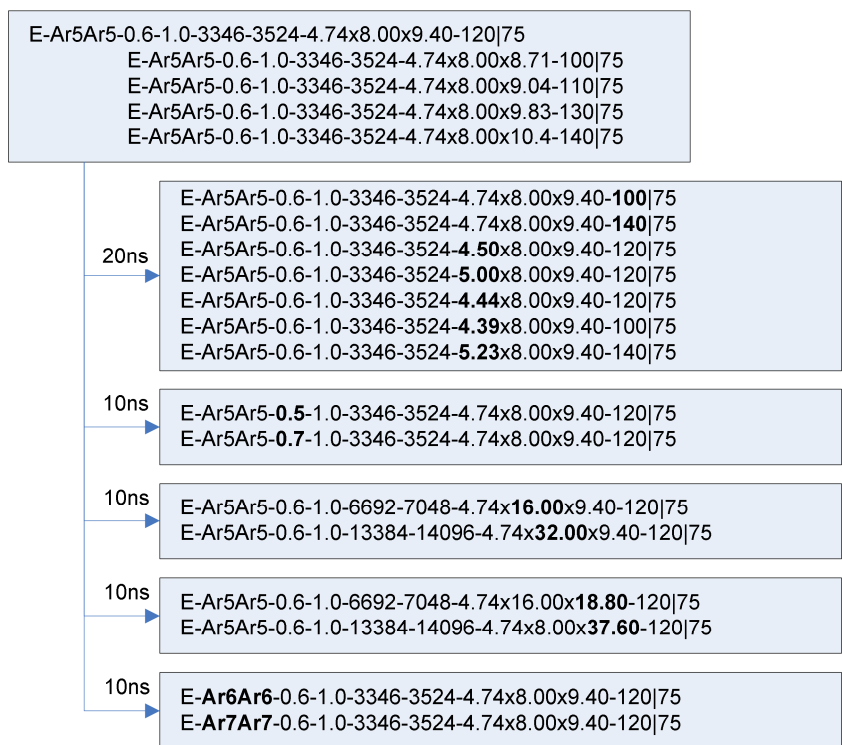


Figure 21 Sketch of a nonequilibrium interfacial system together with the subvolumes for which the local observables are computed
The subvolumes lumped together into the ArA or ArB phases are indicated in different shades of grey. The subvolumes considered in the calculation of the C, M, or H-averages in each phase are labelled with the letters "C", "M", or "H".



a) EMD simulations of heterophasic interfacial systems



b) EMD simulations of homophasic interfacial systems

N-Ar1Ar2-0.6-1.0-3346-3524-4.74x8.00x9.40-100-140-r1|75
N-Ar1Ar2-0.6-1.0-6795-24-4.74x8.00x9.40-100-140|75
N-Ar1Ar2-0.6-1.0-20-7091-4.74x8.00x9.40-100-140|75

20ns

N-Ar1Ar2-0.6-**0.6**-3346-3524-4.74x8.00x9.40-100-140|75
N-Ar1Ar2-0.6-**0.6**-6585-250-3524-4.74x8.00x9.40-100-140|75
N-Ar1Ar2-0.6-**0.6**-251-6715-3524-4.74x8.00x9.40-100-140|75

N-Ar1Ar2-0.6-**1.2**-3346-3524-4.74x8.00x9.40-100-140|75
N-Ar1Ar2-0.6-**1.2**-6804-16-3524-4.74x8.00x9.40-100-140|75
N-Ar1Ar2-0.6-**1.2**-13-7123-3524-4.74x8.00x9.40-100-140|75

5ns

N-Ar1Ar2-0.6-1.0-3346-3524-4.74x8.00x9.40-100-140-**a**|75
N-Ar1Ar2-0.6-1.0-3346-3524-4.74x8.00x9.40-100-140-**b**|75
N-Ar1Ar2-0.6-1.0-3346-3524-4.74x8.00x9.40-100-140-**c**|75
N-Ar1Ar2-0.6-1.0-3346-3524-4.74x8.00x9.40-100-140-**d**|75
N-Ar1Ar2-0.6-1.0-3346-3524-4.74x8.00x9.40-100-140-**e**|75
N-Ar1Ar2-0.6-1.0-3346-3524-4.74x8.00x9.40-100-140-**f**|75
N-Ar1Ar2-0.6-1.0-3346-3524-4.74x8.00x9.40-100-140-**g**|75
N-Ar1Ar2-0.6-1.0-3346-3524-4.74x8.00x9.40-100-140-**h**|75
N-Ar1Ar2-0.6-1.0-3346-3524-4.74x8.00x9.40-100-140-**i**|75
N-Ar1Ar2-0.6-1.0-3346-3524-4.74x8.00x9.40-100-140-**j**|75
N-Ar1Ar2-0.6-1.0-3346-3524-4.74x8.00x9.40-100-140-**ls**|75

10ns

N-Ar1**Ar3**-0.6-1.0-3346-3524-4.74x8.00x9.40-100-140|75
N-Ar1**Ar3**-0.6-1.0-6797-22-4.74x8.00x9.40-100-140|75
N-Ar1**Ar3**-0.6-1.0-20-7089-4.74x8.00x9.40-100-140|75

N-Ar1**Ar4**-0.6-1.0-3346-3524-4.74x8.00x9.40-100-140|75
N-Ar1**Ar4**-0.6-1.0-6799-22-4.74x8.00x9.40-100-140|75
N-Ar1**Ar4**-0.6-1.0-19-7088-4.74x8.00x9.40-100-140|75

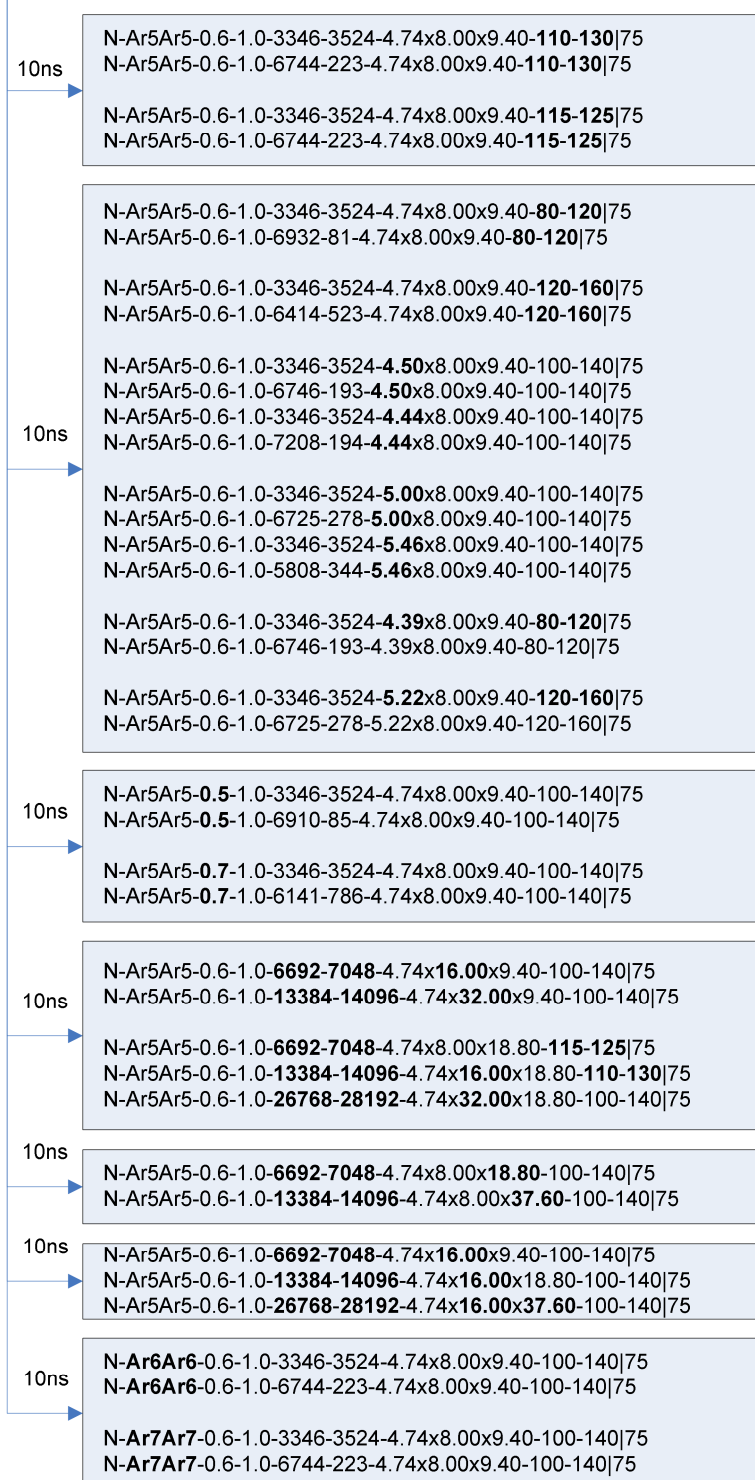
10ns

N-**Ar5Ar5**-0.6-1.0-3346-3524-4.74x8.00x9.40-100-140|75

c) NEMD simulations of heterophasic interfacial systems

N-Ar5Ar5-0.6-1.0-3346-3524-4.74x8.00x9.40-100-140|75
N-Ar5Ar5-0.6-1.0-6744-223-4.74x8.00x9.40-100-140|75

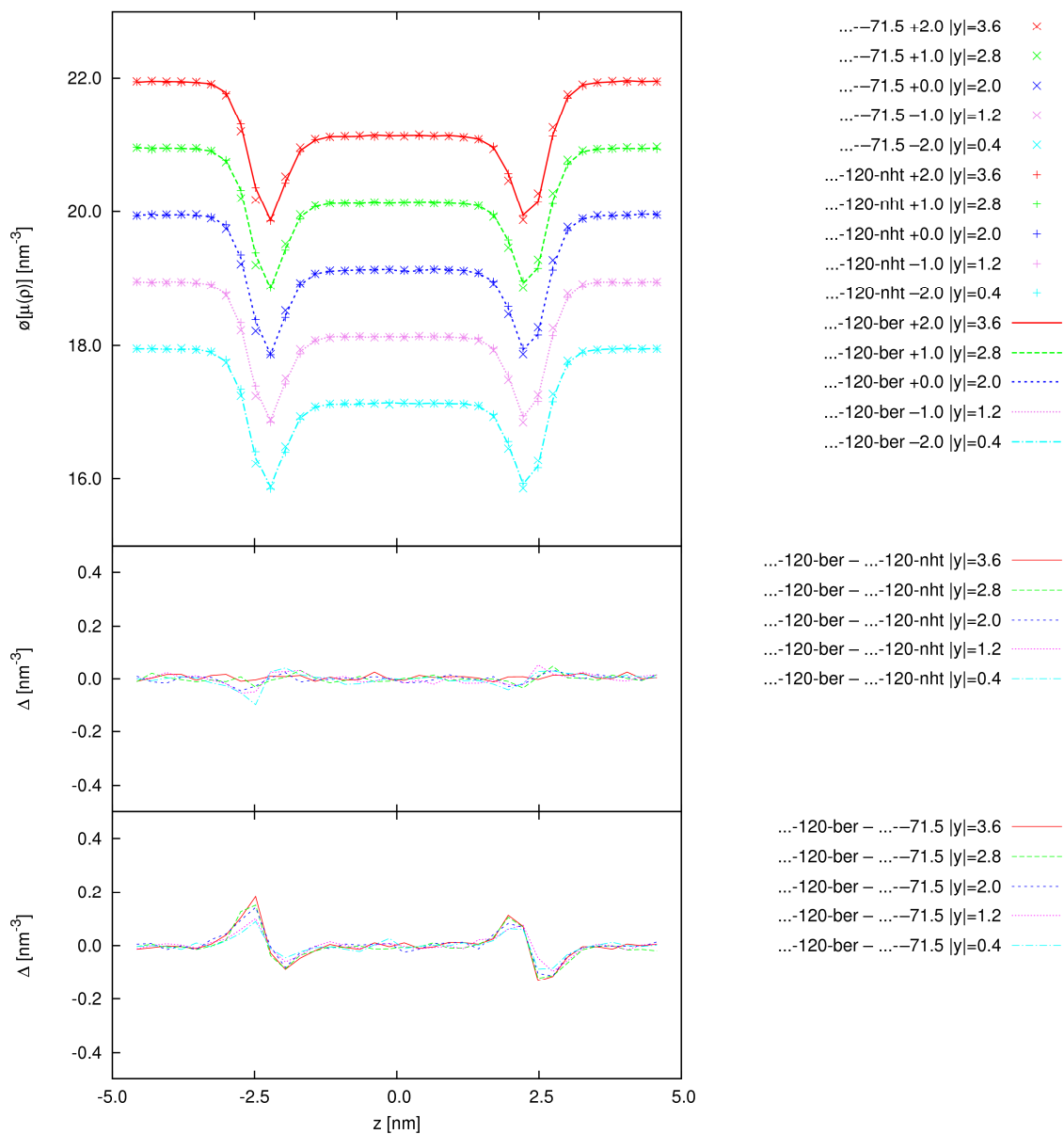
N-Ar5Ar5-0.6-1.0-6767-200-4.74x8.00x9.40-100-140|75
N-Ar5Ar5-0.6-1.0-6817-150-4.73x8.00x9.40-100-140|75
N-Ar5Ar5-0.6-1.0-6867-100-4.72x8.00x9.40-100-140|75
N-Ar5Ar5-0.6-1.0-6917-50-4.71x8.00x9.40-100-140|75
N-Ar5Ar5-0.6-1.0-6967-0-4.71x8.00x9.40-100-140|75



d) NEMD simulations of homophasic interfacial and their corresponding one-phase systems

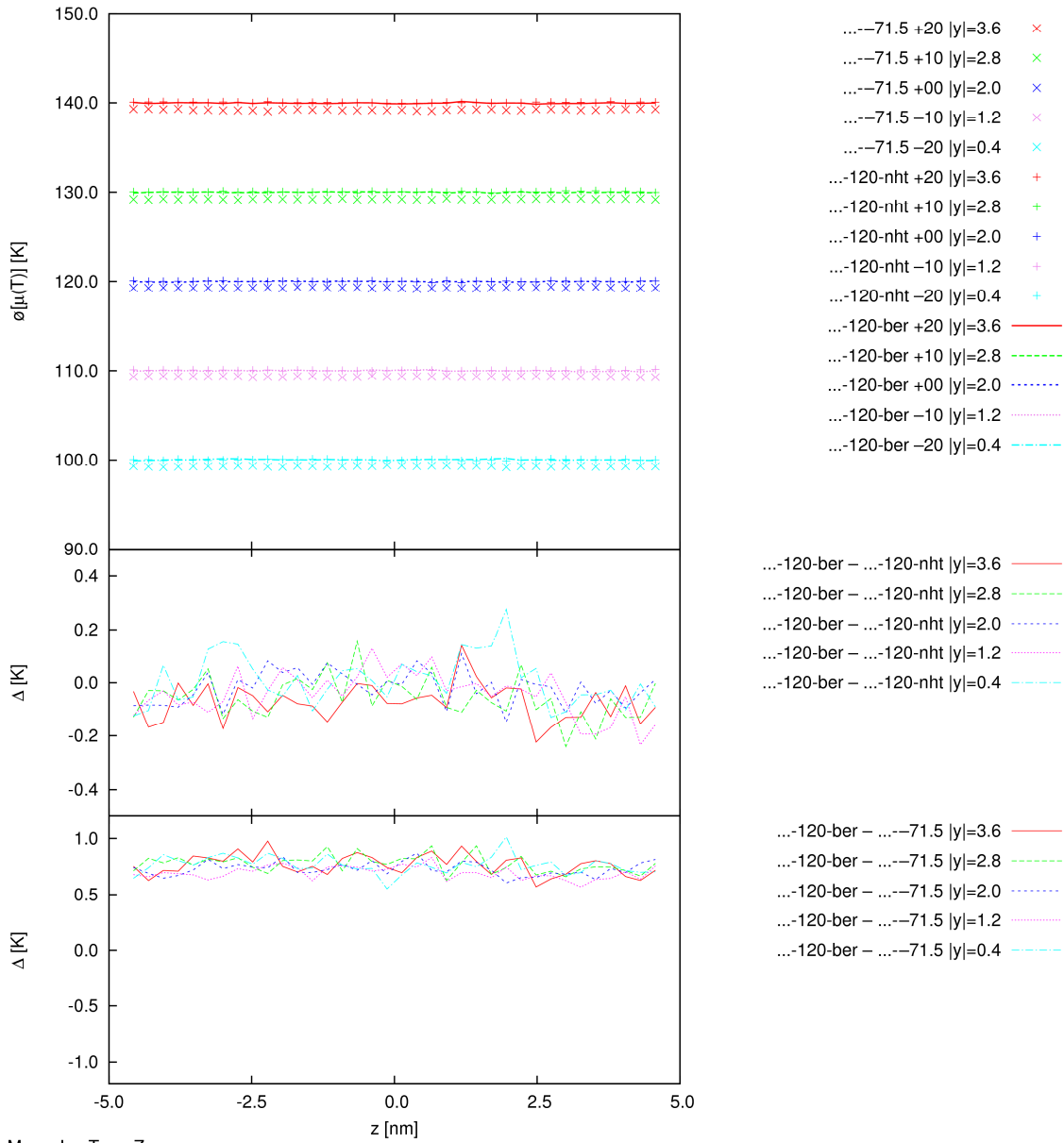
Figure 22 Production simulations of the different systems in chronological order

We give additionally the lengths of the preparational simulations. Bold symbols indicate the altered simulation parameters.



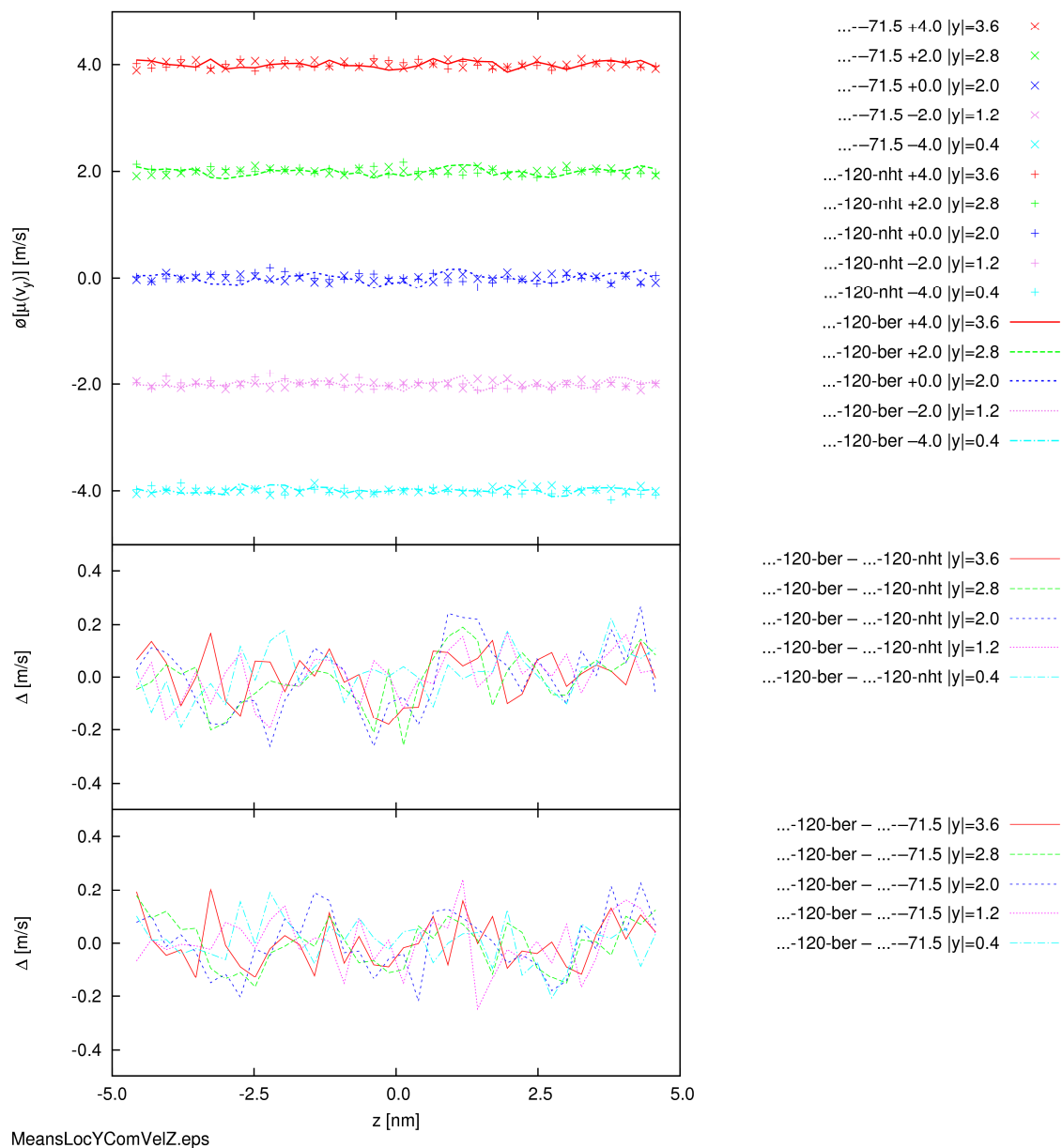
MeansLocDenOverallZ.eps

a) Density profiles

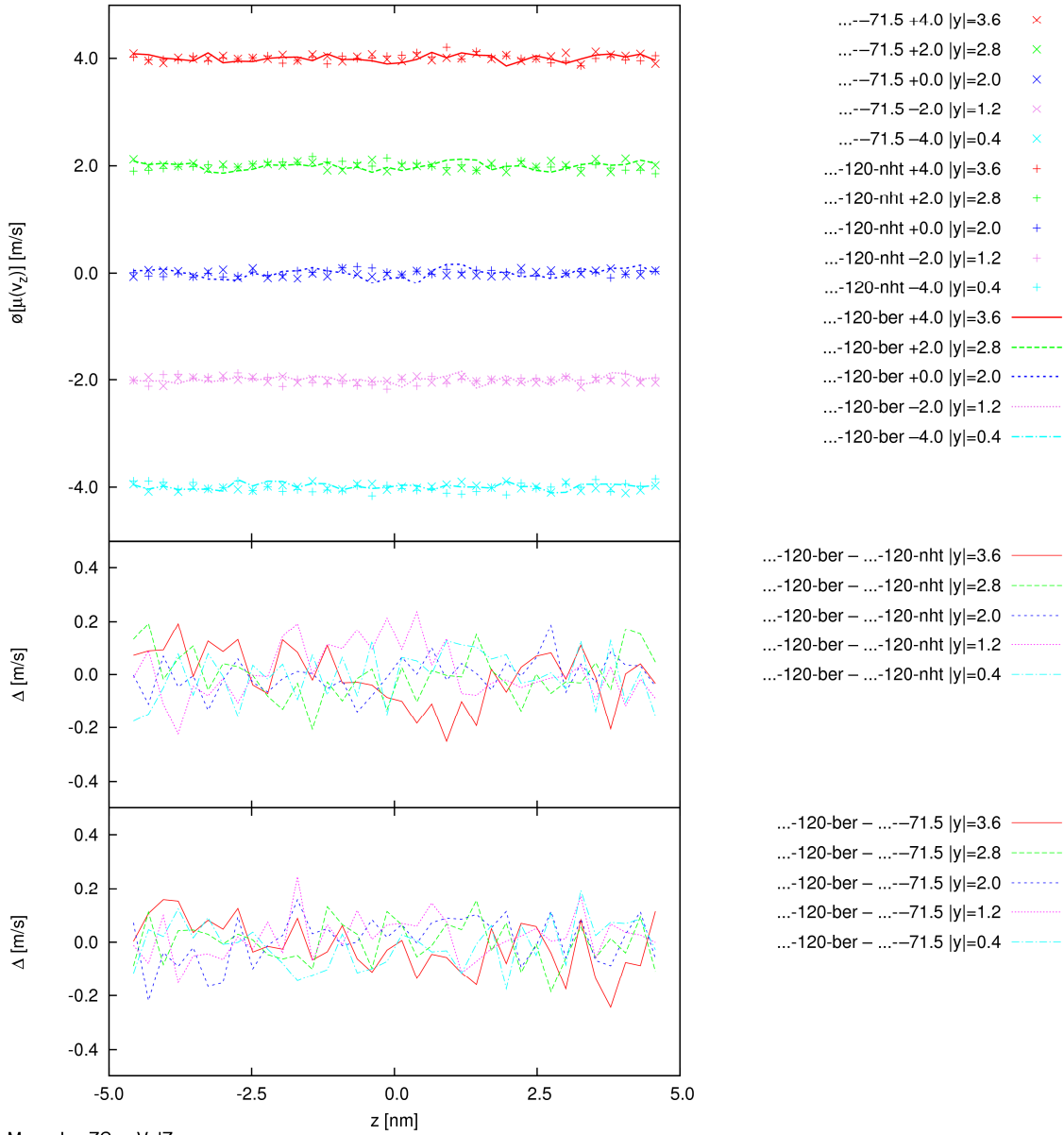


MeansLocTempZ.eps

b) Temperature profiles



MeansLocYComVelZ.eps



c) Com velocity components

Figure 23 Comparison of selected local observables in different production simulations of the first heterophasic equilibrium interfacial system E-Ar1Ar2-0.6-1.0-3346-3524-4.74x8.00x9.40-120-ber, E-Ar1Ar2-0.6-1.0-3346-3524-4.74x8.00x9.40-120-nvt, and E-Ar1Ar2-0.6-1.0-3346-3524-4.74x8.00x9.40-71.5; They start from different initial phase points obtained through the first, second or third preparation route.

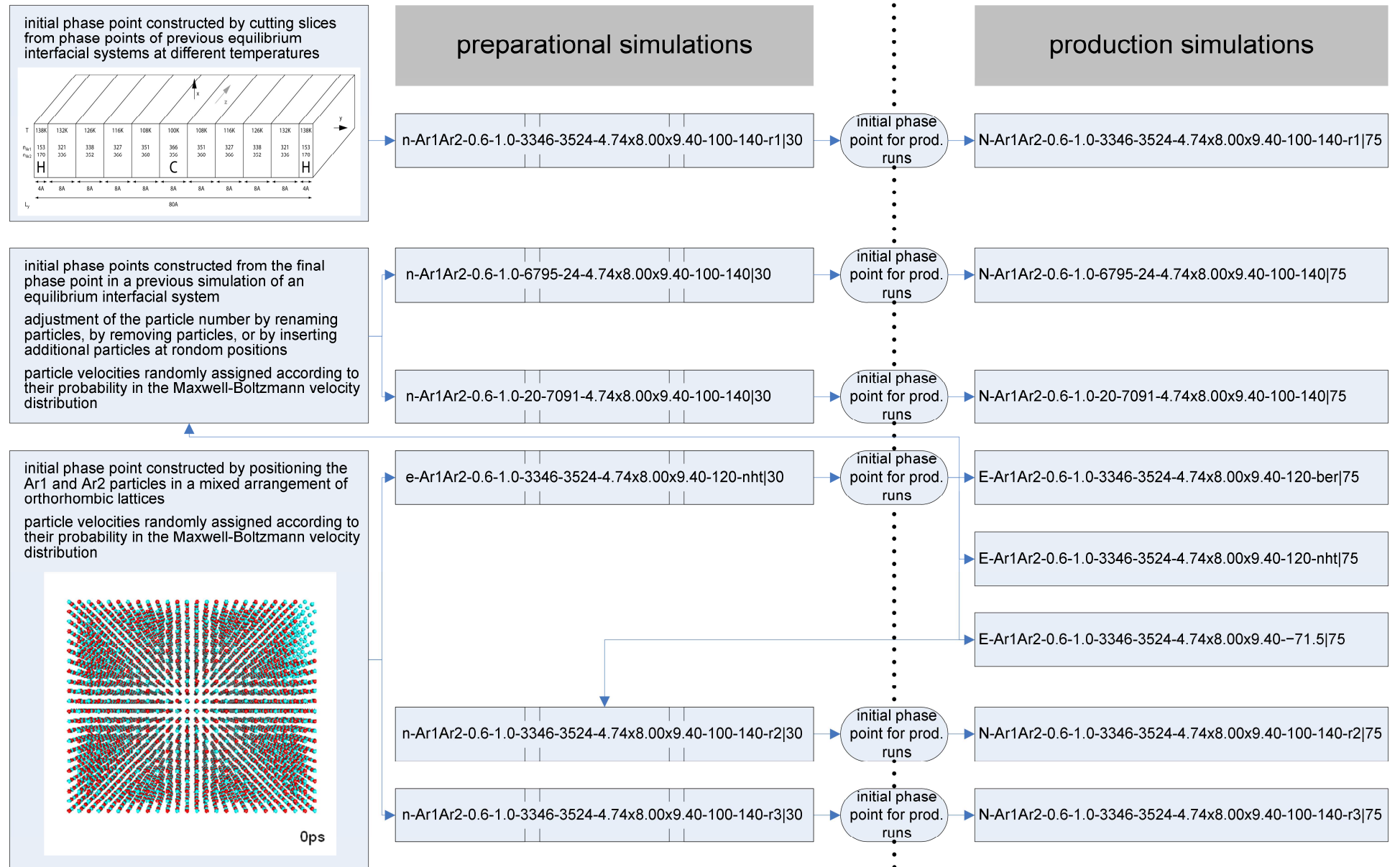
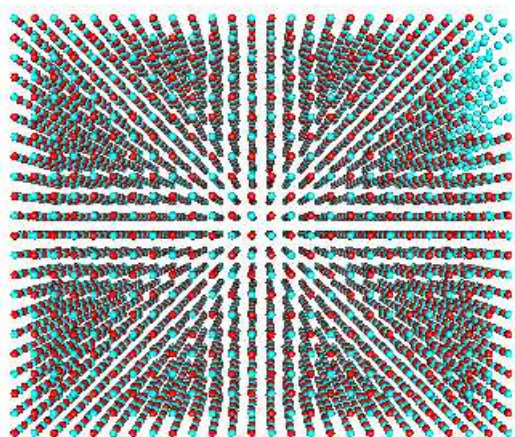
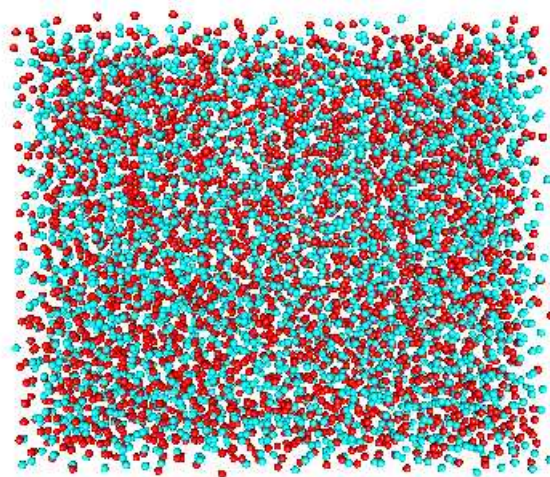


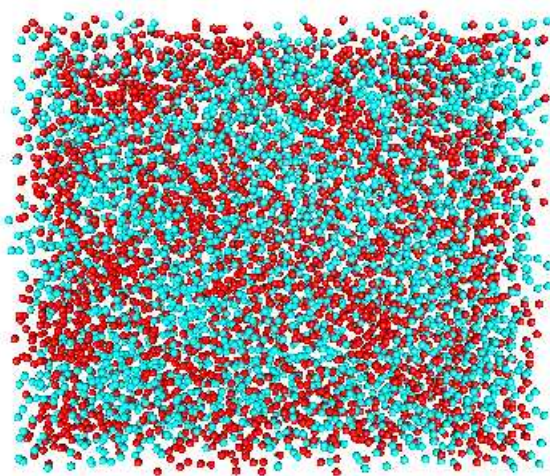
Figure 24 Sequence of the preparational and production simulations of the first systems
 N-Ar1Ar2-0.6-1.0-3346-3524-4.74x8.00x9.40-100-140 and E-Ar1Ar2-0.6-1.0-3346-3524-4.74x8.00x9.40-120



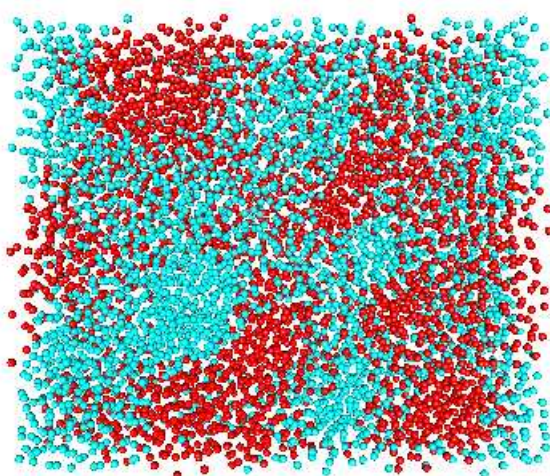
0ps



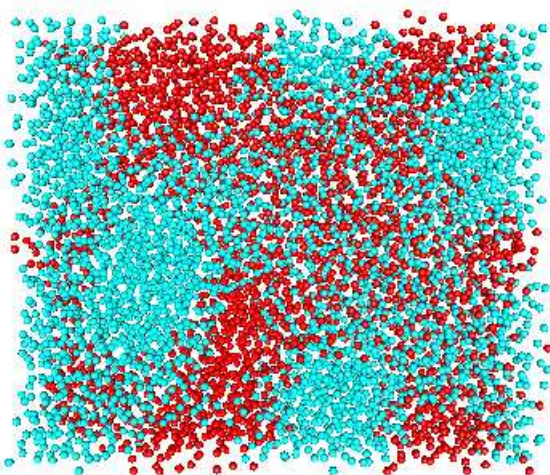
5ps



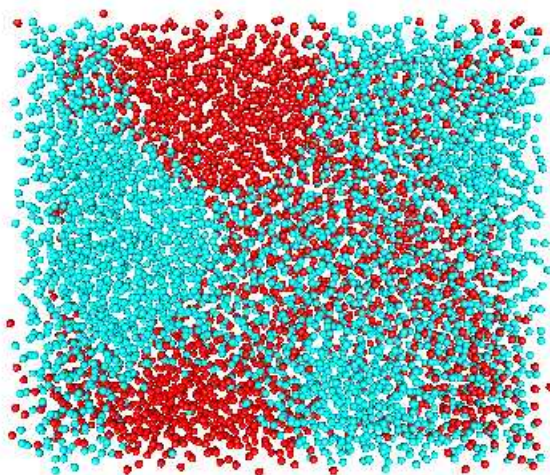
50ps



250ps



500ps



700ps

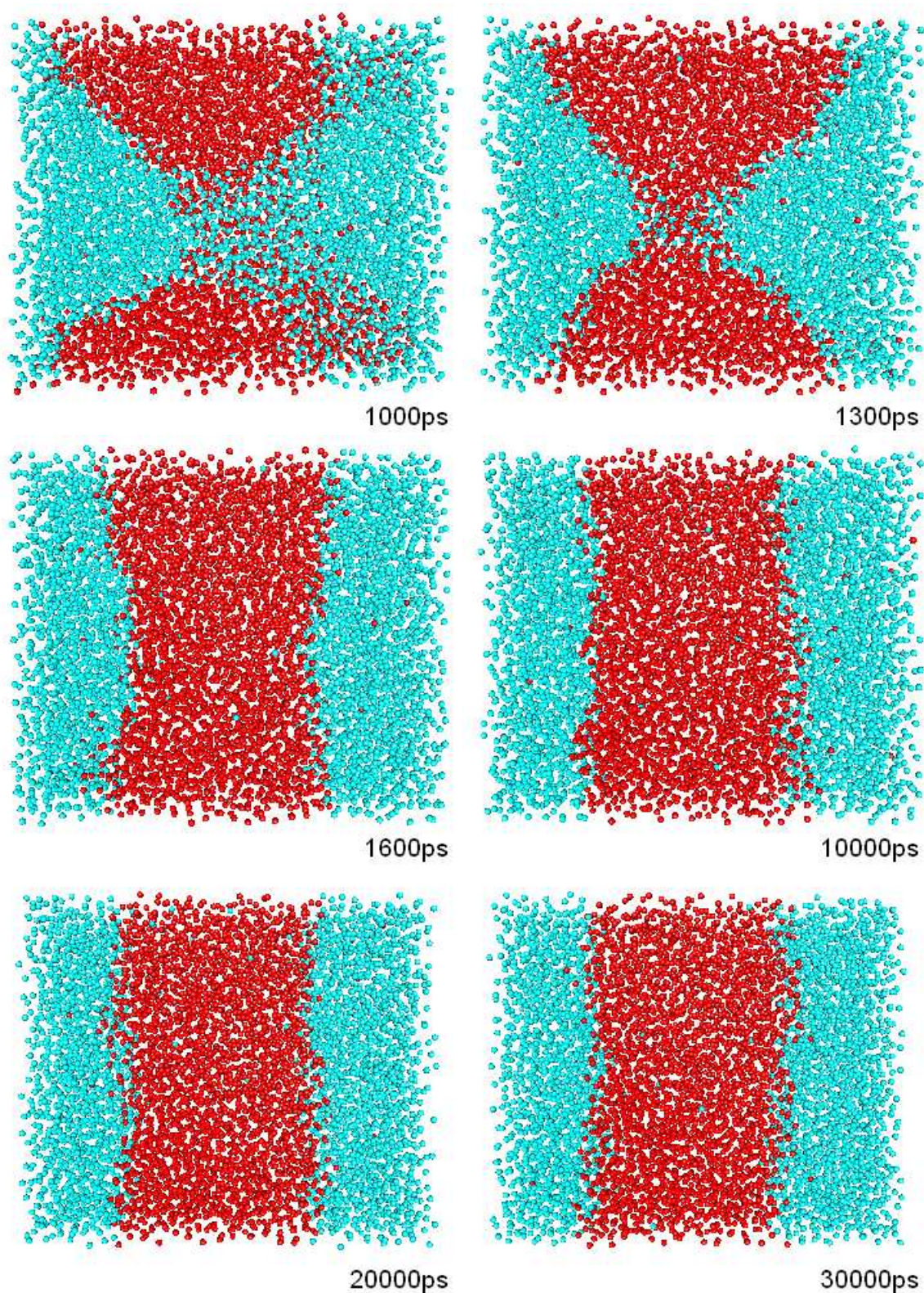
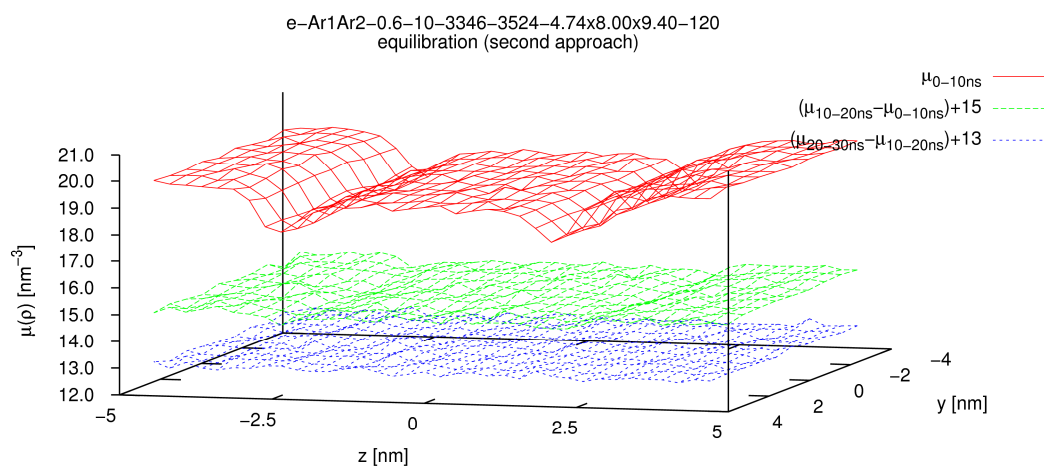
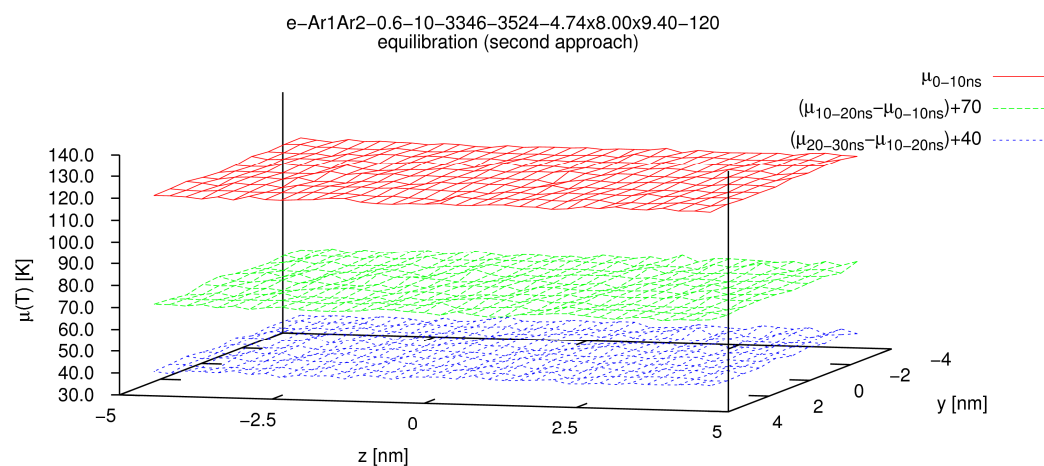


Figure 25 Selected snapshots of the demixing in the equilibration simulation e-Ar1Ar2-0.6-1.0-3346-3524-4.74x8.00x9.40-120 (second preparation route)



MeansLocDenOverallYZ-diff.eps

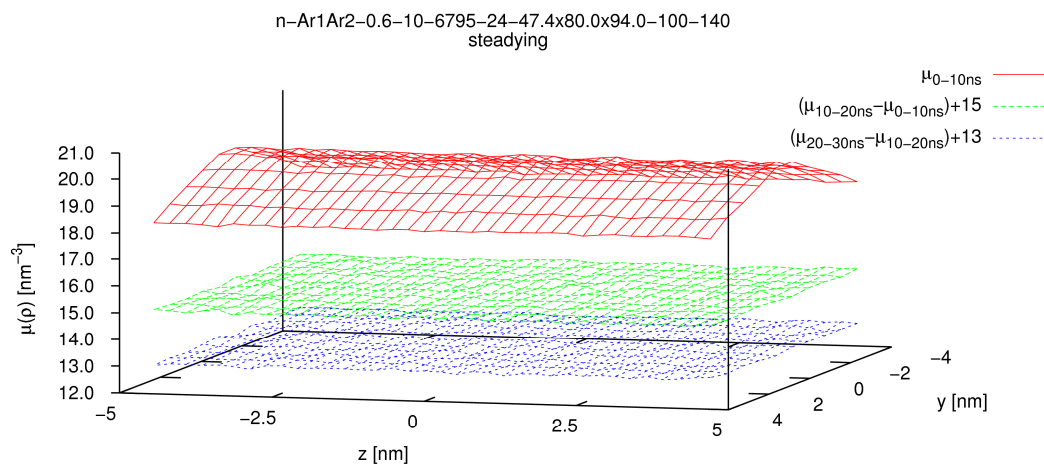
a) Densities



MeansLocTempYZ-diff.eps

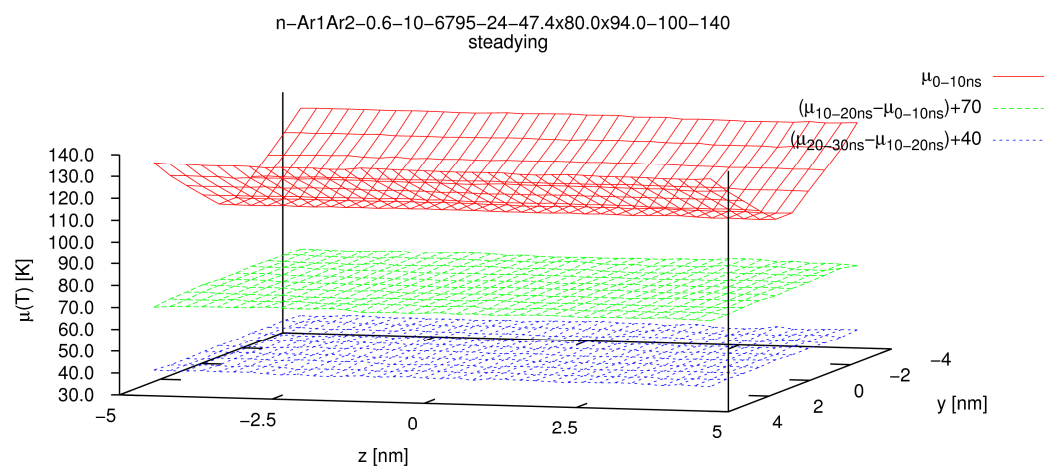
b) Temperatures

Figure 26 Local densities determined over three 10ns long successive segments of the equilibration simulation e-Ar1Ar2-0.6-1.0-3346-3524-4.74x8.00x9.40-120 (second preparation route)
Note that only the changes from the first to the second and from the second to the third segment are displayed for better readability.



MeansLocDenOverallYZ-diff.eps

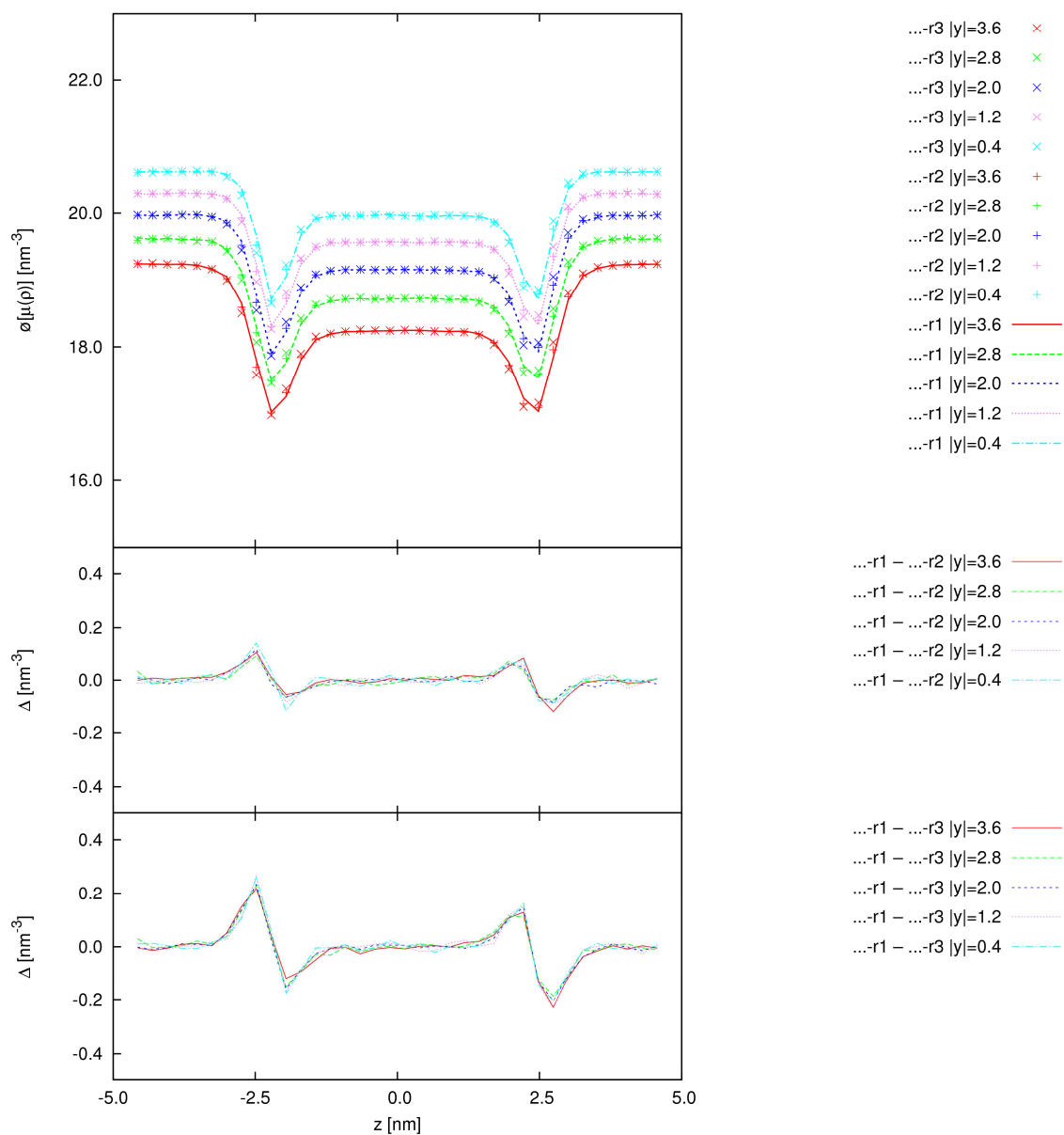
a) Densities



MeansLocTempYZ-diff.eps

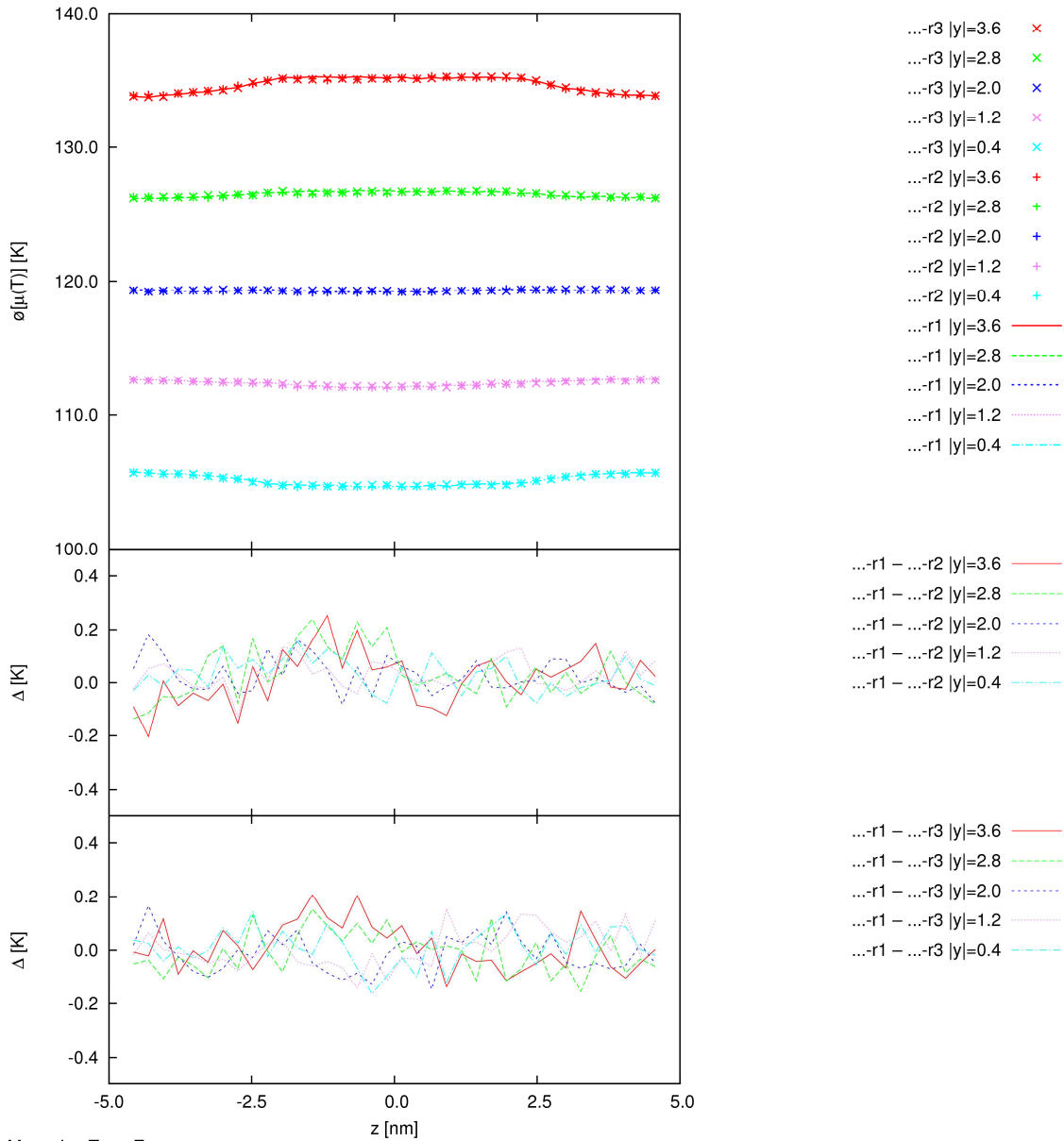
b) Temperatures

Figure 27 Local observables determined over three 10ns long successive segments of the steadying simulation n-Ar1Ar2-0.6-1.0-6795-24-4.74x8.00x9.40-100-140
Note that only the changes from the first to the second and from the second to the third segment are displayed for better readability.



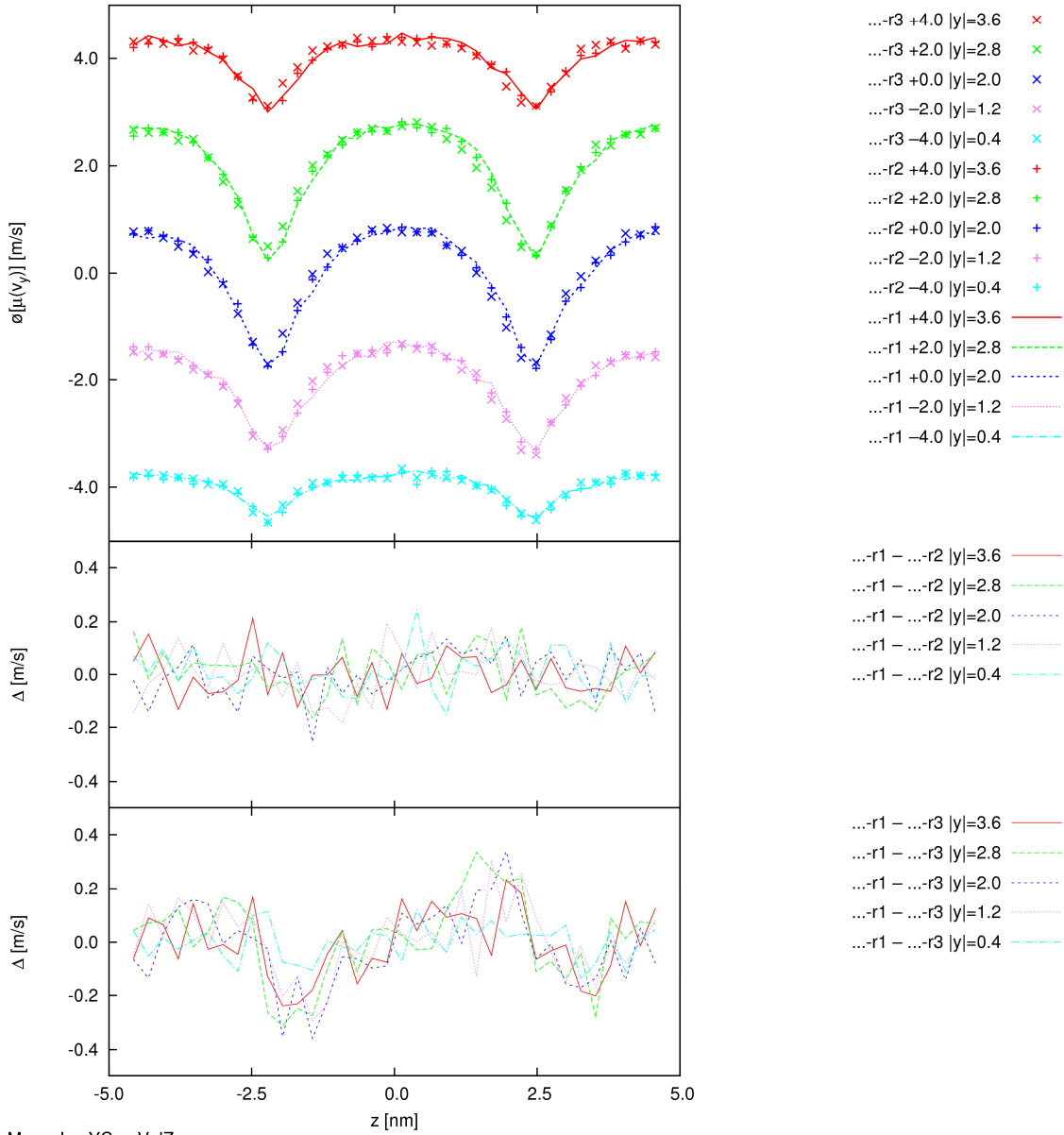
MeansLocDenOverallZ.eps

a) Density profiles



MeansLocTempZ.eps

b) Temperature profiles



MeansLocYComVelZ.eps

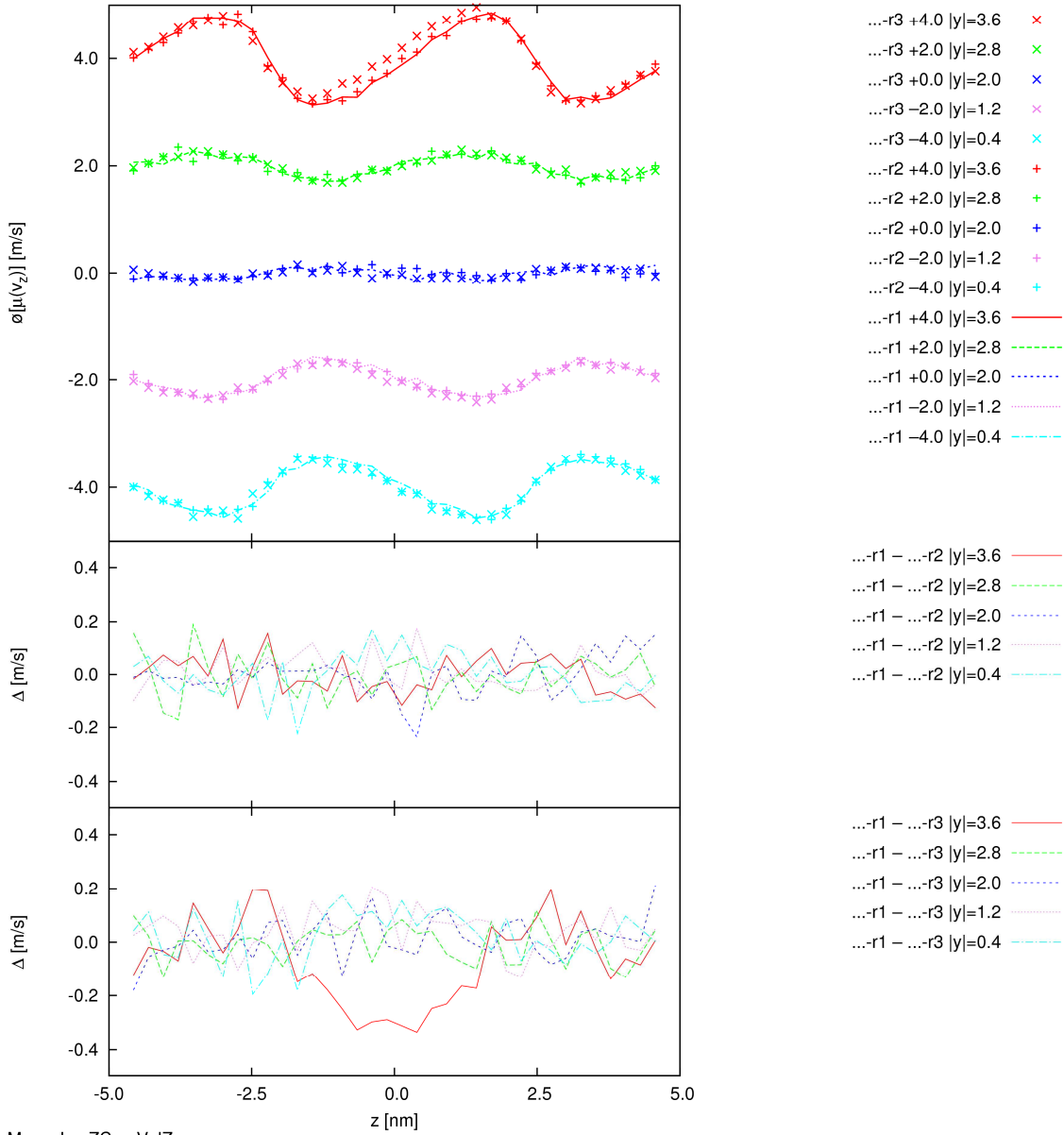


Figure 28 Comparison of selected local observables in separate production simulations of the first heterophasic nonequilibrium interfacial system N-Ar1Ar2-0.6-1.0-3346-3524-4.74x8.00x9.40-100-140-r1, N-Ar1Ar2-0.6-1.0-3346-3524-4.74x8.00x9.40-100-140-r2, and N-Ar1Ar2-0.6-1.0-3346-3524-4.74x8.00x9.40-100-140-r3 They start from different initial phase points obtained through the first, second or third preparation route.

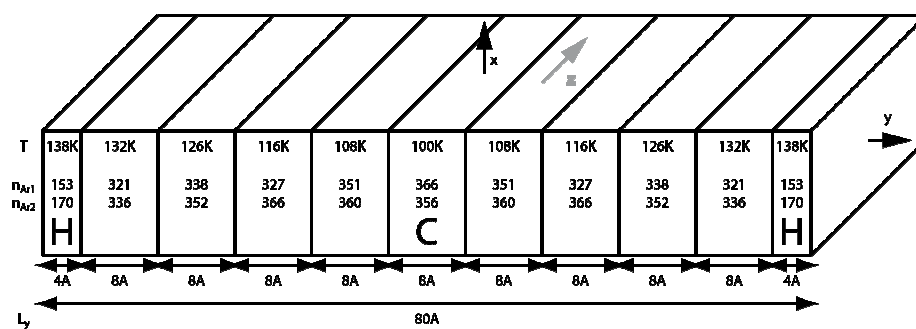
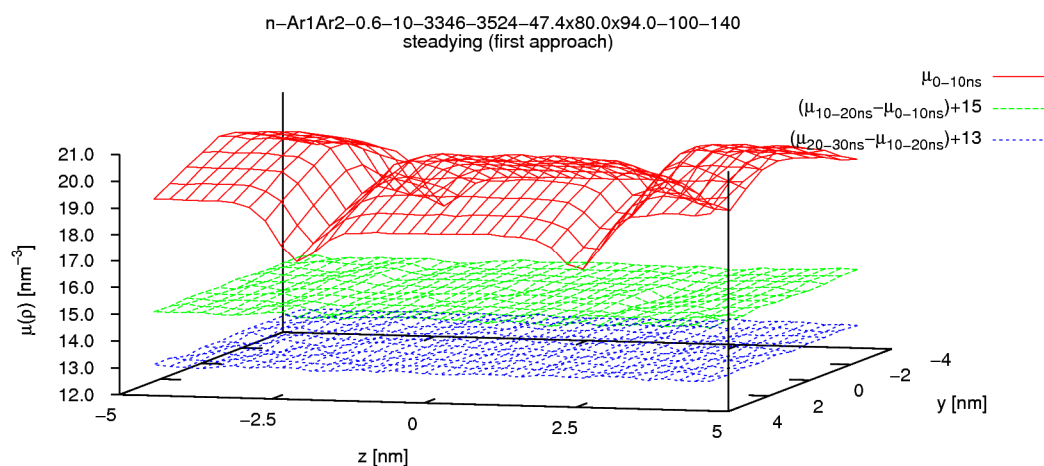
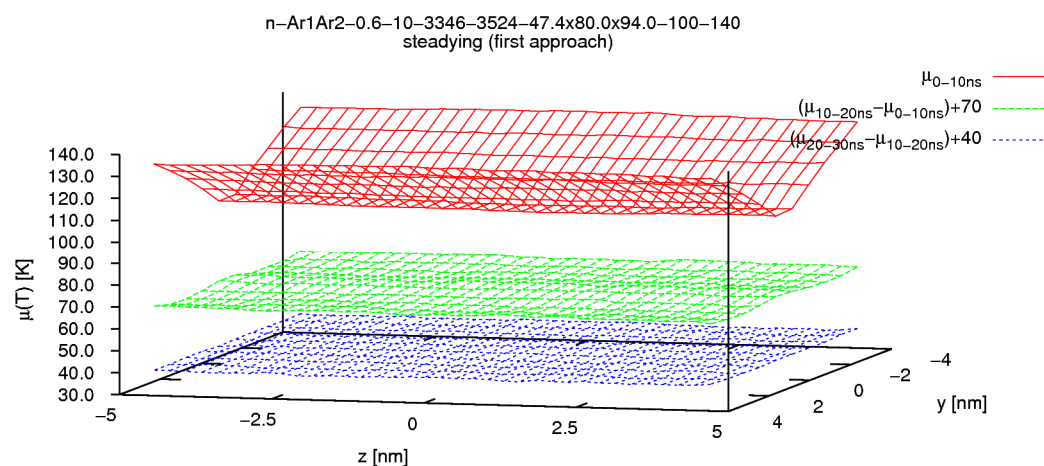


Figure 29 Preparation of an initial phase point from cut-outs of phase points in Buhn's NPT simulations. We link the different cut-outs together in y -direction to obtain a phase point that resembles one to be found in the first nonequilibrium interfacial system. The figure shows additionally the numbers of particles found in the different cut-outs.



MeansLocDenOverallYZ-diff.eps

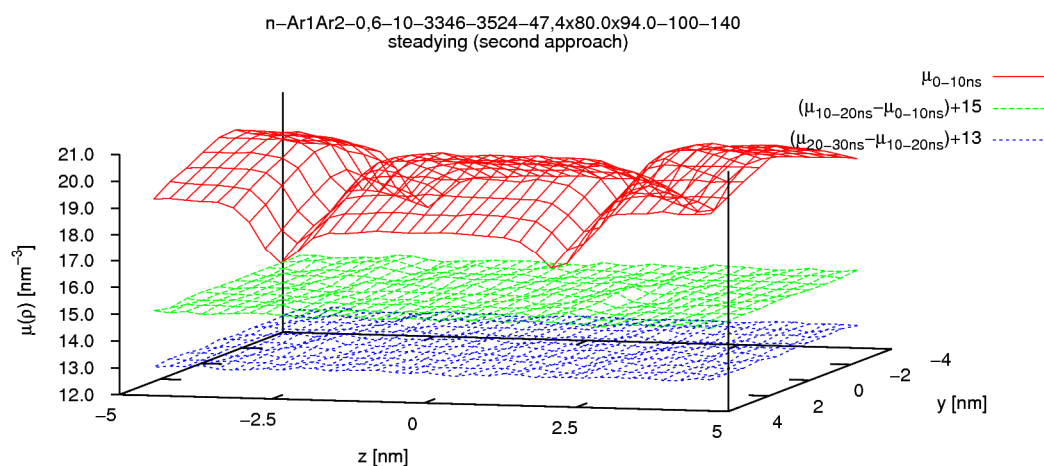
a) Densities



MeansLocTempYZ-diff.eps

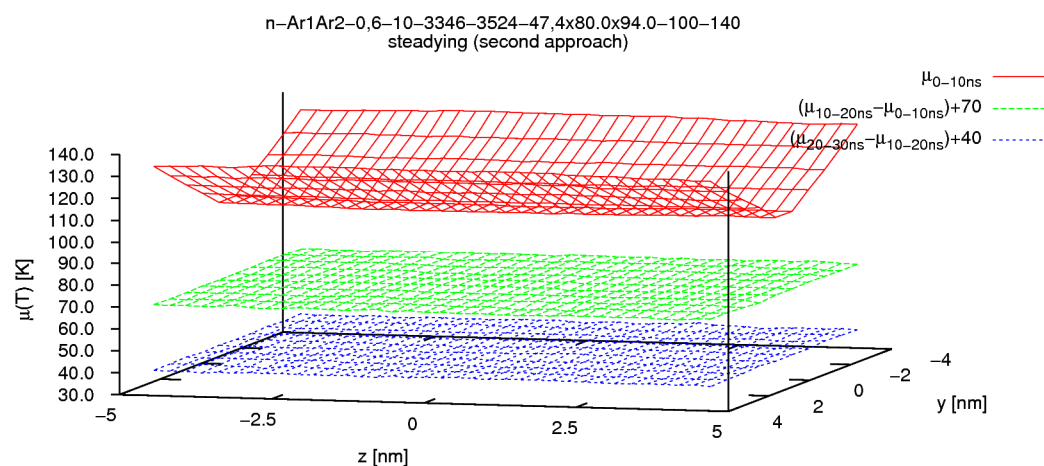
b) Temperatures

Figure 30 Local observables determined over three 10ns long successive segments of the steading simulation n-Ar1Ar2-0.6-1.0-3346-3524-4.74x8.00x9.40-100-140 (first preparation route)
Note that only the changes from the first to the second and from the second to the third segment are displayed for better readability.



MeansLocDenOverallYZ-diff.eps

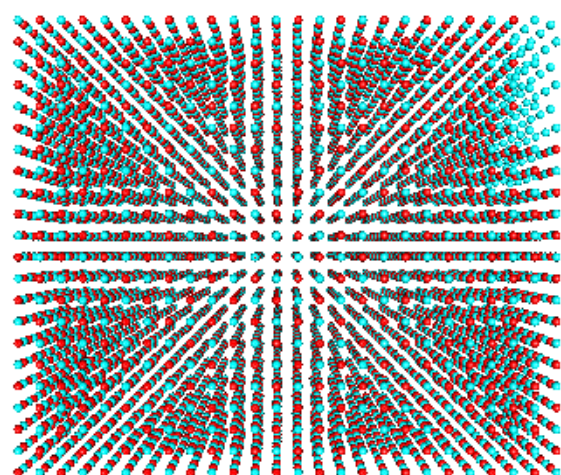
a) Densities



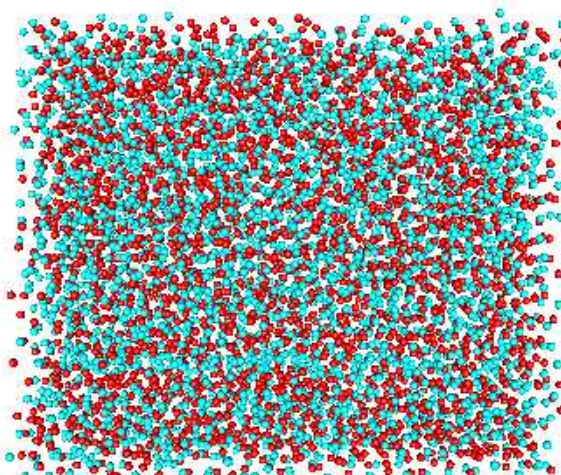
MeansLocTempYZ-diff.eps

b) Temperatures

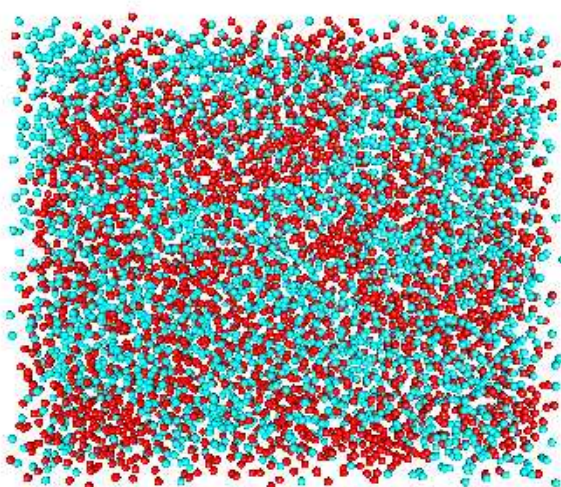
Figure 31 Local observables determined over three 10ns long successive segments of the steading simulation n-Ar1Ar2-0.6-1.0-3346-3524-4.74x8.00x9.40-100-140 (second preparation route)
Note that only the changes from the first to the second and from the second to the third segment are displayed for better readability.



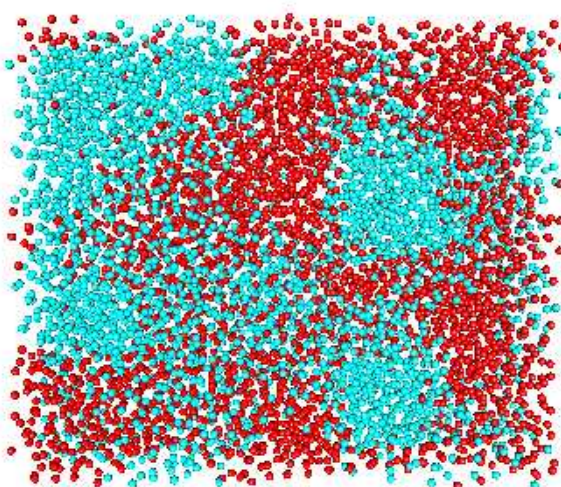
0ps



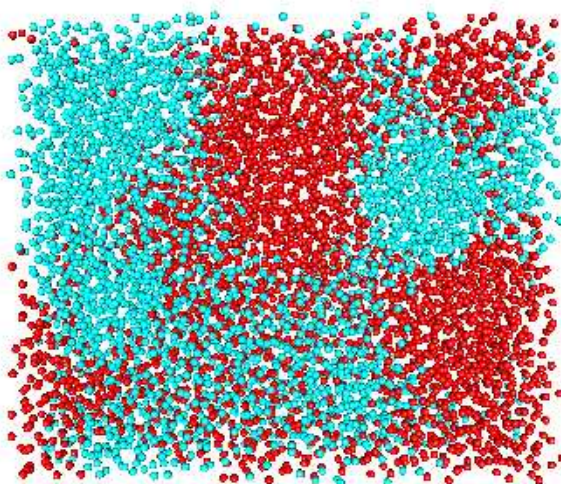
5ps



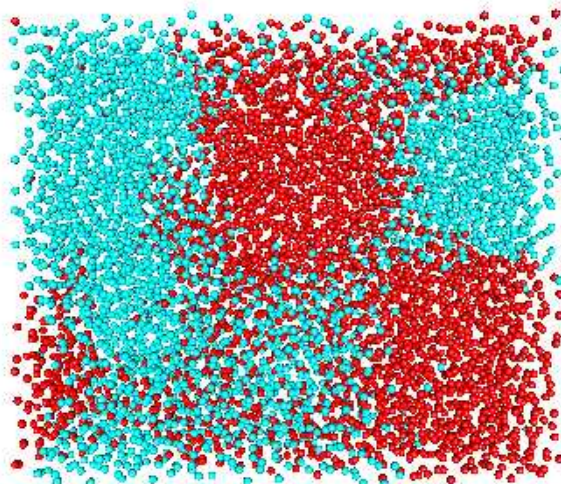
50ps



250ps



400ps



500ps

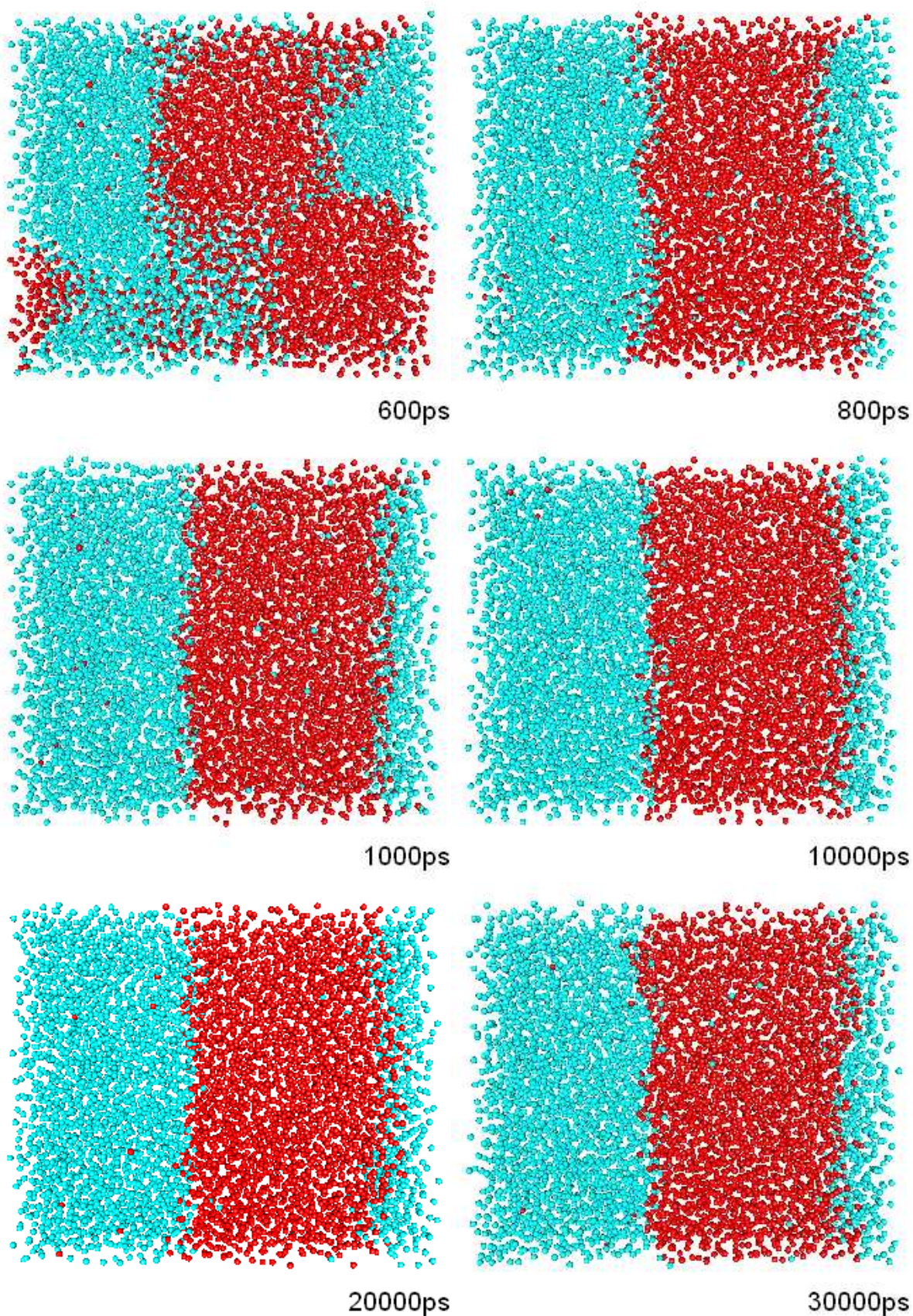
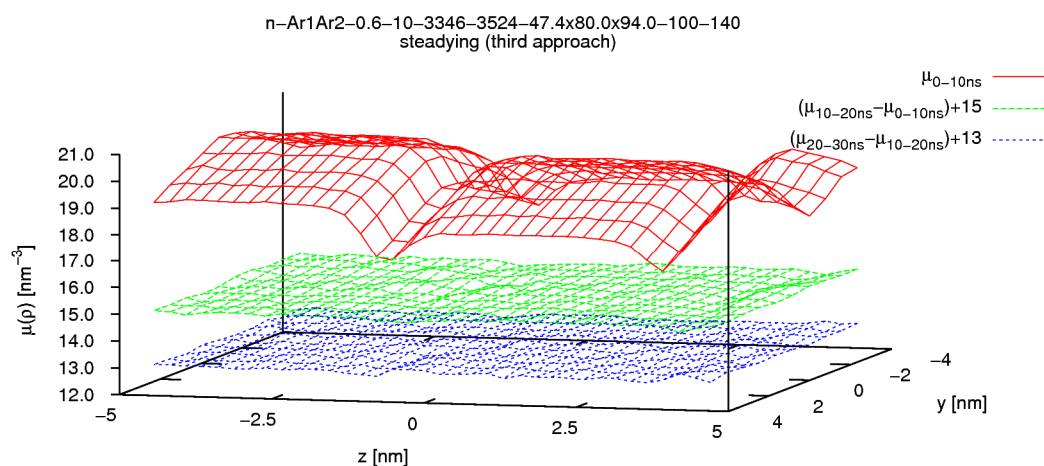
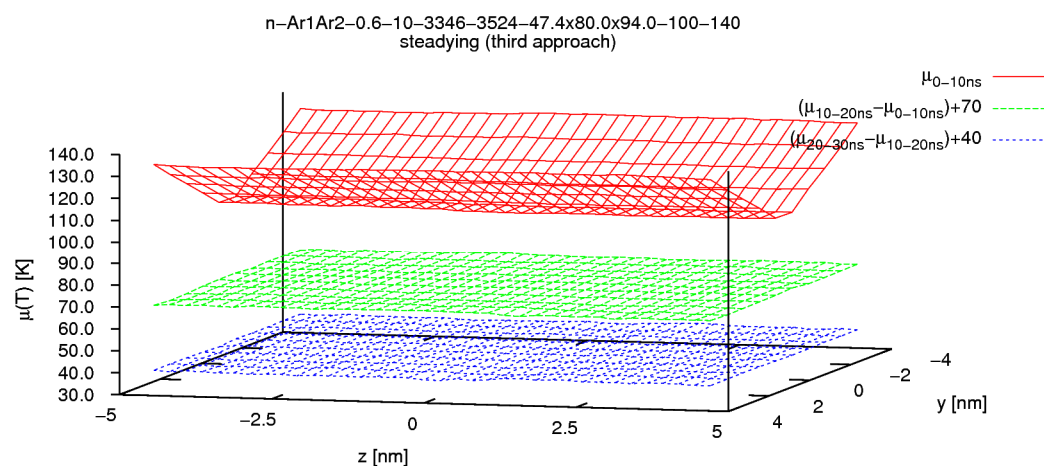


Figure 32 Selected snapshots of the demixing in the steadying simulation n-Ar1Ar2-0.6-1.0-3346-3524-4.74x8.00x9.40-100-140 (third preparation route)



MeansLocDenOverallYZ-diff.eps

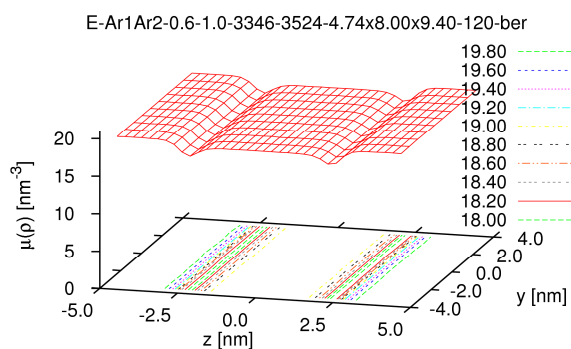
a) Densities



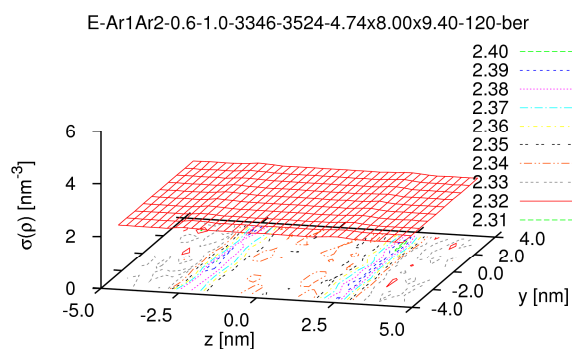
MeansLocTempYZ-diff.eps

b) Temperatures

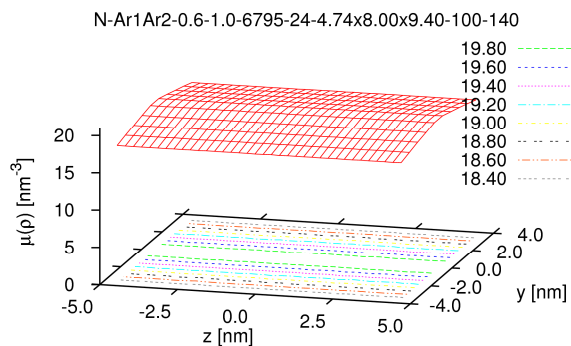
Figure 33 Local observables determined over three 10ns long successive segments of the steading simulation N-Ar1Ar2-0.6-1.0-3346-3524-4.74x8.00x9.40-100-140 (third preparation route)
Note that only the changes from the first to the second and from the second to the third segment are displayed for better readability.



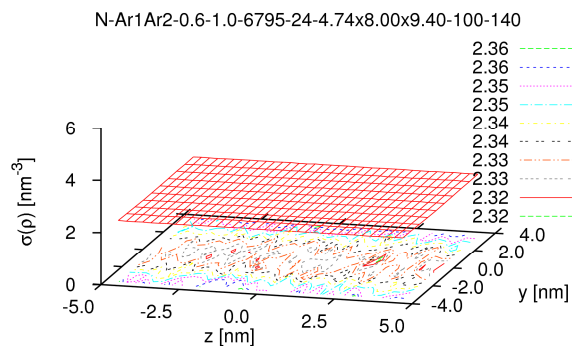
MeansLocDenOverallYZ.eps



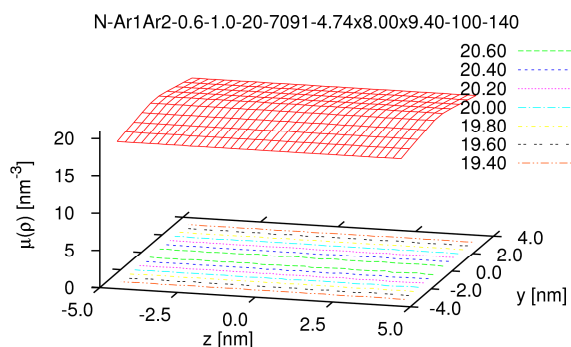
SigmaLocDenOverallYZ.eps



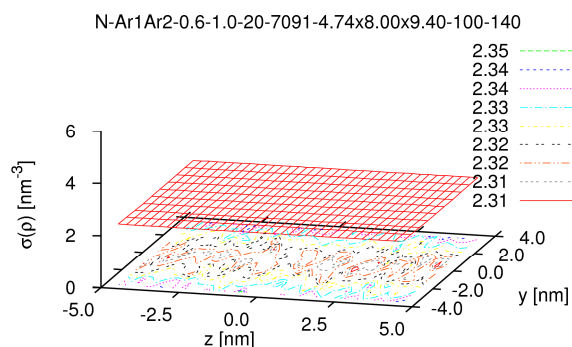
MeansLocDenOverallYZ.eps



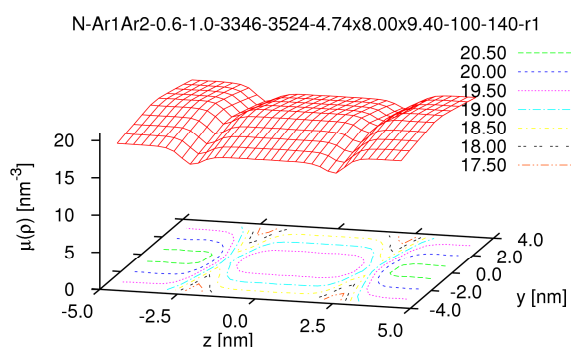
SigmaLocDenOverallYZ.eps



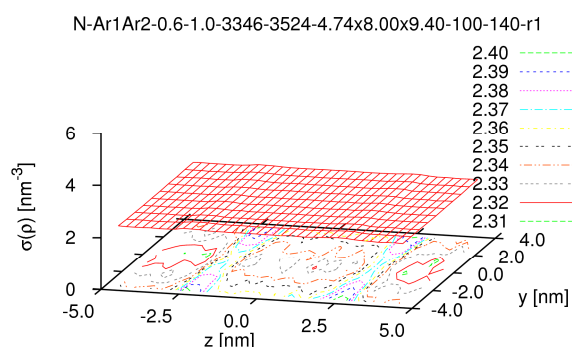
MeansLocDenOverallYZ.eps



SigmaLocDenOverallYZ.eps

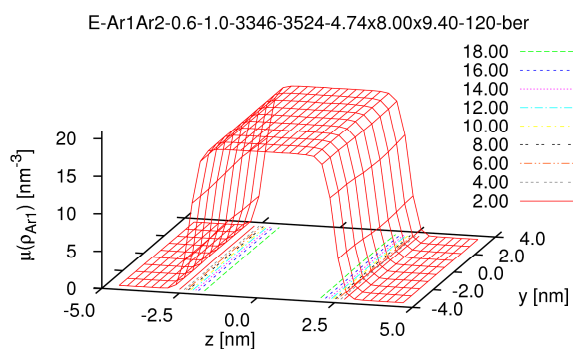


MeansLocDenOverallYZ.eps

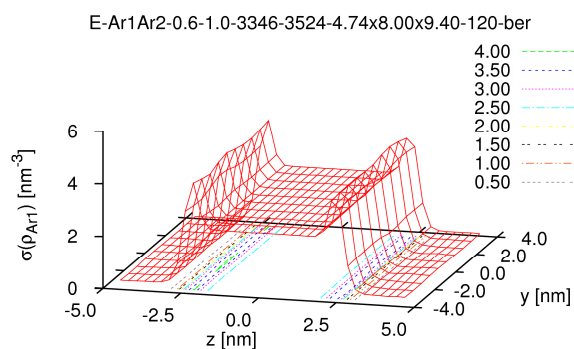


SigmaLocDenOverallYZ.eps

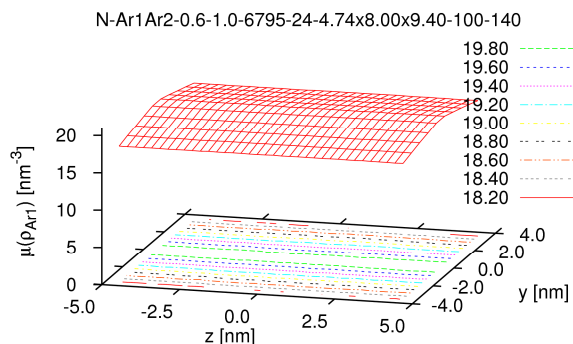
a) Densities



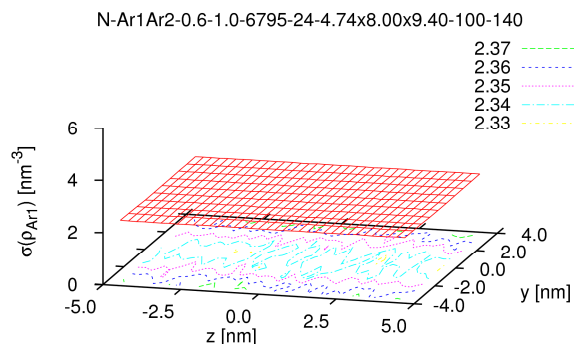
MeansLocDenAr1YZ.eps



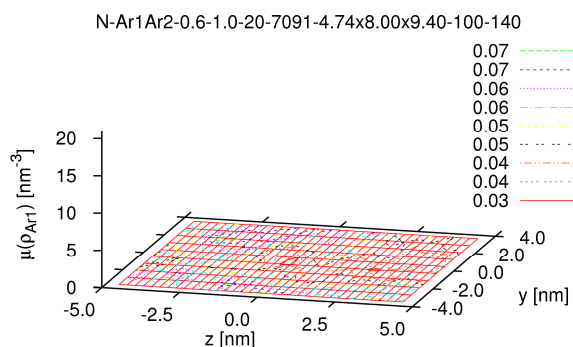
SigmaLocDenAr1YZ.eps



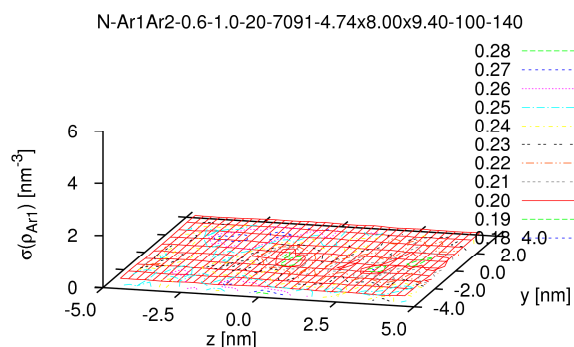
MeansLocDenAr1YZ.eps



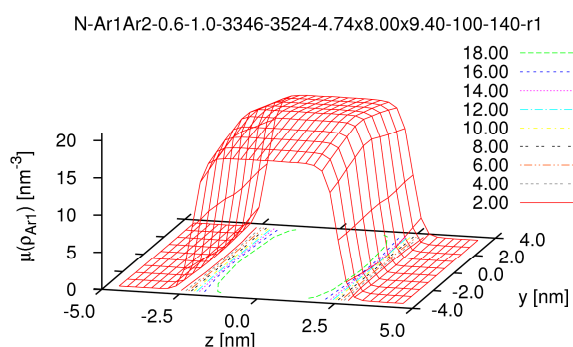
SigmaLocDenAr1YZ.eps



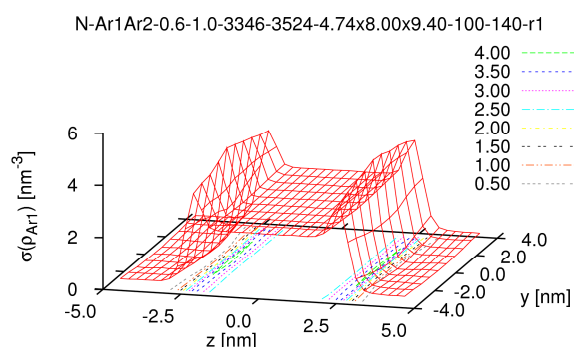
MeansLocDenAr1YZ.eps



SigmaLocDenAr1YZ.eps

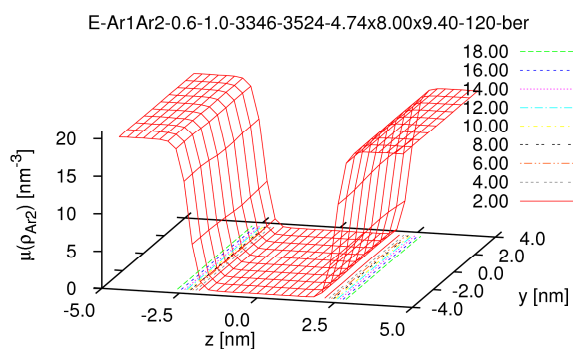


MeansLocDenAr1YZ.eps

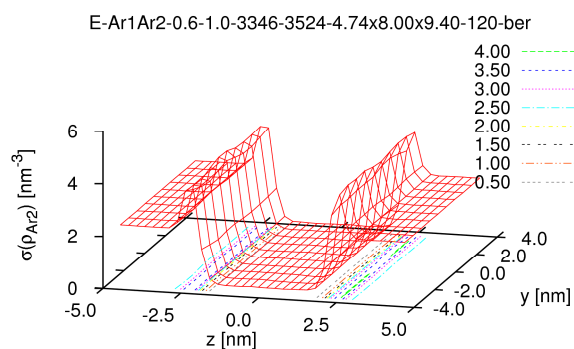


SigmaLocDenAr1YZ.eps

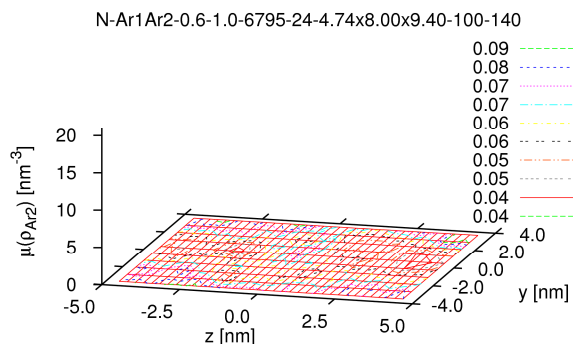
b) ArA partial densities



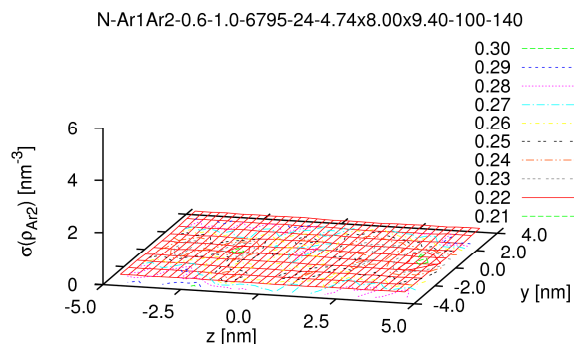
MeansLocDenAr2YZ.eps



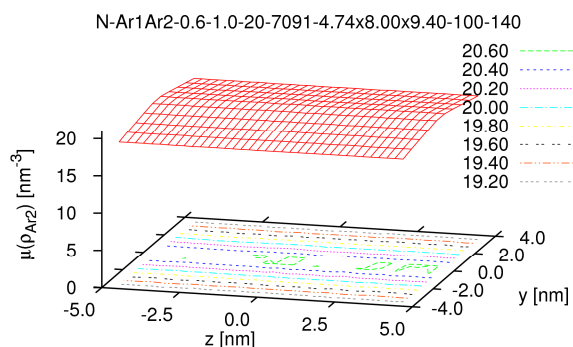
SigmaLocDenAr2YZ.eps



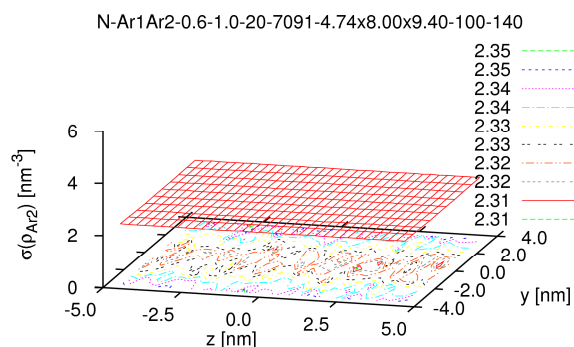
MeansLocDenAr2YZ.eps



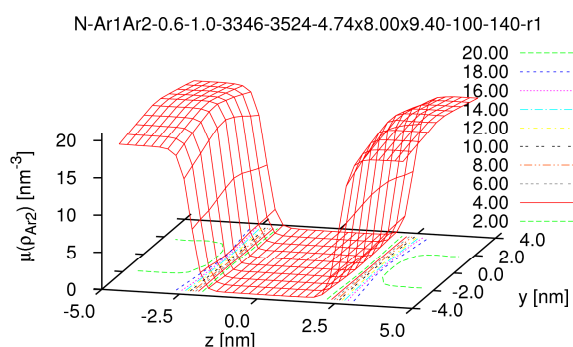
SigmaLocDenAr2YZ.eps



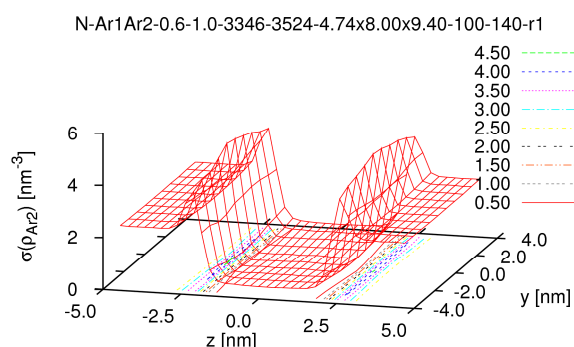
MeansLocDenAr2YZ.eps



SigmaLocDenAr2YZ.eps

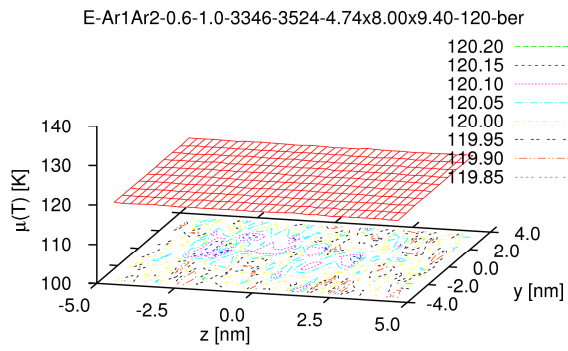


MeansLocDenAr2YZ.eps

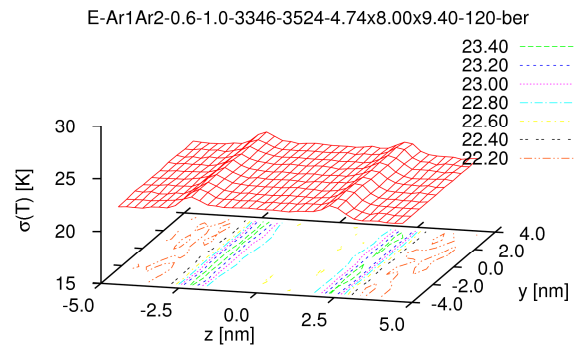


SigmaLocDenAr2YZ.eps

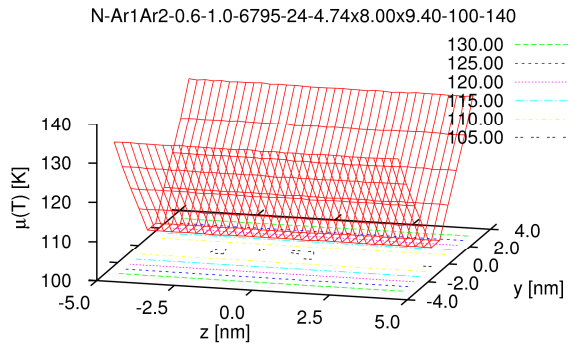
c) ArB partial densities



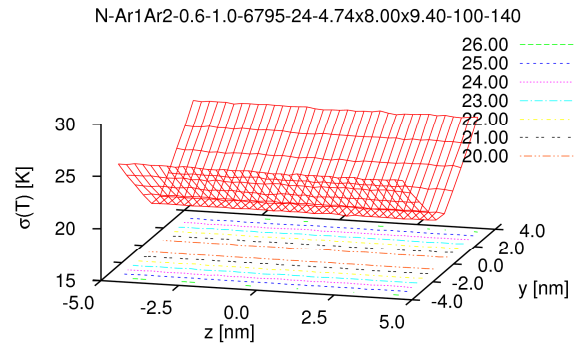
MeansLocTempYZ.eps



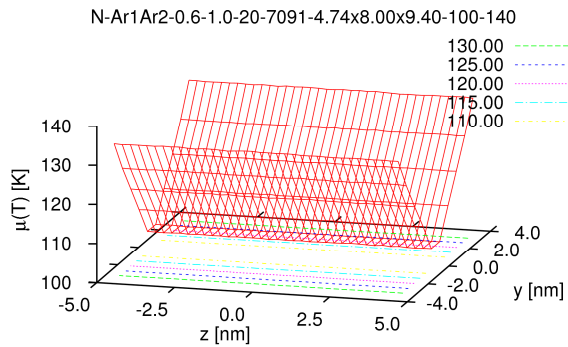
SigmaLocTempYZ.eps



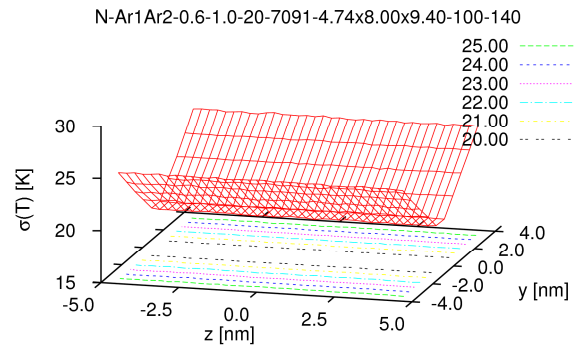
MeansLocTempYZ.eps



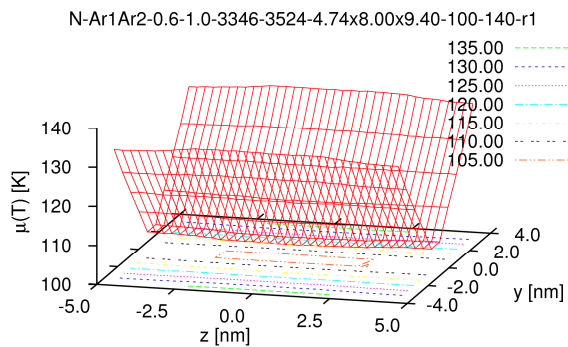
SigmaLocTempYZ.eps



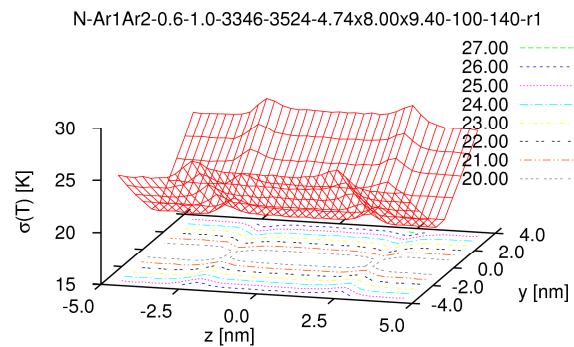
MeansLocTempYZ.eps



SigmaLocTempYZ.eps

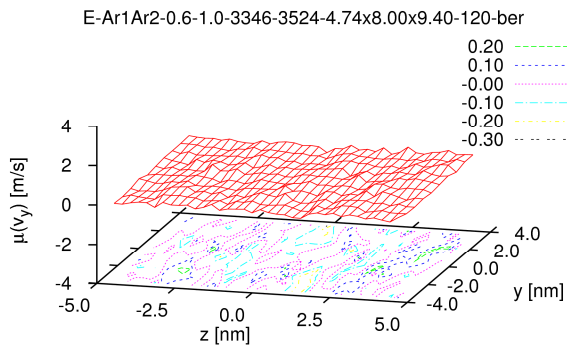


MeansLocTempYZ.eps

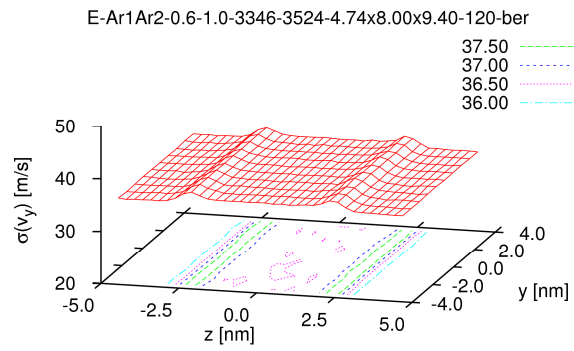


SigmaLocTempYZ.eps

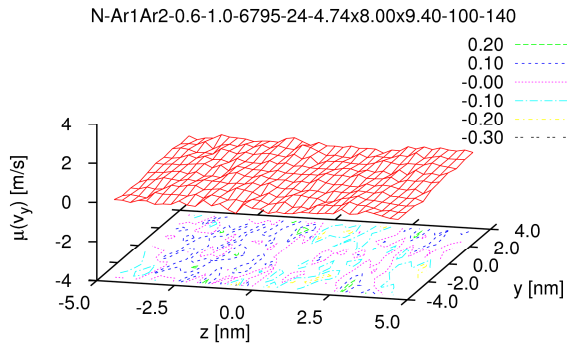
d) Temperatures



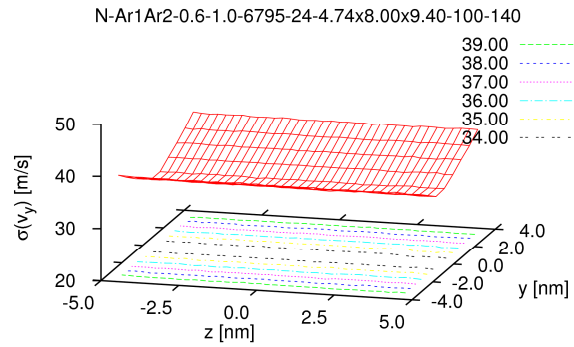
MeansLocYComVelYZ.eps



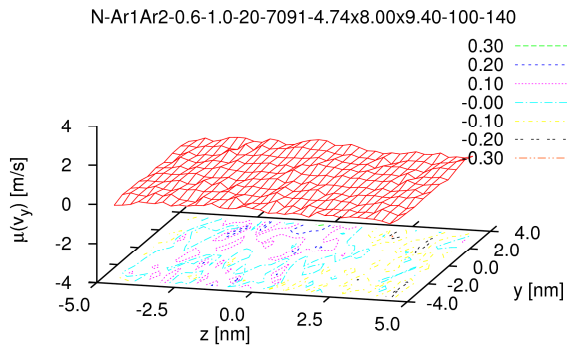
SigmaLocYComVelYZ.eps



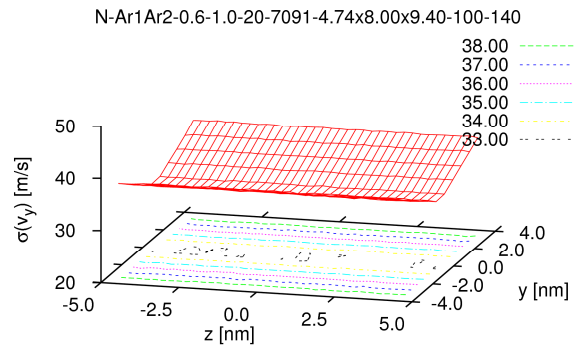
MeansLocYComVelYZ.eps



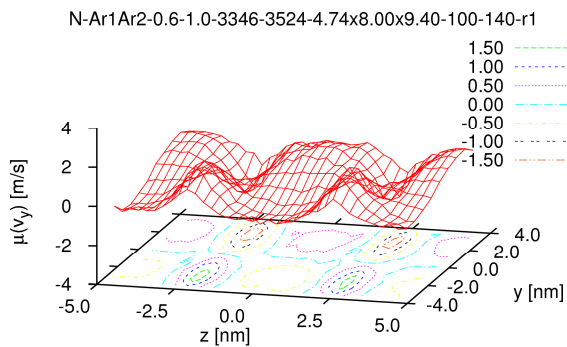
SigmaLocYComVelYZ.eps



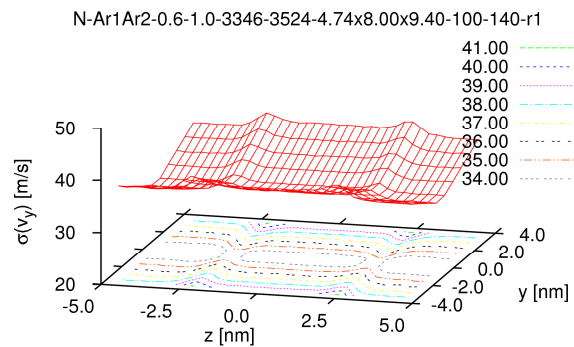
MeansLocYComVelYZ.eps



SigmaLocYComVelYZ.eps

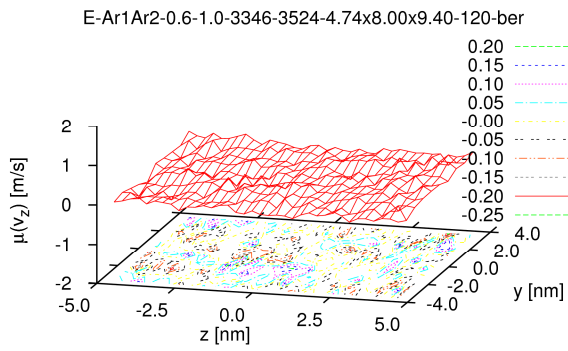


MeansLocYComVelYZ.eps

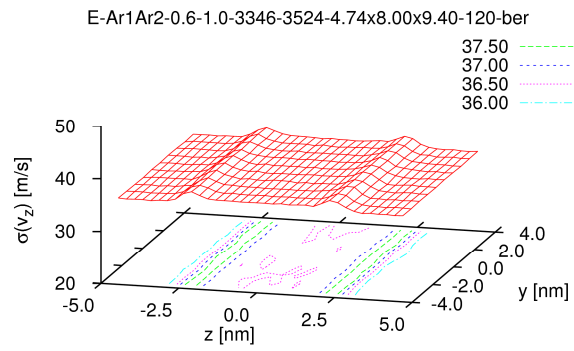


SigmaLocYComVelYZ.eps

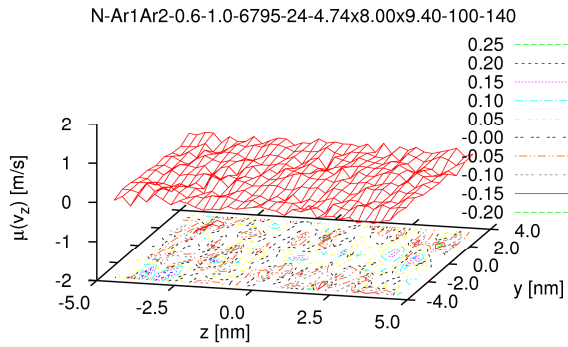
e) Com y-velocities



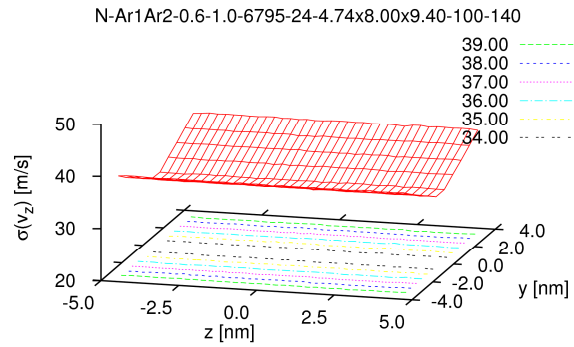
MeansLocZComVelYZ.eps



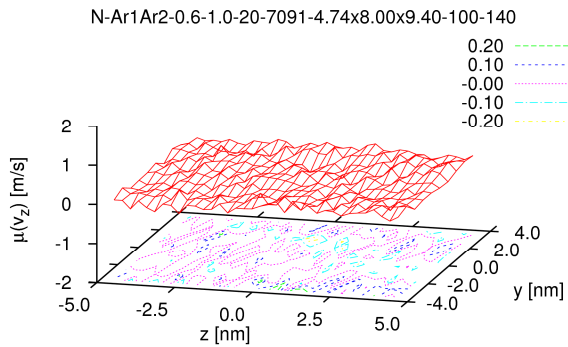
SigmaLocZComVelYZ.eps



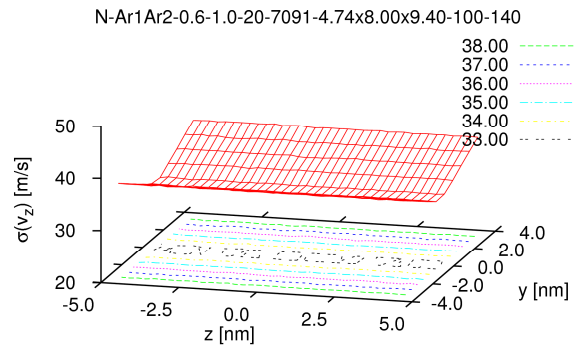
MeansLocZComVelYZ.eps



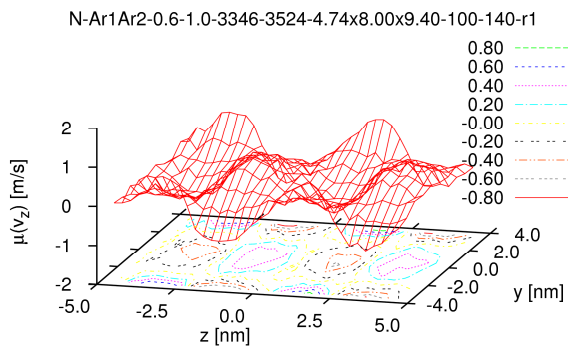
SigmaLocZComVelYZ.eps



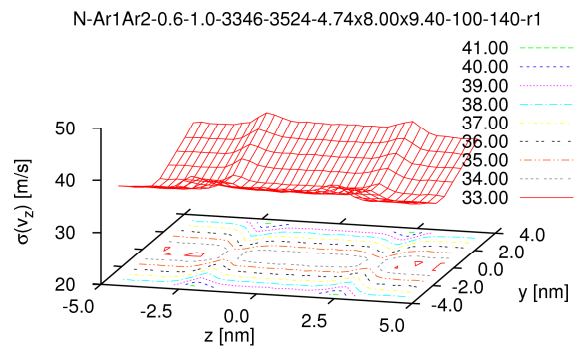
MeansLocZComVelYZ.eps



SigmaLocZComVelYZ.eps

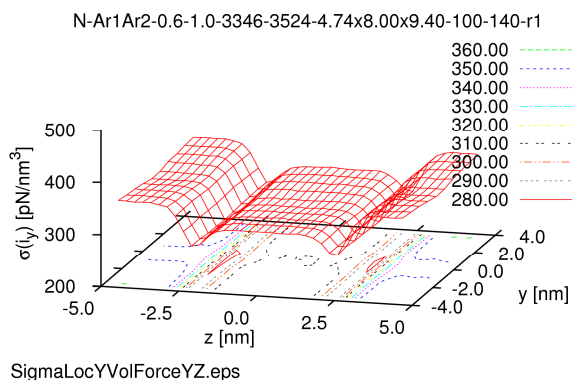
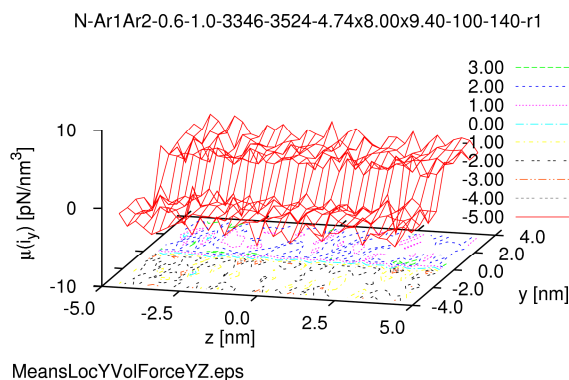
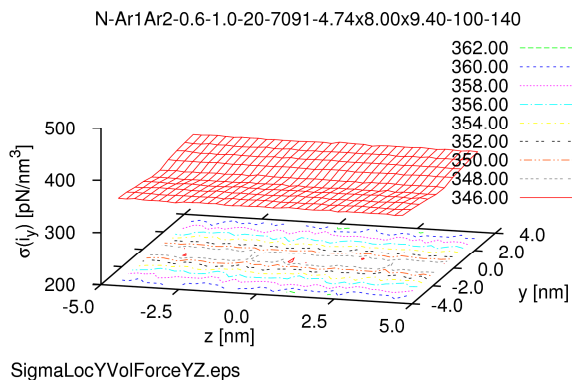
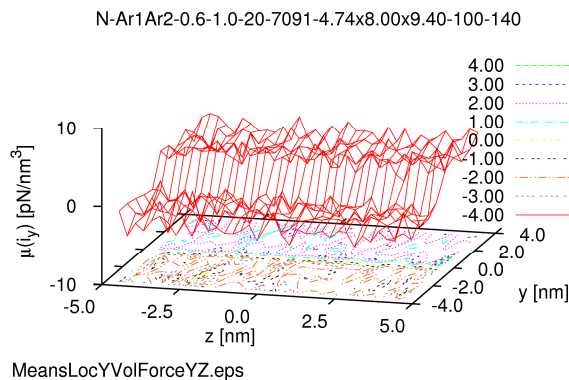
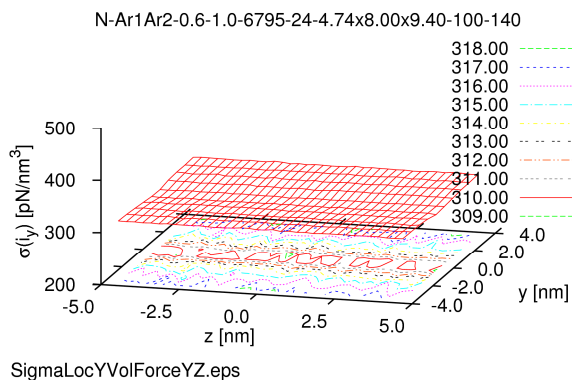
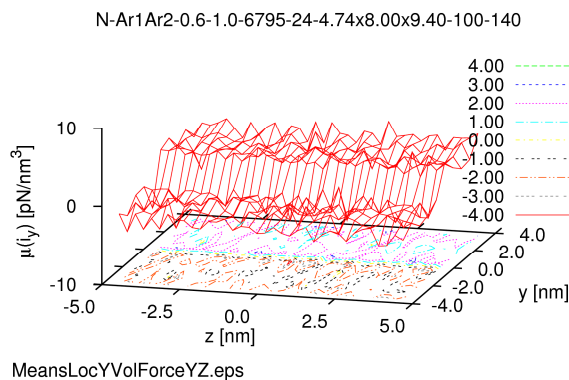
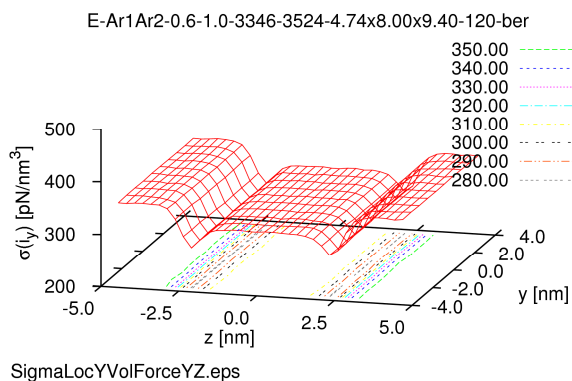
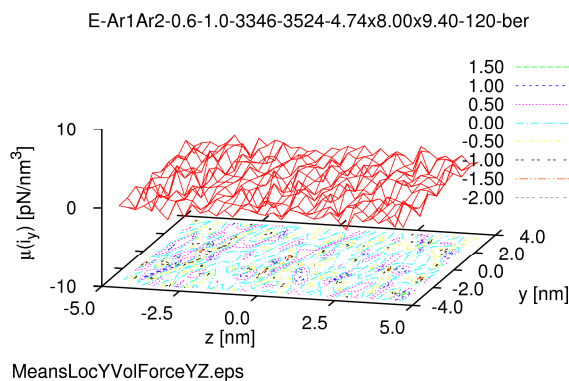


MeansLocZComVelYZ.eps

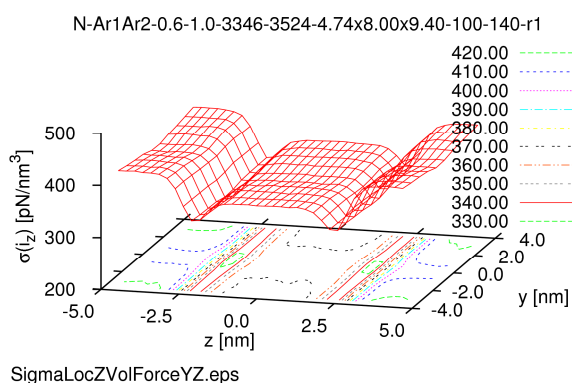
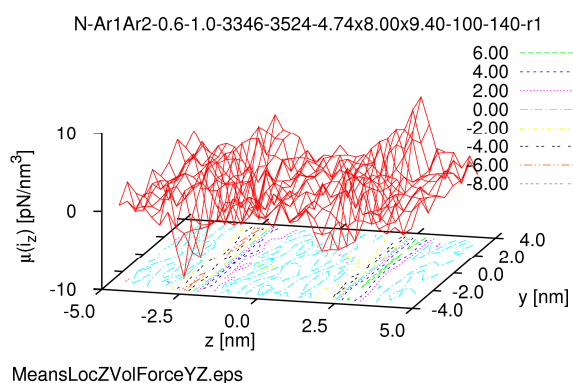
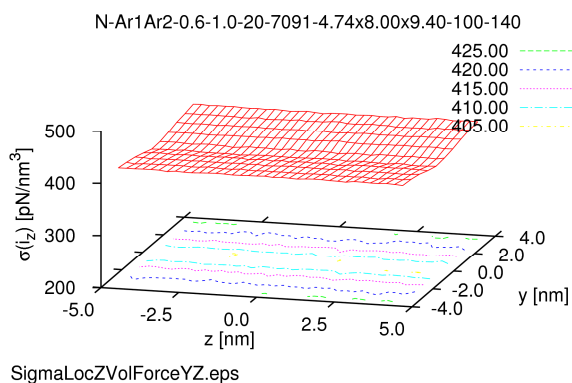
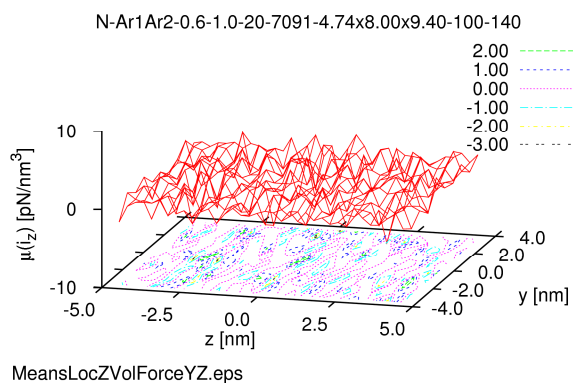
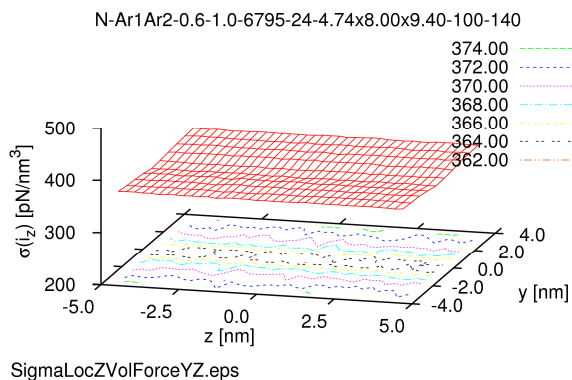
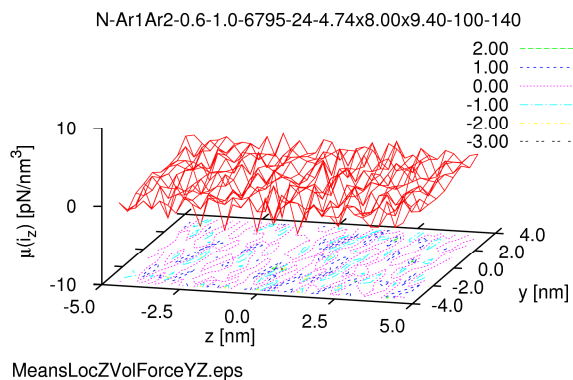
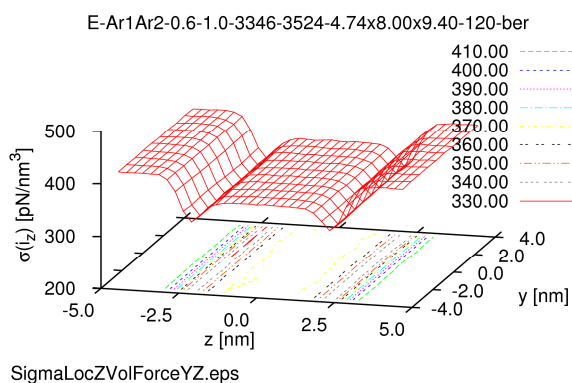
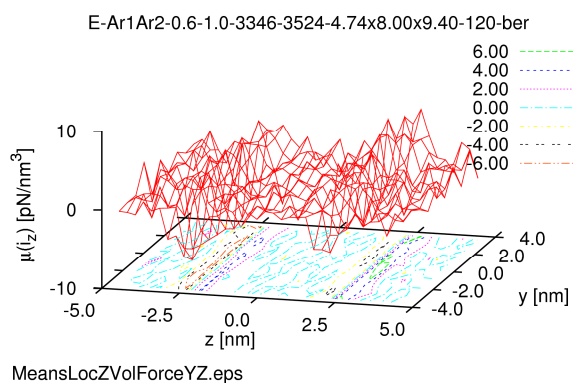


SigmaLocZComVelYZ.eps

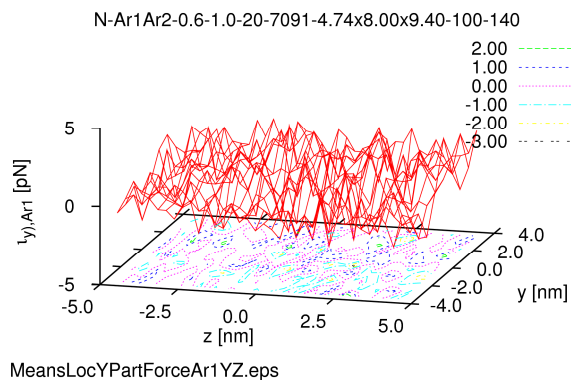
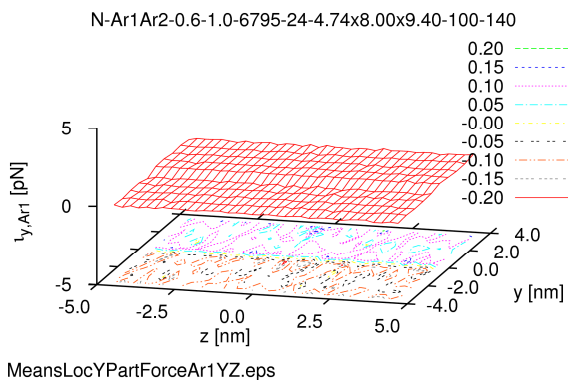
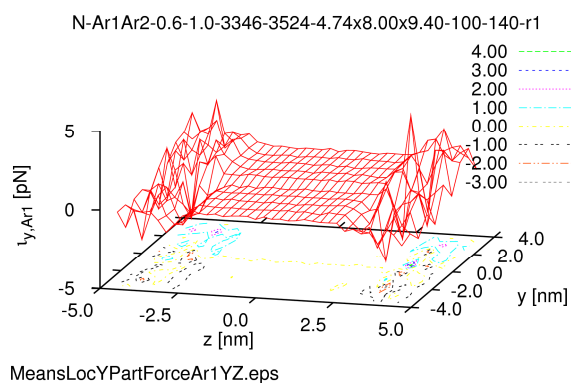
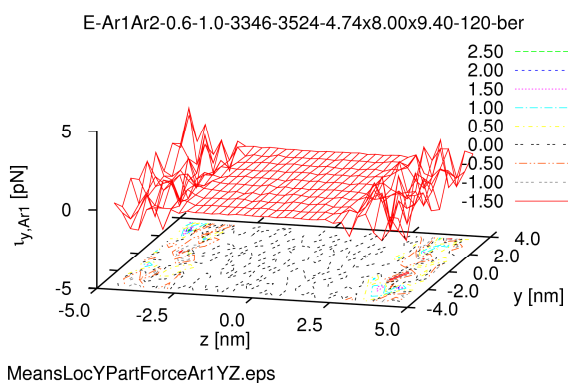
f) Com z-velocities



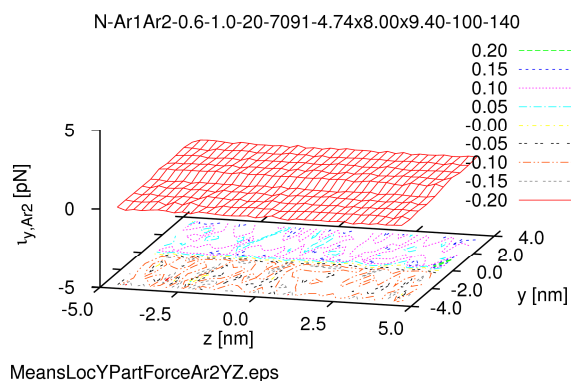
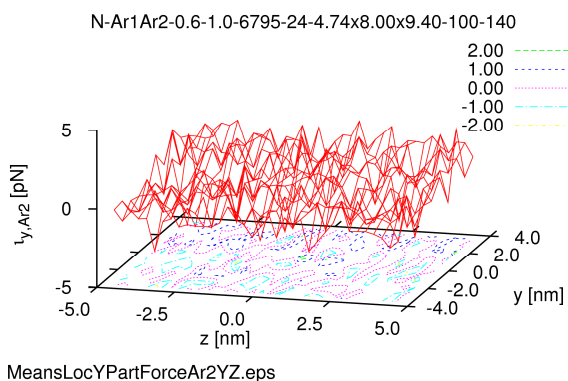
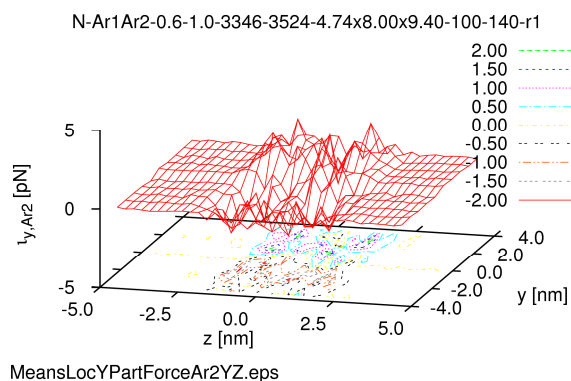
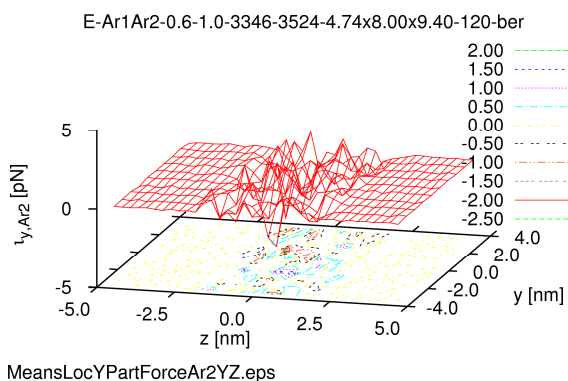
g) Interatomic volume y-forces



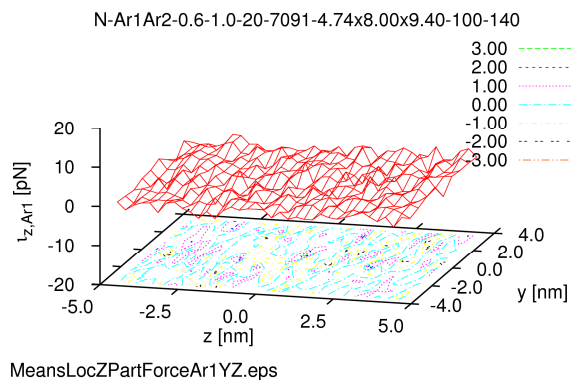
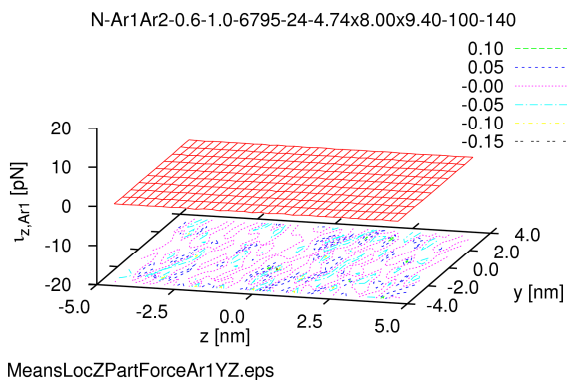
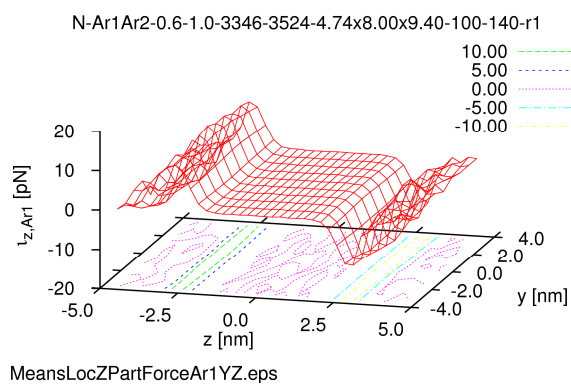
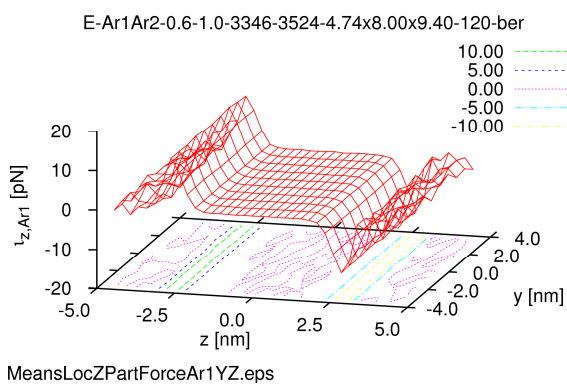
h) Interatomic volume z-forces



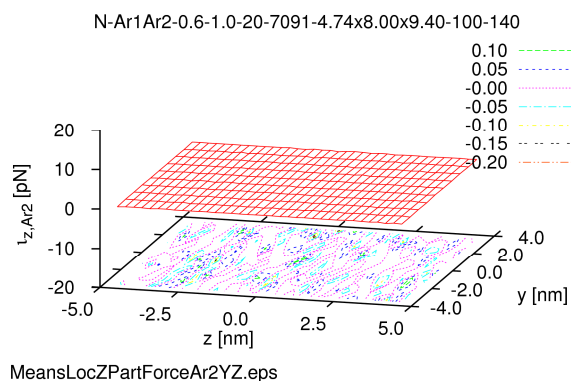
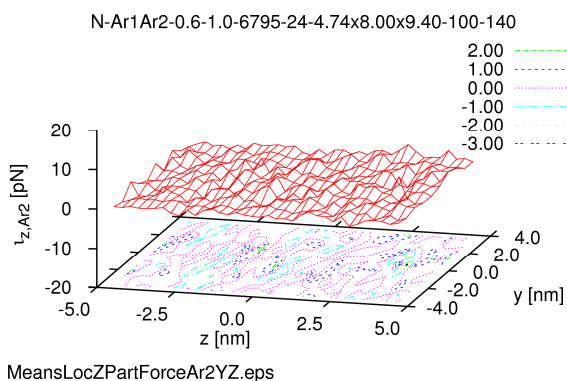
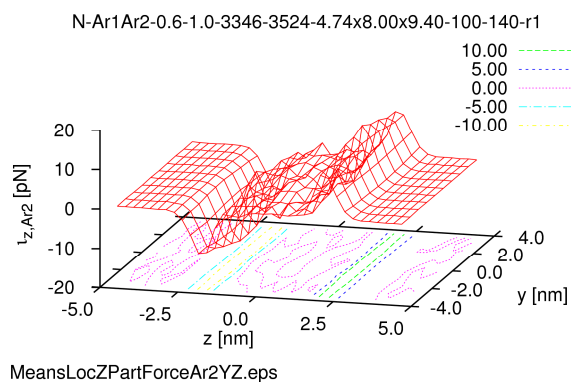
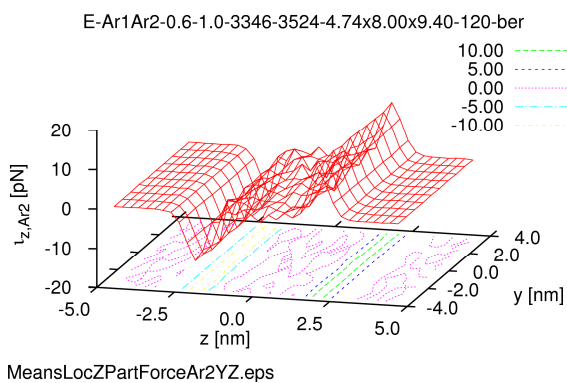
i) Interatomic ArA particle y-forces



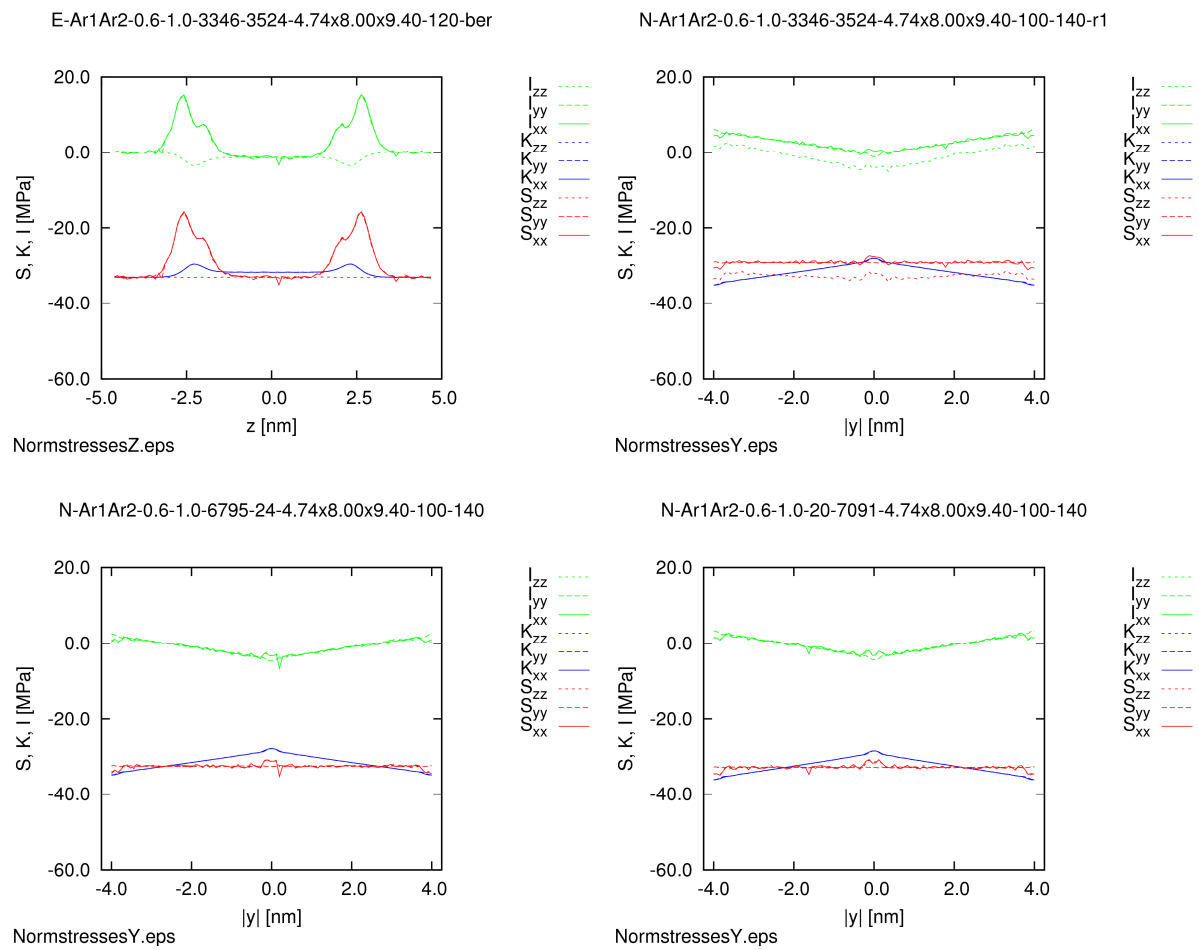
j) Interatomic ArB particle y-forces



k) Interatomic ArA particle z-forces



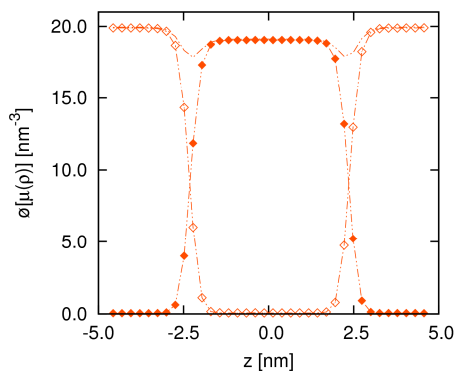
l) Interatomic ArB particle z-forces



m) Normal stresses

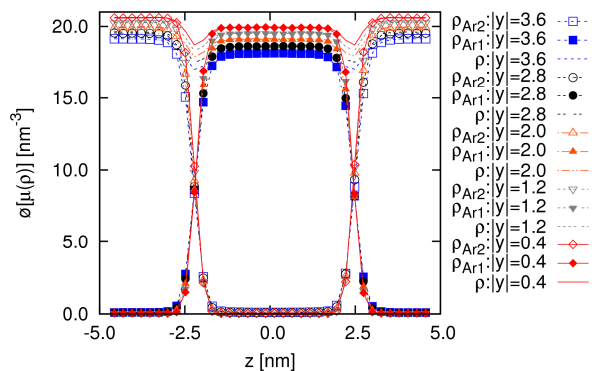
Figure 34 Detailed distributions of the local observables in the first heterophasic nonequilibrium interfacial system and its corresponding ones
N-Ar1Ar2-0.6-1.0-3346-3524-4.74x8.00x9.40-100-140-r1,
E-Ar1Ar2-0.6-1.0-3346-3524-4.74x8.00x9.40-120-ber,
N-Ar1Ar2-0.6-1.0-6795-24-4.74x8.00x9.40-100-140,
and N-Ar1Ar2-0.6-1.0-20-7091-4.74x8.00x9.40-100-140

E-Ar1Ar2-0.6-1.0-3346-3524-4.74x8.00x9.40-120-ber



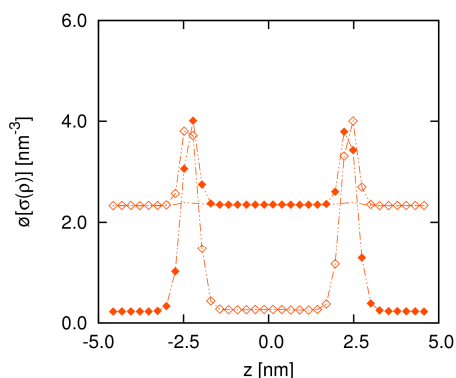
MeansLocDenZ.eps

N-Ar1Ar2-0.6-1.0-3346-3524-4.74x8.00x9.40-100-140-r1



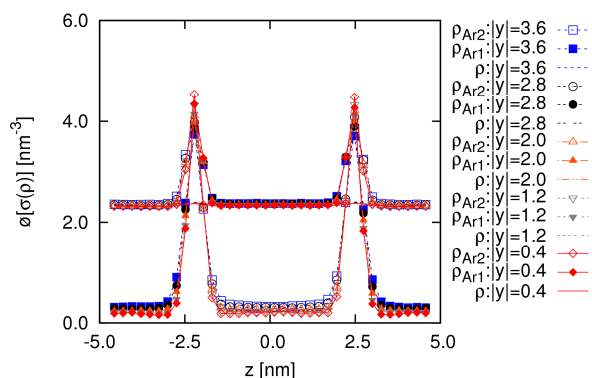
MeansLocDenZ.eps

E-Ar1Ar2-0.6-1.0-3346-3524-4.74x8.00x9.40-120-ber



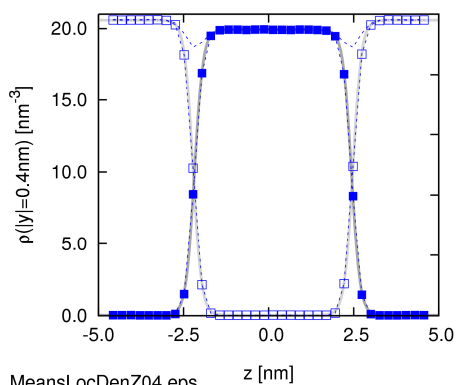
SigmaLocDenZ.eps

N-Ar1Ar2-0.6-1.0-3346-3524-4.74x8.00x9.40-100-140-r1



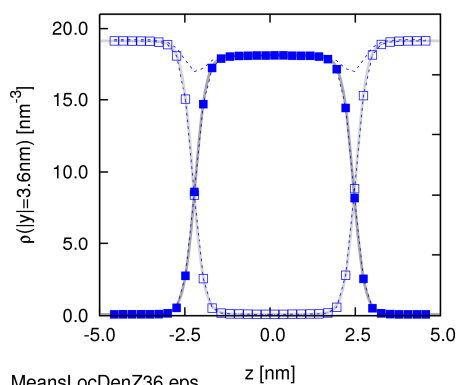
SigmaLocDenZ.eps

N-Ar1Ar2-0.6-1.0-3346-3524-4.74x8.00x9.40-100-140-r1



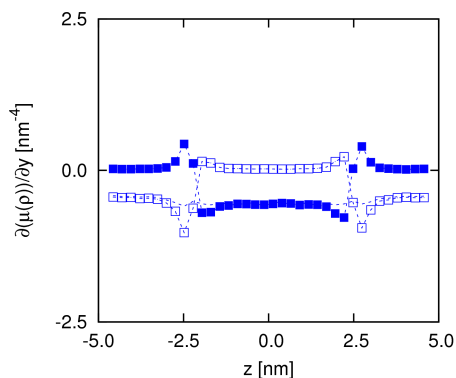
MeansLocDenZ04.eps

N-Ar1Ar2-0.6-1.0-3346-3524-4.74x8.00x9.40-100-140-r1



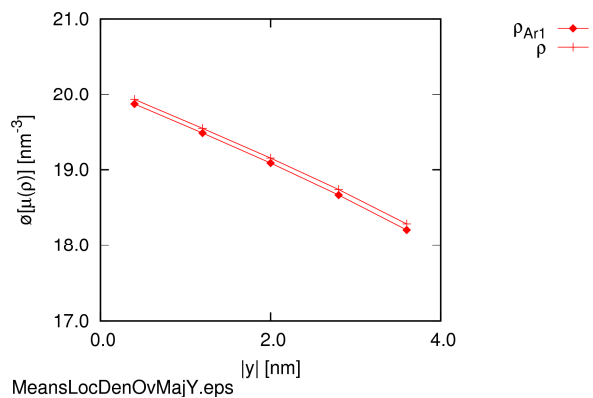
MeansLocDenZ36.eps

N-Ar1Ar2-0.6-1.0-3346-3524-4.74x8.00x9.40-100-140-r1

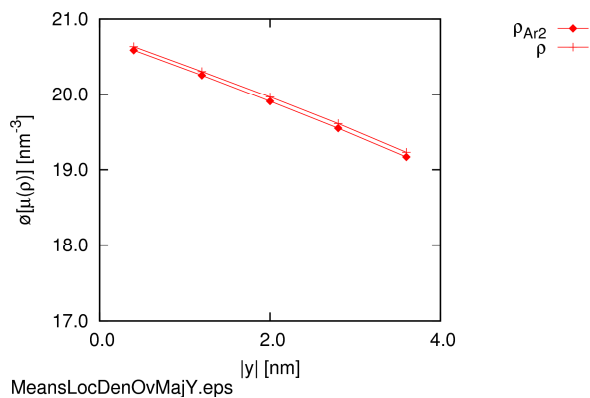


MeansLocDenYGradZ.eps

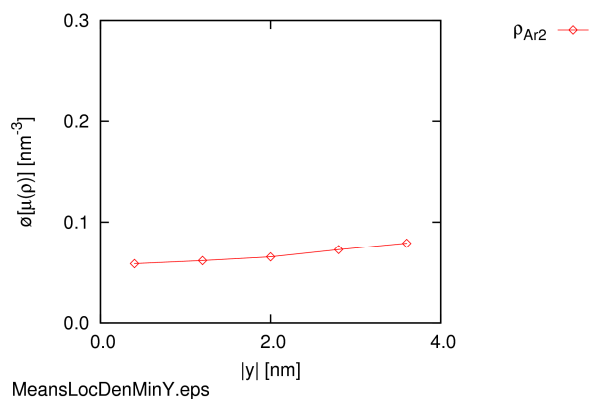
N-Ar1Ar2-0.6-1.0-6795-24-4.74x8.00x9.40-100-140



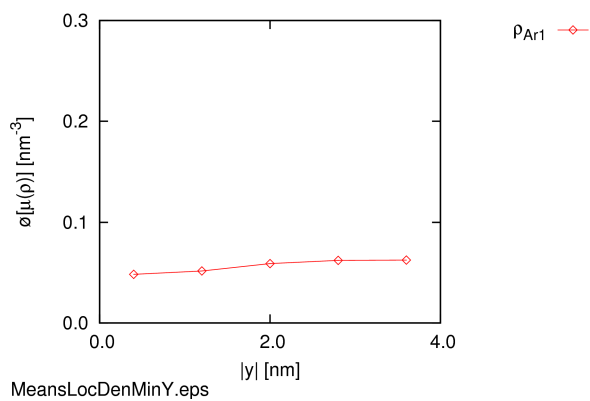
N-Ar1Ar2-0.6-1.0-20-7091-4.74x8.00x9.40-100-140



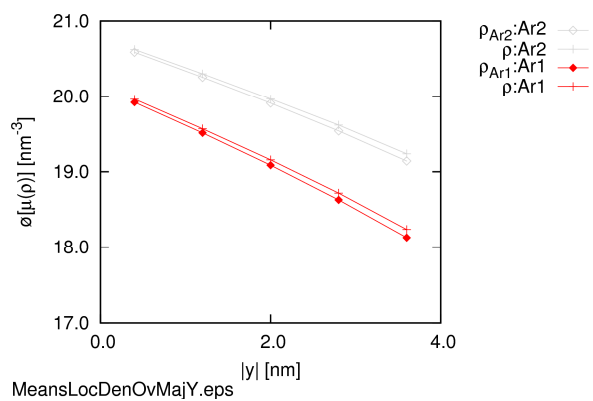
N-Ar1Ar2-0.6-1.0-6795-24-4.74x8.00x9.40-100-140



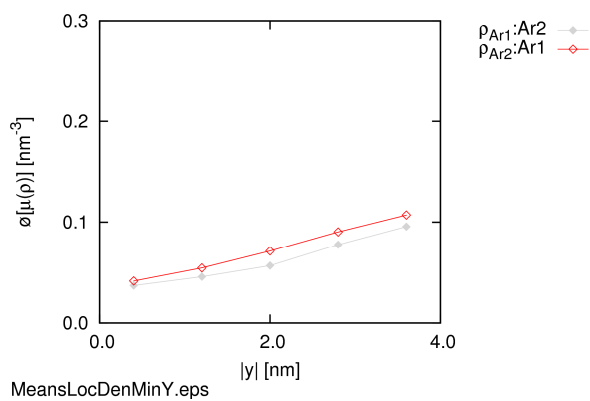
N-Ar1Ar2-0.6-1.0-20-7091-4.74x8.00x9.40-100-140



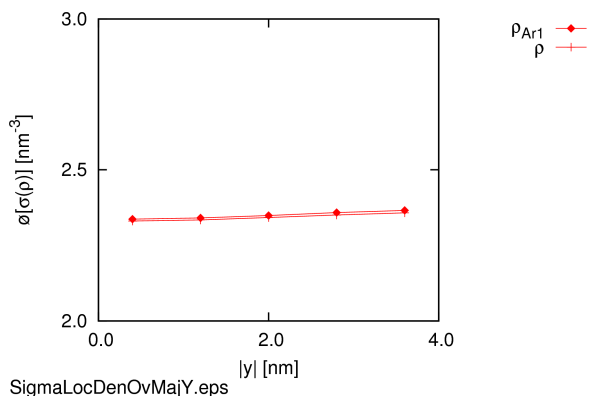
N-Ar1Ar2-0.6-1.0-3346-3524-4.74x8.00x9.40-100-140-r1



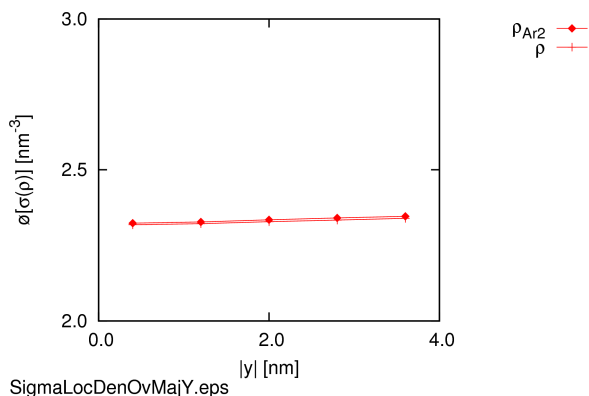
N-Ar1Ar2-0.6-1.0-3346-3524-4.74x8.00x9.40-100-140-r1



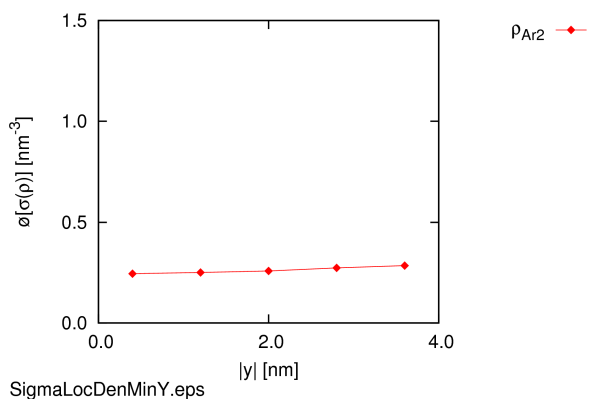
N-Ar1Ar2-0.6-1.0-6795-24-4.74x8.00x9.40-100-140



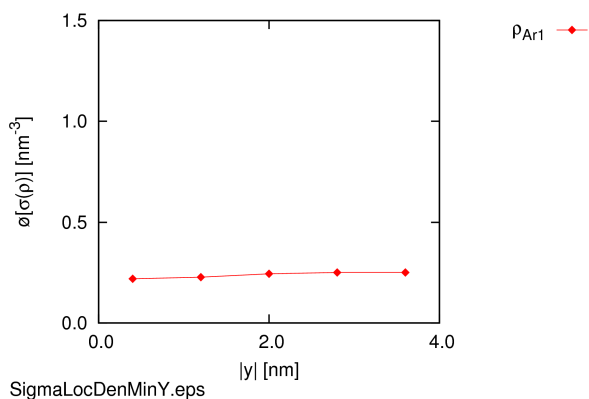
N-Ar1Ar2-0.6-1.0-20-7091-4.74x8.00x9.40-100-140



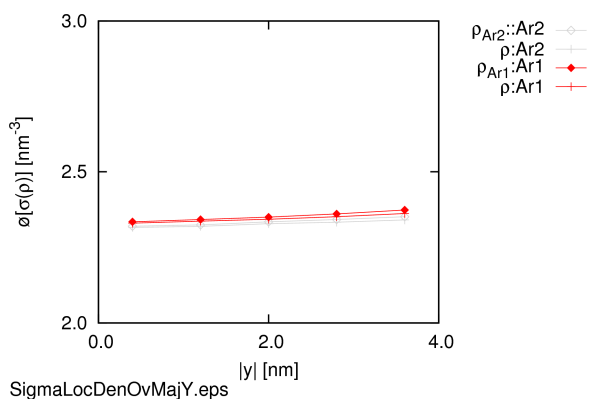
N-Ar1Ar2-0.6-1.0-6795-24-4.74x8.00x9.40-100-140



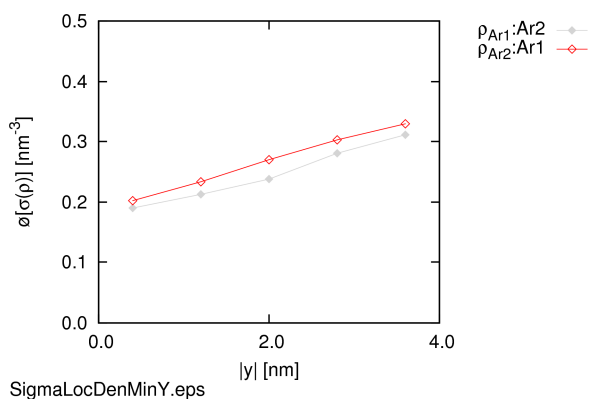
N-Ar1Ar2-0.6-1.0-20-7091-4.74x8.00x9.40-100-140



N-Ar1Ar2-0.6-1.0-3346-3524-4.74x8.00x9.40-100-140-r1

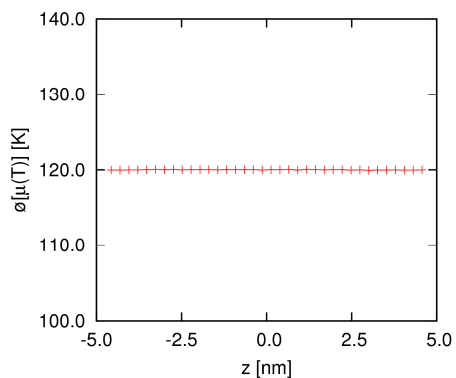


N-Ar1Ar2-0.6-1.0-3346-3524-4.74x8.00x9.40-100-140-r1



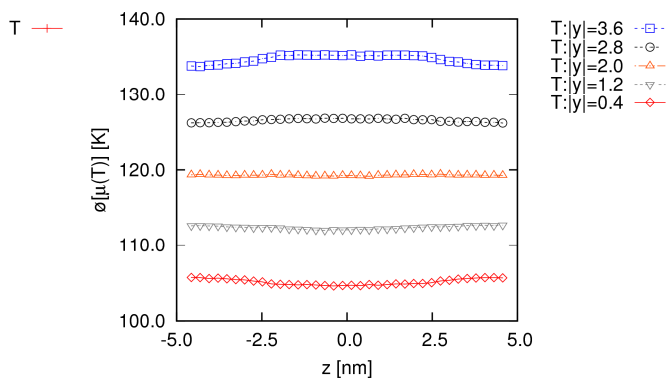
a) Densities

E-Ar1Ar2-0.6-1.0-3346-3524-4.74x8.00x9.40-120-ber



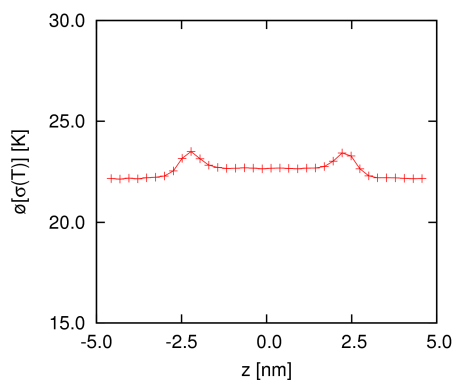
MeansLocTempZ.eps

N-Ar1Ar2-0.6-1.0-3346-3524-4.74x8.00x9.40-100-140-r1



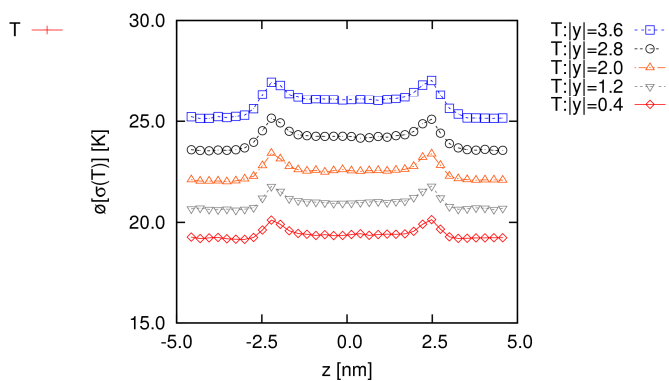
MeansLocTempZ.eps

E-Ar1Ar2-0.6-1.0-3346-3524-4.74x8.00x9.40-120-ber



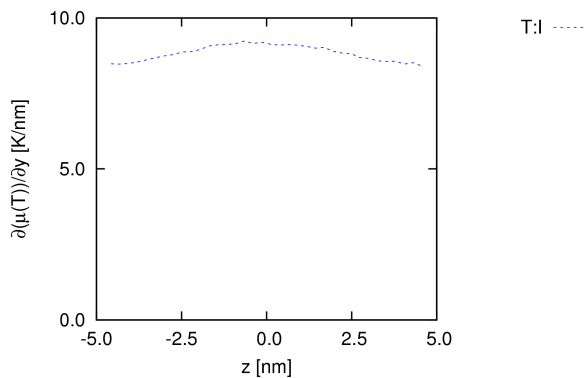
SigmaLocTempZ.eps

N-Ar1Ar2-0.6-1.0-3346-3524-4.74x8.00x9.40-100-140-r1

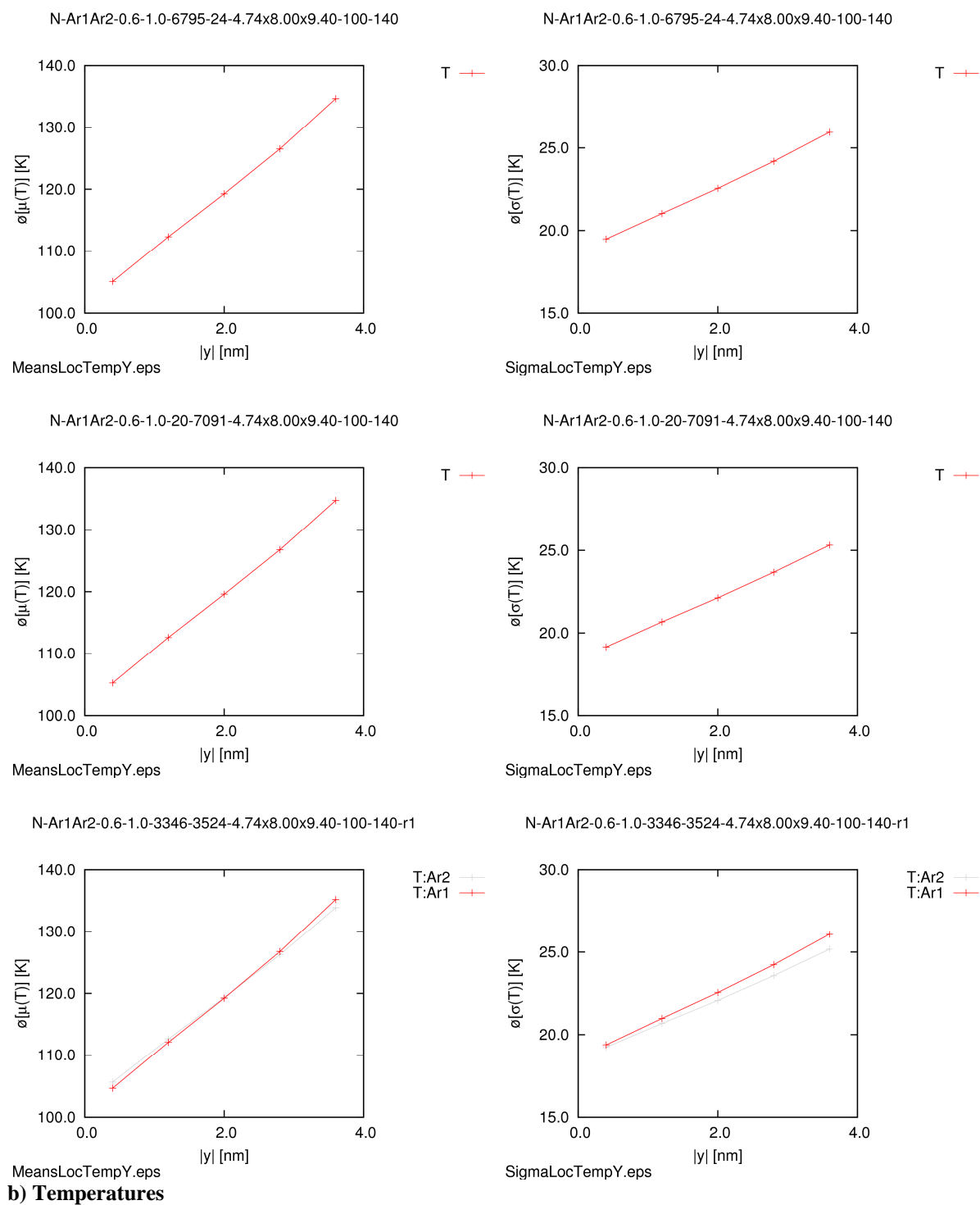


SigmaLocTempZ.eps

N-Ar1Ar2-0.6-1.0-3346-3524-4.74x8.00x9.40-100-140-r1

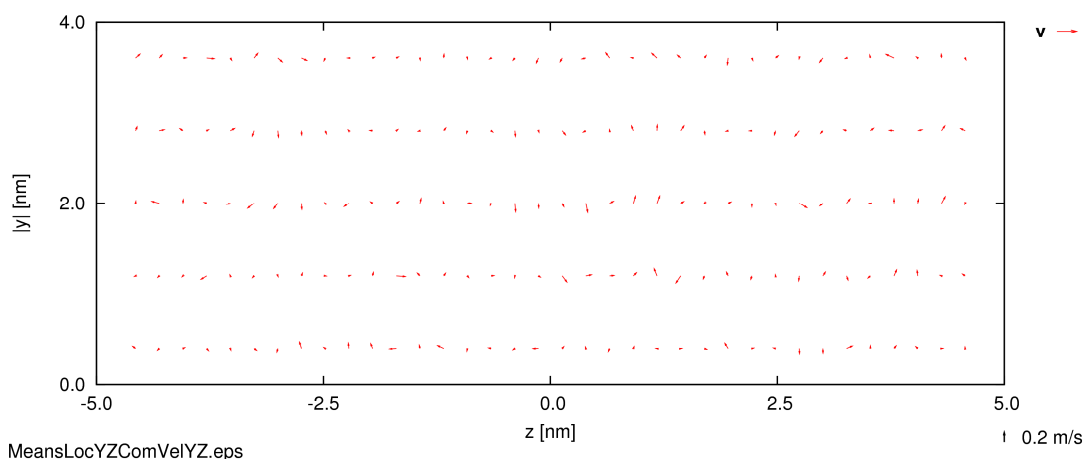


MeansLocTempYGradZ.eps

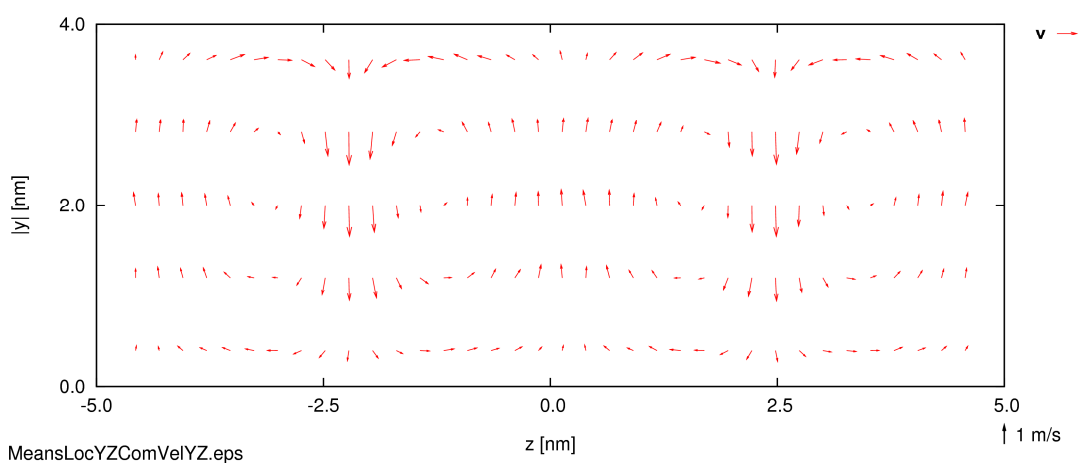


b) Temperatures

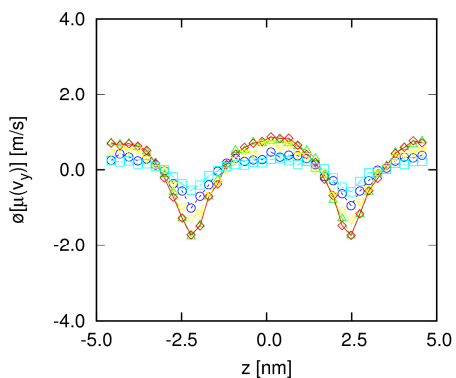
E-Ar1Ar2-0.6-1.0-3346-3524-4.74x8.00x9.40-120-ber



N-Ar1Ar2-0.6-1.0-3346-3524-4.74x8.00x9.40-100-140-r1

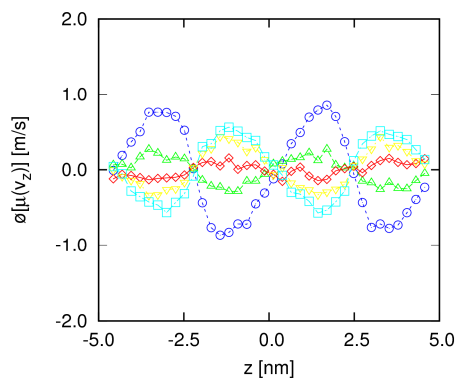


N-Ar1Ar2-0.6-1.0-3346-3524-4.74x8.00x9.40-100-140-r1



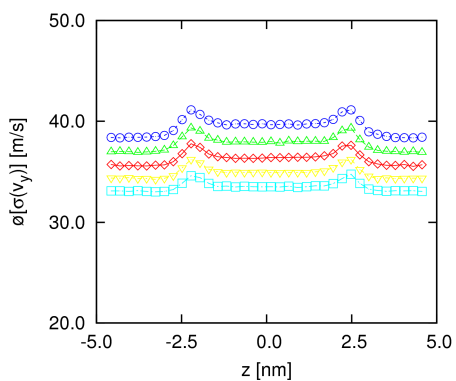
MeansLocYComVelZ.eps

N-Ar1Ar2-0.6-1.0-3346-3524-4.74x8.00x9.40-100-140-r1



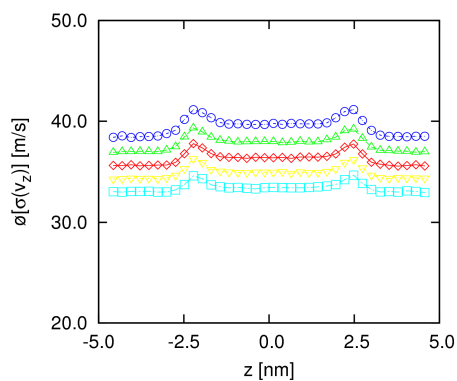
MeansLocZComVelZ.eps

N-Ar1Ar2-0.6-1.0-3346-3524-4.74x8.00x9.40-100-140-r1

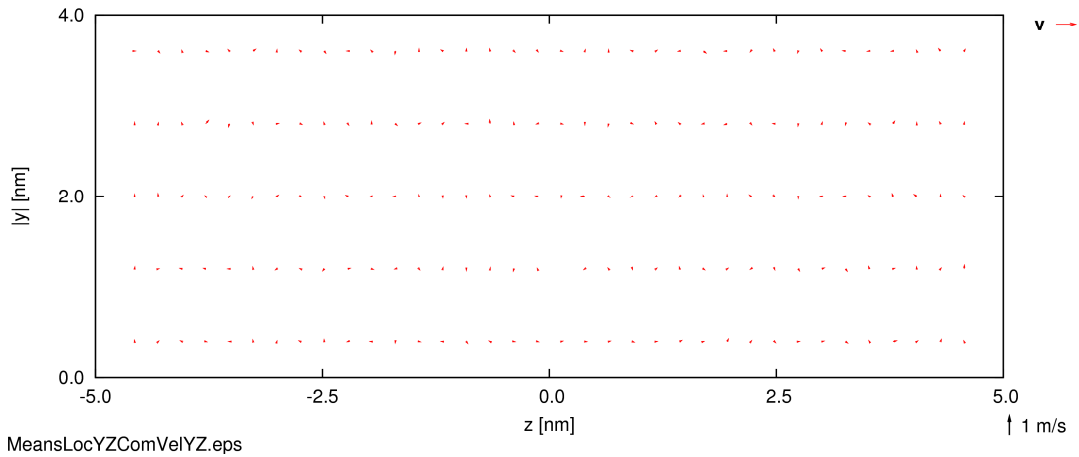


SigmaLocYComVelZ.eps

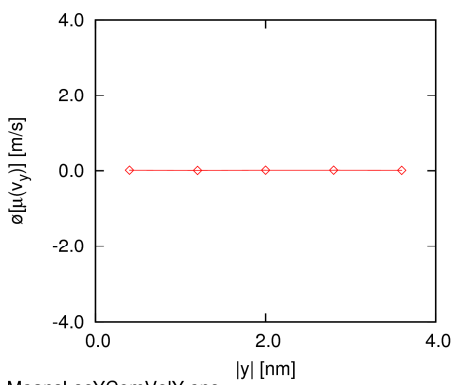
N-Ar1Ar2-0.6-1.0-3346-3524-4.74x8.00x9.40-100-140-r1



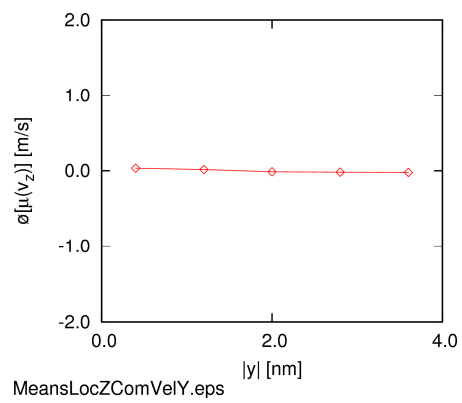
SigmaLocZComVelZ.eps



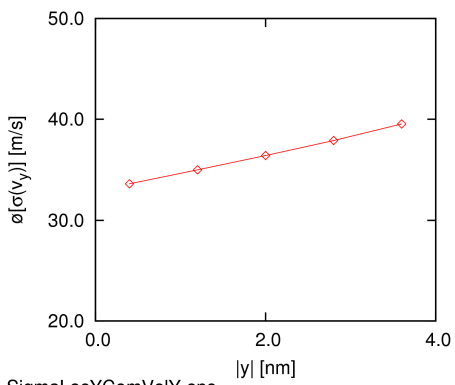
N-Ar1Ar2-0.6-1.0-6795-24-4.74x8.00x9.40-100-140



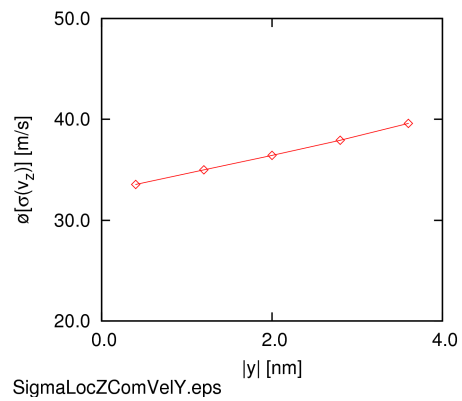
N-Ar1Ar2-0.6-1.0-6795-24-4.74x8.00x9.40-100-140

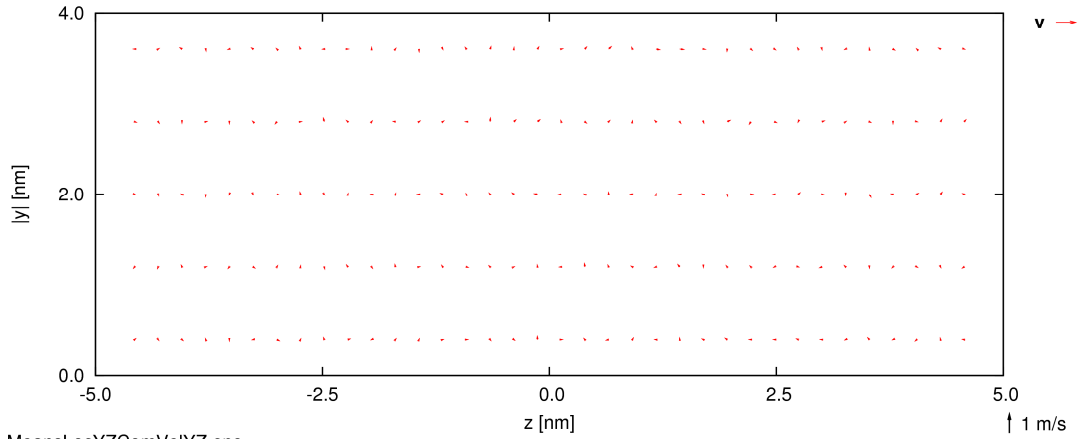


N-Ar1Ar2-0.6-1.0-6795-24-4.74x8.00x9.40-100-140

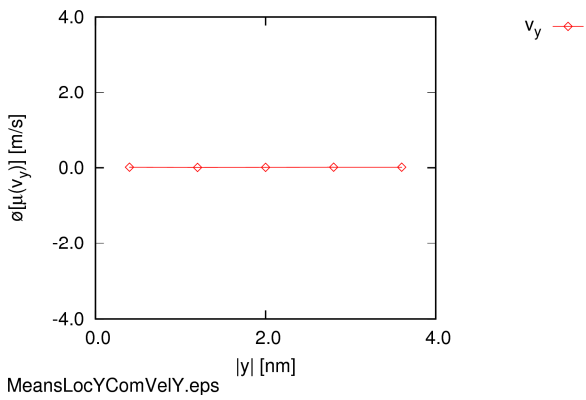


N-Ar1Ar2-0.6-1.0-6795-24-4.74x8.00x9.40-100-140

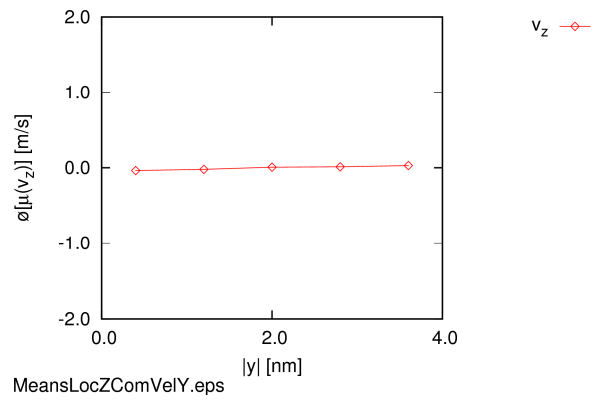




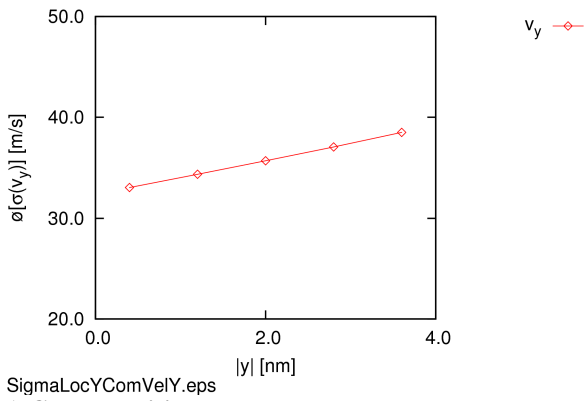
N-Ar1Ar2-0.6-1.0-20-7091-4.74x8.00x9.40-100-140



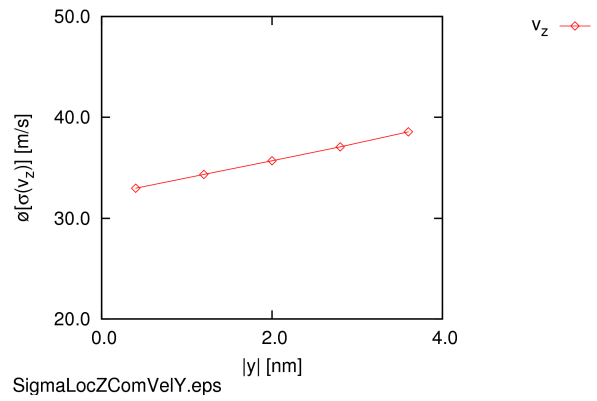
N-Ar1Ar2-0.6-1.0-20-7091-4.74x8.00x9.40-100-140



N-Ar1Ar2-0.6-1.0-20-7091-4.74x8.00x9.40-100-140

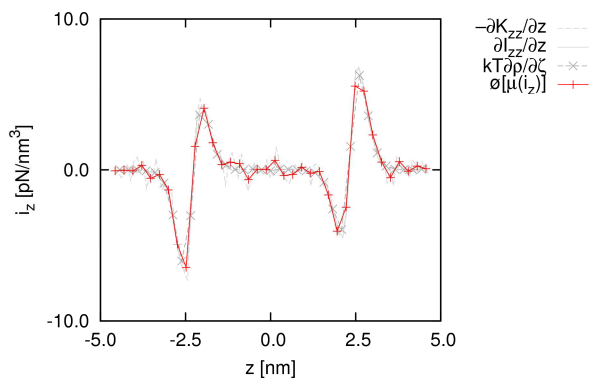


N-Ar1Ar2-0.6-1.0-20-7091-4.74x8.00x9.40-100-140



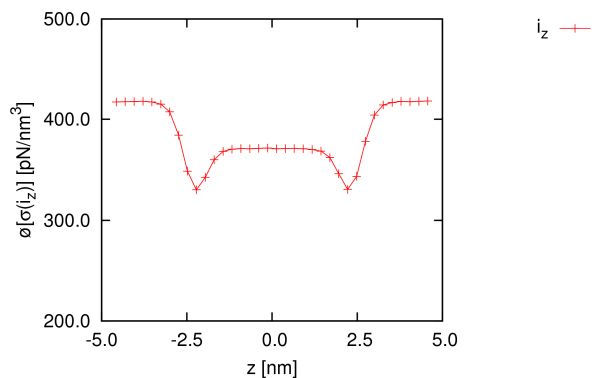
c) Com velocities

E-Ar1Ar2-0.6-1.0-3346-3524-4.74x8.00x9.40-120-ber



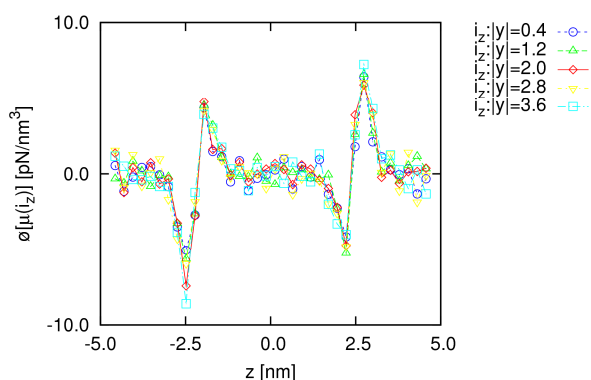
MeansLocZVolForceZ2.eps

E-Ar1Ar2-0.6-1.0-3346-3524-4.74x8.00x9.40-120-ber



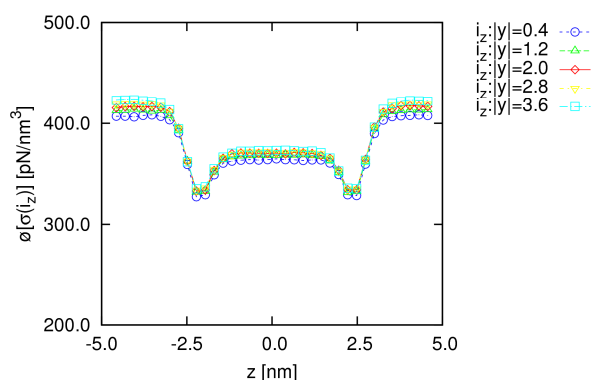
SigmaLocZVolForceZ.eps

N-Ar1Ar2-0.6-1.0-3346-3524-4.74x8.00x9.40-100-140-r1



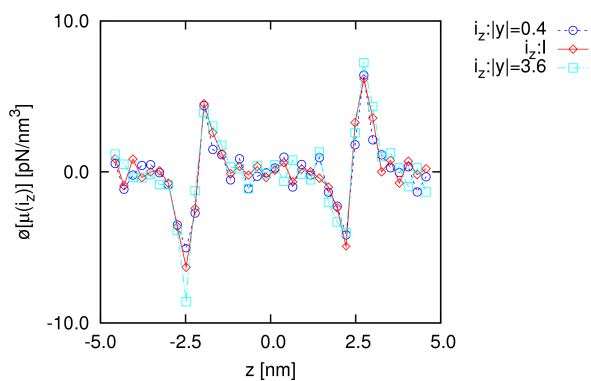
MeansLocZVolForceZ.eps

N-Ar1Ar2-0.6-1.0-3346-3524-4.74x8.00x9.40-100-140-r1



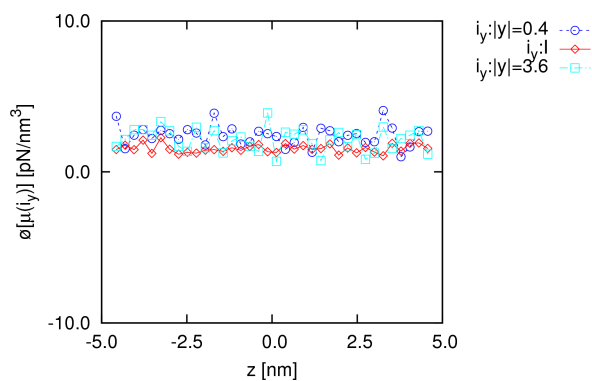
SigmaLocZVolForceZ.eps

N-Ar1Ar2-0.6-1.0-3346-3524-4.74x8.00x9.40-100-140-r1



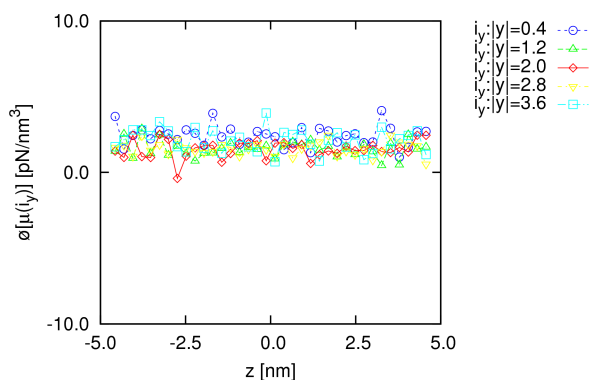
MeansLocZVolForceZ2.eps

N-Ar1Ar2-0.6-1.0-3346-3524-4.74x8.00x9.40-100-140-r1



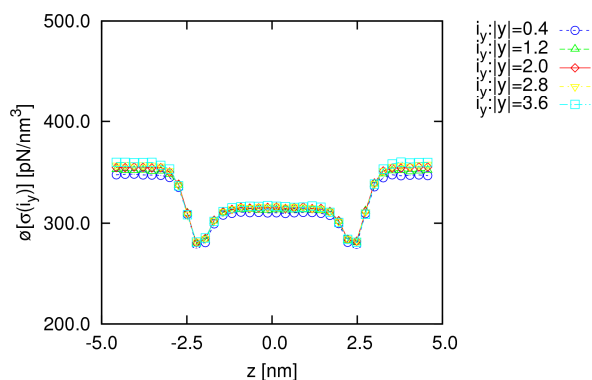
MeansLocYVolForceZ2.eps

N-Ar1Ar2-0.6-1.0-3346-3524-4.74x8.00x9.40-100-140-r1



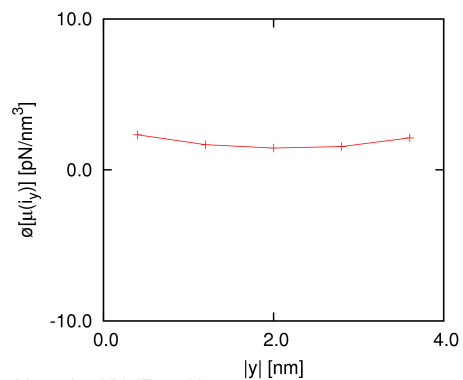
MeansLocYVolForceZ.eps

N-Ar1Ar2-0.6-1.0-3346-3524-4.74x8.00x9.40-100-140-r1



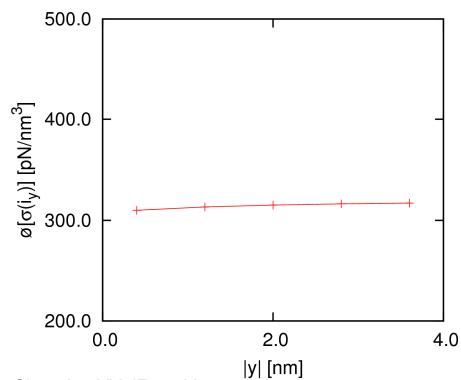
SigmaLocYVolForceZ.eps

N-Ar1Ar2-0.6-1.0-6795-24-4.74x8.00x9.40-100-140



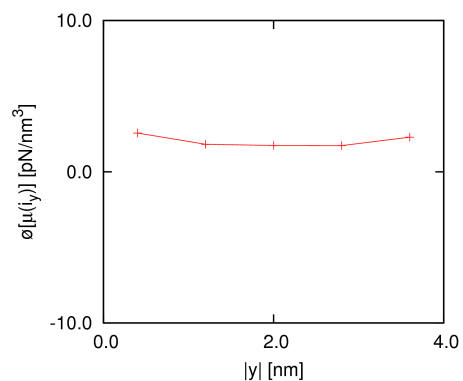
MeansLocYVolForceY.eps

N-Ar1Ar2-0.6-1.0-6795-24-4.74x8.00x9.40-100-140



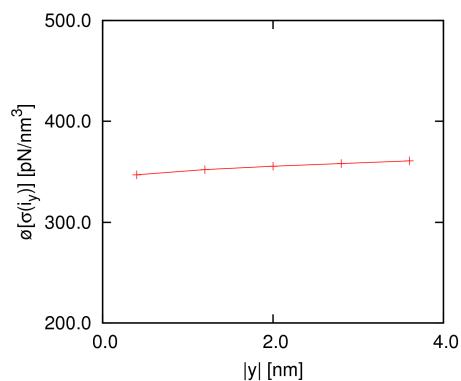
SigmaLocYVolForceY.eps

N-Ar1Ar2-0.6-1.0-20-7091-4.74x8.00x9.40-100-140



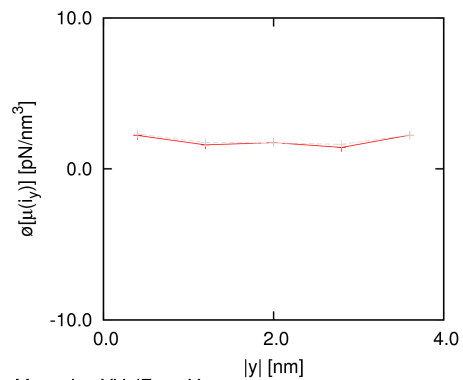
MeansLocYVolForceY.eps

N-Ar1Ar2-0.6-1.0-20-7091-4.74x8.00x9.40-100-140



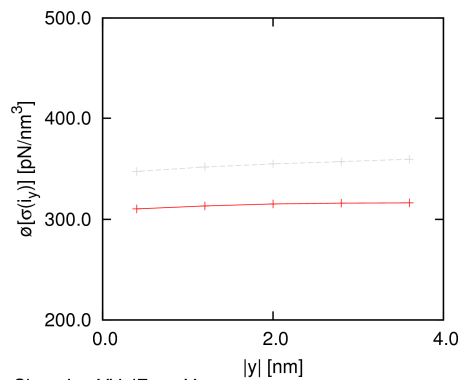
SigmaLocYVolForceY.eps

N-Ar1Ar2-0.6-1.0-3346-3524-4.74x8.00x9.40-100-140-r1



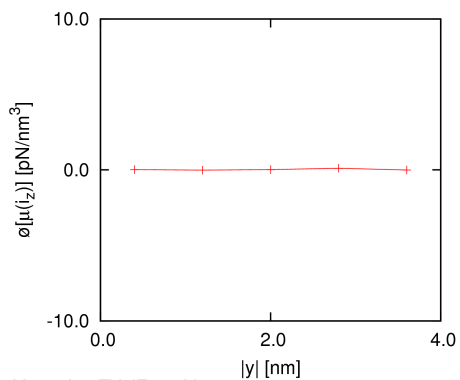
MeansLocYVolForceY.eps

N-Ar1Ar2-0.6-1.0-3346-3524-4.74x8.00x9.40-100-140-r1

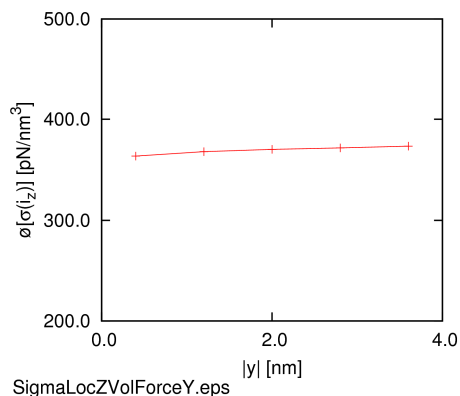


SigmaLocYVolForceY.eps

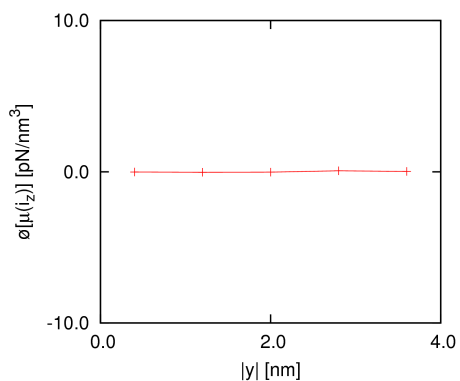
N-Ar1Ar2-0.6-1.0-6795-24-4.74x8.00x9.40-100-140



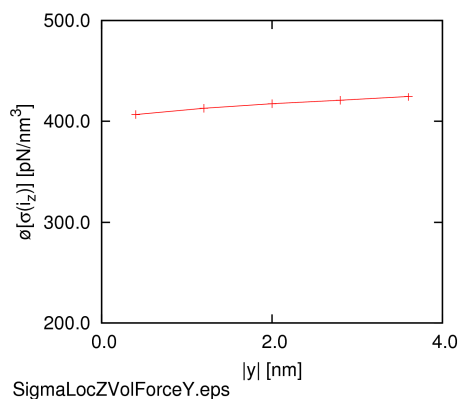
N-Ar1Ar2-0.6-1.0-6795-24-4.74x8.00x9.40-100-140



N-Ar1Ar2-0.6-1.0-20-7091-4.74x8.00x9.40-100-140

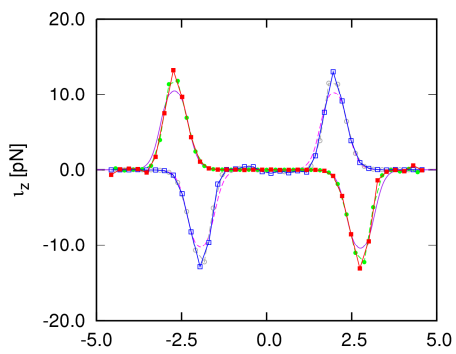


N-Ar1Ar2-0.6-1.0-20-7091-4.74x8.00x9.40-100-140



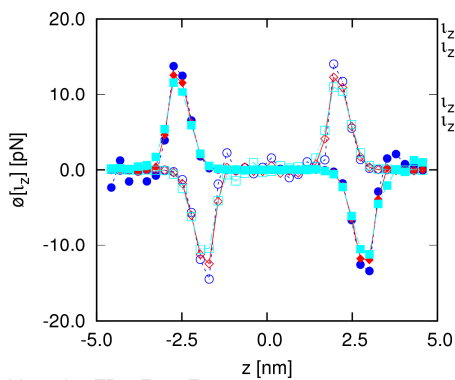
d) Volume forces

E-Ar1Ar2-0.6-1.0-3346-3524-4.74x8.00x9.40-120-ber



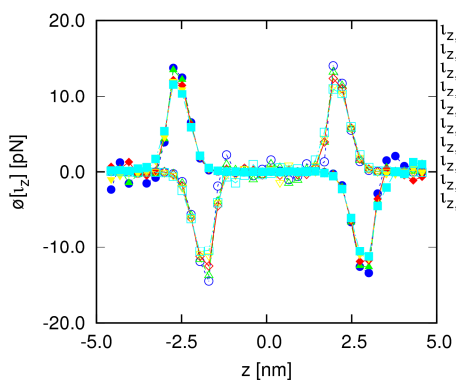
MeansLocZPartForceZ2.eps^z [nm]

N-Ar1Ar2-0.6-1.0-3346-3524-4.74x8.00x9.40-100-140-r1



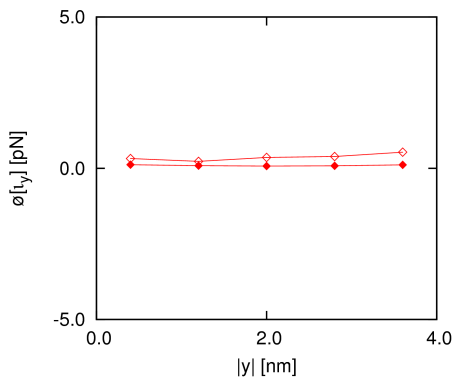
MeansLocZPartForceZ2.eps

N-Ar1Ar2-0.6-1.0-3346-3524-4.74x8.00x9.40-100-140-r1



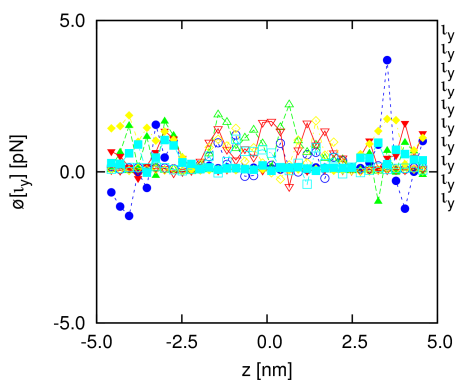
MeansLocZPartForceZ2.eps

N-Ar1Ar2-0.6-1.0-6795-24-4.74x8.00x9.40-100-140



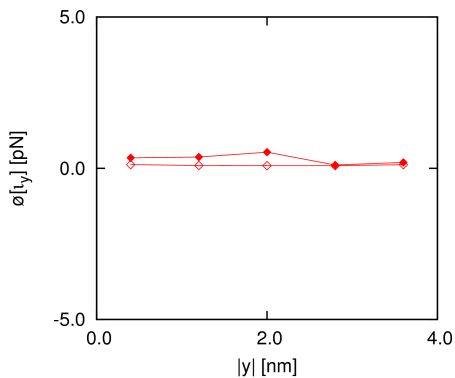
MeansLocYPartForceY2.eps

N-Ar1Ar2-0.6-1.0-3346-3524-4.74x8.00x9.40-100-140-r1



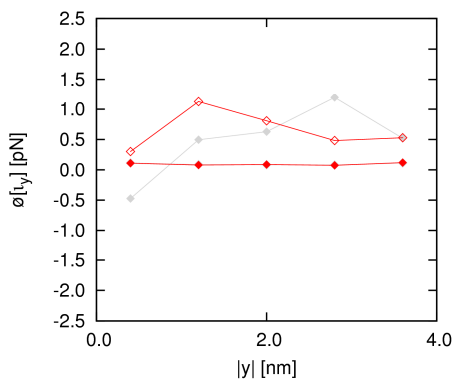
MeansLocYPartForceZ2.eps

N-Ar1Ar2-0.6-1.0-20-7091-4.74x8.00x9.40-100-140



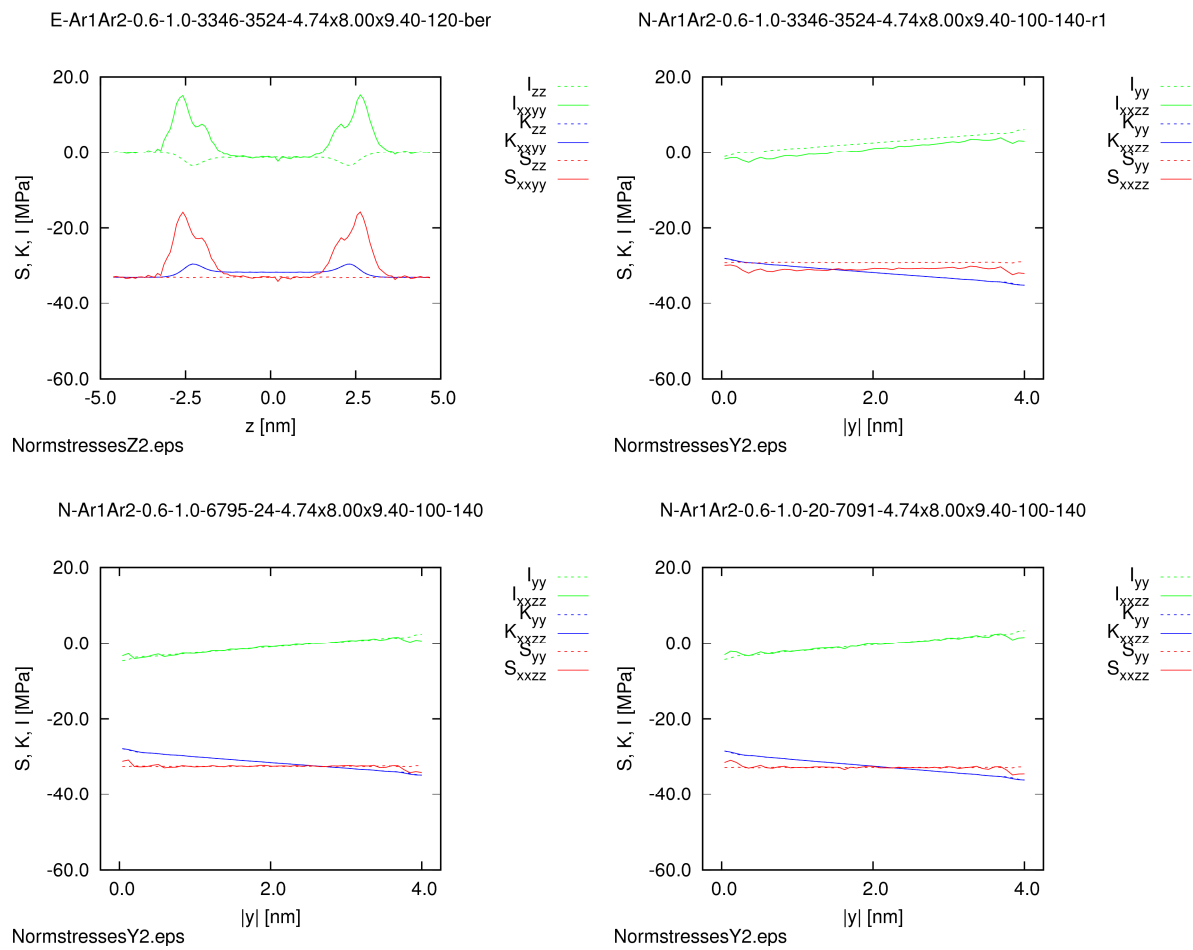
MeansLocYPartForceY2.eps

N-Ar1Ar2-0.6-1.0-3346-3524-4.74x8.00x9.40-100-140-r1



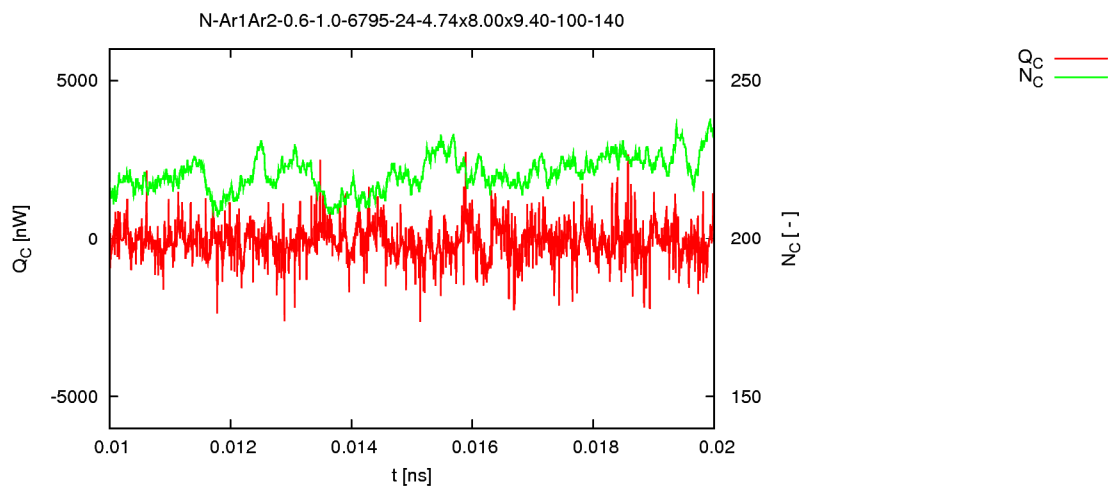
MeansLocYPartForceY2.eps

e) Particle forces



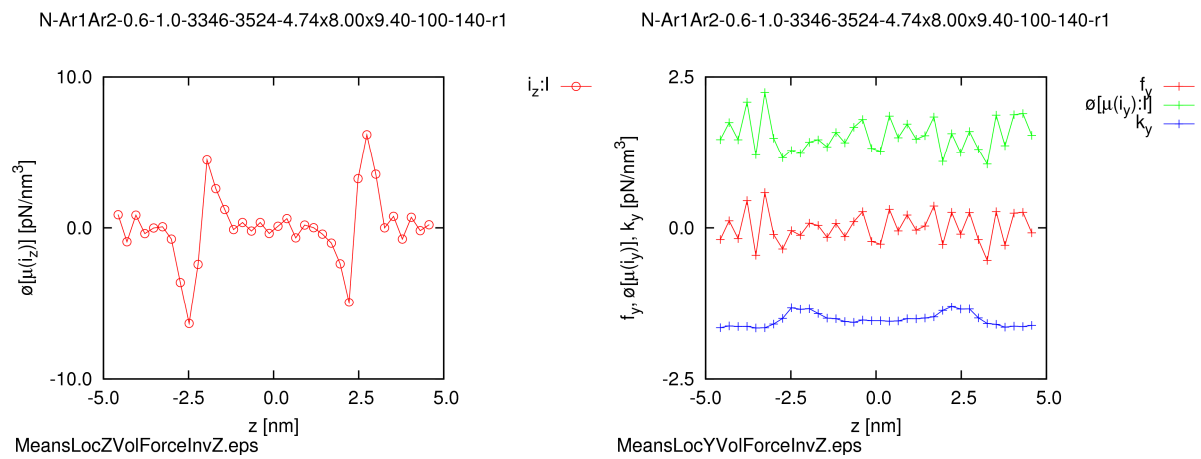
f) Normal stresses

Figure 35 Spatially averaged distributions of the local observables in the first heterophasic nonequilibrium interfacial system and its corresponding ones
N-Ar1Ar2-0.6-1.0-3346-3524-4.74x8.00x9.40-100-140-r1,
E-Ar1Ar2-0.6-1.0-3346-3524-4.74x8.00x9.40-120-ber,
N-Ar1Ar2-0.6-1.0-6795-24-4.74x8.00x9.40-100-140,
and N-Ar1Ar2-0.6-1.0-20-7091-4.74x8.00x9.40-100-140
We plot additionally the fitted hyperbolic tangent density z -profiles in the interfacial systems.

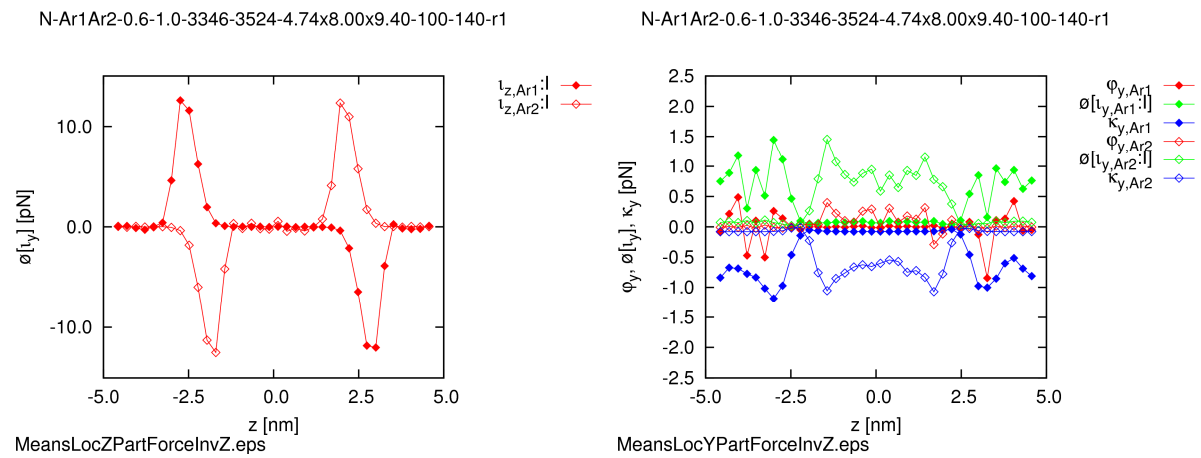


ExcerptHeatFluxColdT.eps

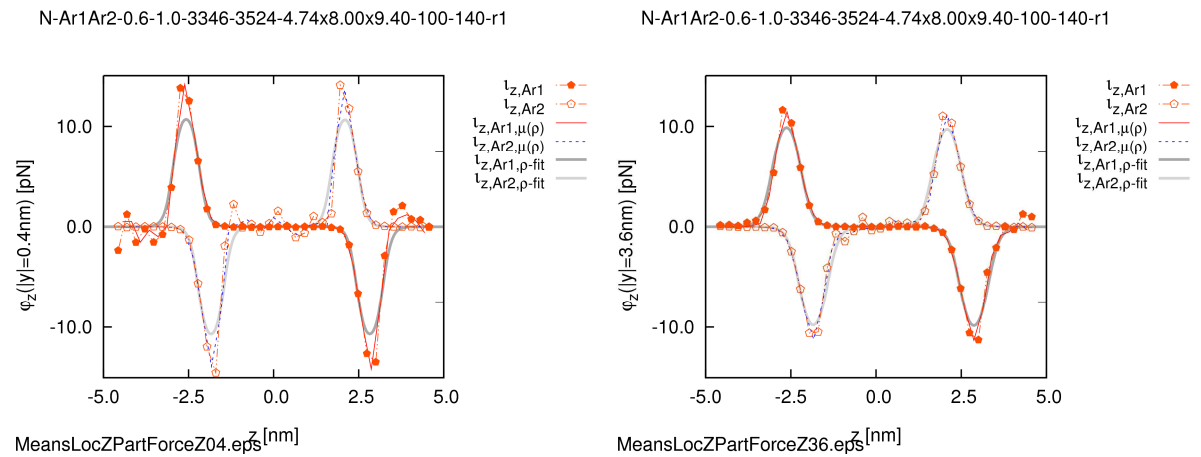
Figure 36 Excerpt of the instantaneous heat fluxes coupled into or out of the hot thermostated region and the numbers of the particles residing in it in N-Ar1Ar2-0.6-1.0-6795-24-4.74x8.00x9.40-100-140



a) I-averages of the interatomic and kinetic volume y-forces as well as their sum as function of z

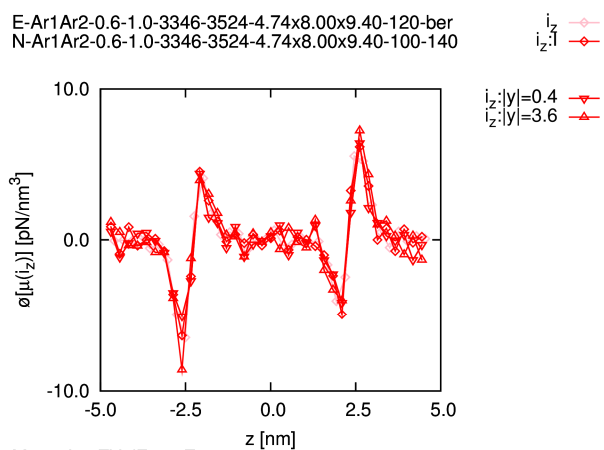


b) I-averages of the interatomic and kinetic particle y-forces as well as their sum as function of z

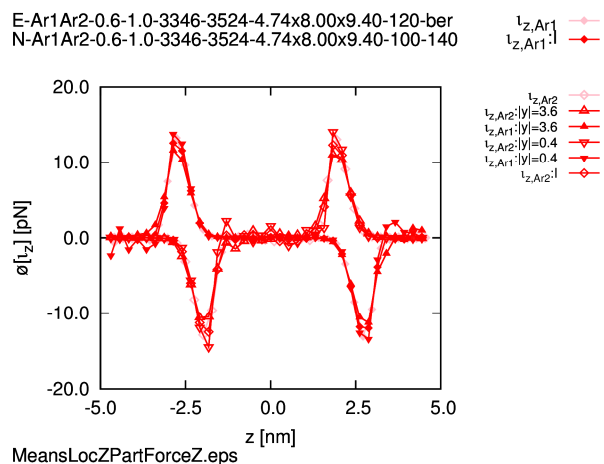


c) Particle z-forces obtained in the simulation compared to those computed from the partial density profiles by using the BGY equation using the absolute y-coordinates of $|y|=0.4\text{nm}$ and of $|y|=3.6\text{nm}$ as an example

Figure 37 Consistency of the local observables in the first heterophasic nonequilibrium interfacial system N-Ar1Ar2-0.6-1.0-3346-3524-4.74x8.00x9.40-100-140-r1



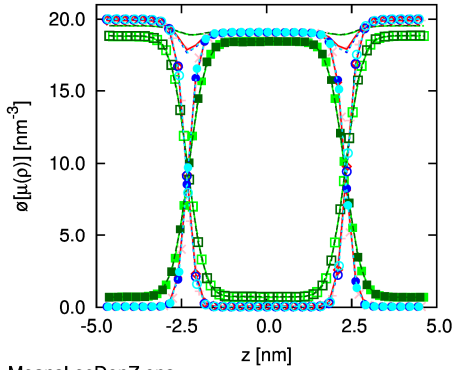
c) Volume forces



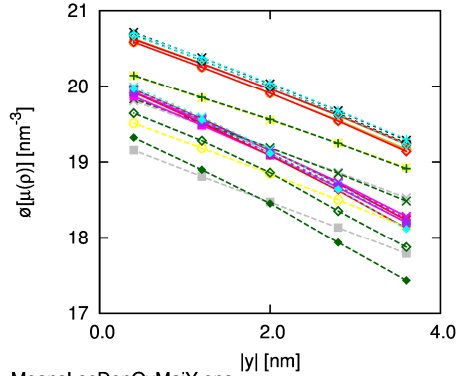
d) Particle forces

Figure 38 Comparison of the summarised local observables in the corresponding first heterophasic interfacial systems
E-Ar1Ar2-0.6-1.0-3346-3524-4.74x8.00x9.40-120 and N-Ar1Ar2-0.6-1.0-3346-3524-4.74x8.00x9.40-100-140

E-Ar1Ar2-0.6-1.0-3346-3524-4.74x8.00x9.40-120-ber ρ — N-Ar1Ar2-0.6-1.0-6795-24-4.74x8.00x9.40-100-140 ρ —
 N-Ar1Ar2-0.6-1.0-3346-3524-4.74x8.00x9.40-100-140-r1 $\rho:|y|=2.0$ — N-Ar1Ar2-0.6-1.0-20-7091-4.74x8.00x9.40-100-140 ρ —
 E-Ar1Ar2-0.6-0.6-3346-3524-4.74x8.00x9.40-120 ρ — N-Ar1Ar2-0.6-1.0-3346-3524-4.74x8.00x9.40-100-140-r1 $\rho:|y|=2.0$ —
 N-Ar1Ar2-0.6-0.6-3346-3524-4.74x8.00x9.40-100-140 $\rho:|y|=2.0$ — N-Ar1Ar2-0.6-0.6-6585-250-4.74x8.00x9.40-100-140 ρ —
 E-Ar1Ar2-0.6-1.2-3346-3524-4.74x8.00x9.40-120 ρ — N-Ar1Ar2-0.6-0.6-251-6715-4.74x8.00x9.40-100-140 ρ —
 N-Ar1Ar2-0.6-1.2-3346-3524-4.74x8.00x9.40-100-140 $\rho:|y|=2.0$ — N-Ar1Ar2-0.6-0.6-3346-3524-4.74x8.00x9.40-100-140 $\rho:|y|=2.0$ —
 N-Ar1Ar2-0.6-1.2-6804-16-4.74x8.00x9.40-100-140 ρ —
 N-Ar1Ar2-0.6-1.2-13-7123-4.74x8.00x9.40-100-140 ρ —
 N-Ar1Ar2-0.6-1.2-3346-3524-4.74x8.00x9.40-100-140 $\rho:Ar1$ —



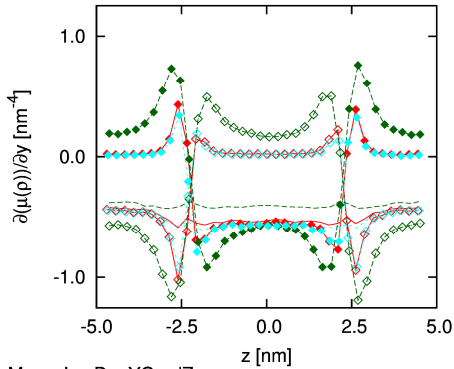
MeansLocDenZ.eps



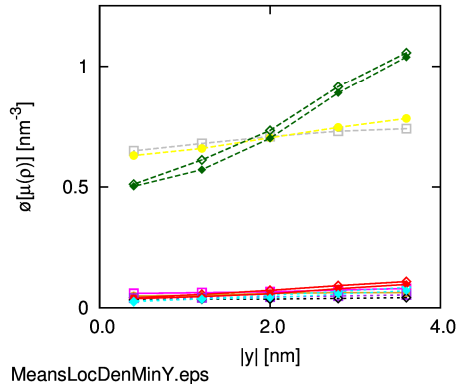
MeansLocDenOvMajY.eps

N-Ar1Ar2-0.6-1.0-3346-3524-4.74x8.00x9.40-100-140-r1 $\rho:l$ —
 N-Ar1Ar2-0.6-0.6-3346-3524-4.74x8.00x9.40-100-140 $\rho:l$ —
 N-Ar1Ar2-0.6-1.2-3346-3524-4.74x8.00x9.40-100-140 $\rho:l$ —

N-Ar1Ar2-0.6-1.0-6795-24-4.74x8.00x9.40-100-140 $\rho:Ar2$ —
 N-Ar1Ar2-0.6-1.0-20-7091-4.74x8.00x9.40-100-140 $\rho:Ar1$ —
 N-Ar1Ar2-0.6-1.0-3346-3524-4.74x8.00x9.40-100-140-r1 $\rho:Ar2:Ar1$ —
 N-Ar1Ar2-0.6-0.6-6585-250-4.74x8.00x9.40-100-140 $\rho:Ar2$ —
 N-Ar1Ar2-0.6-0.6-251-6715-4.74x8.00x9.40-100-140 $\rho:Ar1$ —
 N-Ar1Ar2-0.6-0.6-3346-3524-4.74x8.00x9.40-100-140 $\rho:Ar2:Ar1$ —
 N-Ar1Ar2-0.6-1.2-6804-16-4.74x8.00x9.40-100-140 $\rho:Ar2$ —
 N-Ar1Ar2-0.6-1.2-13-7123-4.74x8.00x9.40-100-140 $\rho:Ar1$ —
 N-Ar1Ar2-0.6-1.2-3346-3524-4.74x8.00x9.40-100-140 $\rho:Ar2:Ar1$ —



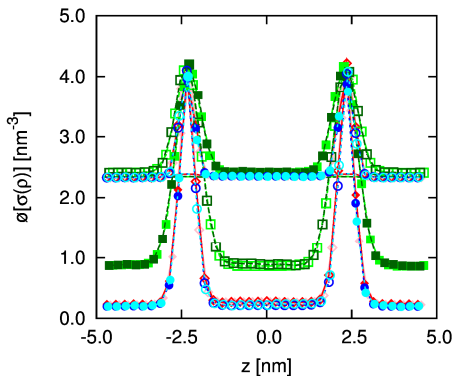
MeansLocDenYGradZ.eps



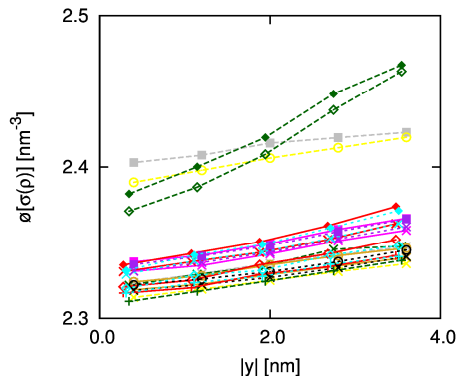
MeansLocDenMinY.eps

E-Ar1Ar2-0.6-1.0-3346-3524-4.74x8.00x9.40-120-ber ρ — N-Ar1Ar2-0.6-1.0-6795-24-4.74x8.00x9.40-100-140 ρ —
 N-Ar1Ar2-0.6-1.0-3346-3524-4.74x8.00x9.40-100-140-r1 $\rho:|y|=2.0$ — N-Ar1Ar2-0.6-1.0-20-7091-4.74x8.00x9.40-100-140 ρ —
 E-Ar1Ar2-0.6-0.6-3346-3524-4.74x8.00x9.40-120 ρ — N-Ar1Ar2-0.6-1.0-3346-3524-4.74x8.00x9.40-100-140-r1 $\rho:|y|=2.0$ —
 N-Ar1Ar2-0.6-0.6-3346-3524-4.74x8.00x9.40-100-140 $\rho:|y|=2.0$ — N-Ar1Ar2-0.6-0.6-6585-250-4.74x8.00x9.40-100-140 ρ —
 E-Ar1Ar2-0.6-1.2-3346-3524-4.74x8.00x9.40-120 ρ — N-Ar1Ar2-0.6-0.6-251-6715-4.74x8.00x9.40-100-140 ρ —
 N-Ar1Ar2-0.6-1.2-3346-3524-4.74x8.00x9.40-100-140 $\rho:|y|=2.0$ — N-Ar1Ar2-0.6-0.6-3346-3524-4.74x8.00x9.40-100-140 $\rho:|y|=2.0$ —
 N-Ar1Ar2-0.6-1.2-6804-16-4.74x8.00x9.40-100-140 ρ —
 N-Ar1Ar2-0.6-1.2-13-7123-4.74x8.00x9.40-100-140 ρ —
 N-Ar1Ar2-0.6-1.2-3346-3524-4.74x8.00x9.40-100-140 $\rho:Ar1$ —

N-Ar1Ar2-0.6-1.0-6795-24-4.74x8.00x9.40-100-140 ρ —
 N-Ar1Ar2-0.6-1.0-20-7091-4.74x8.00x9.40-100-140 ρ —
 N-Ar1Ar2-0.6-1.0-3346-3524-4.74x8.00x9.40-100-140-r1 $\rho:Ar1$ —
 N-Ar1Ar2-0.6-0.6-6585-250-4.74x8.00x9.40-100-140 $\rho:Ar2$ —
 N-Ar1Ar2-0.6-0.6-251-6715-4.74x8.00x9.40-100-140 $\rho:Ar1$ —
 N-Ar1Ar2-0.6-0.6-3346-3524-4.74x8.00x9.40-100-140 $\rho:Ar2:Ar1$ —
 N-Ar1Ar2-0.6-1.2-6804-16-4.74x8.00x9.40-100-140 $\rho:Ar2$ —
 N-Ar1Ar2-0.6-1.2-13-7123-4.74x8.00x9.40-100-140 $\rho:Ar1$ —
 N-Ar1Ar2-0.6-1.2-3346-3524-4.74x8.00x9.40-100-140 $\rho:Ar2:Ar1$ —



SigmaLocDenZ.eps

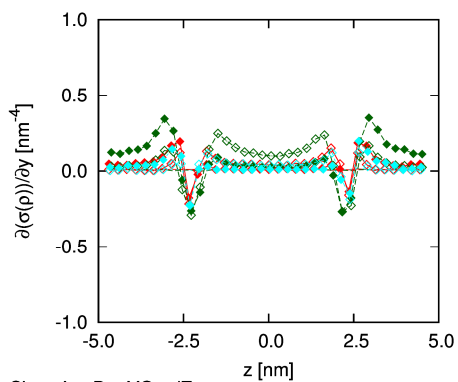


SigmaLocDenOvMajY.eps

N-Ar1Ar2-0.6-1.0-3346-3524-4.74x8.00x9.40-100-140-r1
N-Ar1Ar2-0.6-0.6-3346-3524-4.74x8.00x9.40-100-140
N-Ar1Ar2-0.6-1.2-3346-3524-4.74x8.00x9.40-100-140

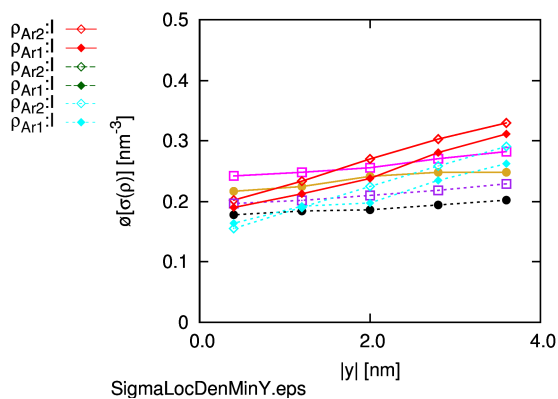
ρ :l — N-Ar1Ar2-0.6-1.0-6795-24-4.74x8.00x9.40-100-140
 ρ :l - - - N-Ar1Ar2-0.6-1.0-20-7091-4.74x8.00x9.40-100-140
 ρ :l - · - - N-Ar1Ar2-0.6-1.0-3346-3524-4.74x8.00x9.40-100-140-r1
N-Ar1Ar2-0.6-0.6-6585-250-4.74x8.00x9.40-100-140
N-Ar1Ar2-0.6-0.6-251-6715-4.74x8.00x9.40-100-140
N-Ar1Ar2-0.6-0.6-3346-3524-4.74x8.00x9.40-100-140
N-Ar1Ar2-0.6-1.2-6804-16-4.74x8.00x9.40-100-140
N-Ar1Ar2-0.6-1.2-13-7123-4.74x8.00x9.40-100-140
N-Ar1Ar2-0.6-1.2-3346-3524-4.74x8.00x9.40-100-140

ρ_{Ar2} — \square
 ρ_{Ar1} — \circ
 $\rho_{Ar2}:Ar1$ — \diamond
 ρ_{Ar2} — \square
 ρ_{Ar1} — \diamond
 ρ_{Ar2} — \square
 ρ_{Ar1} — \diamond
 $\rho_{Ar2}:Ar1$ — \diamond



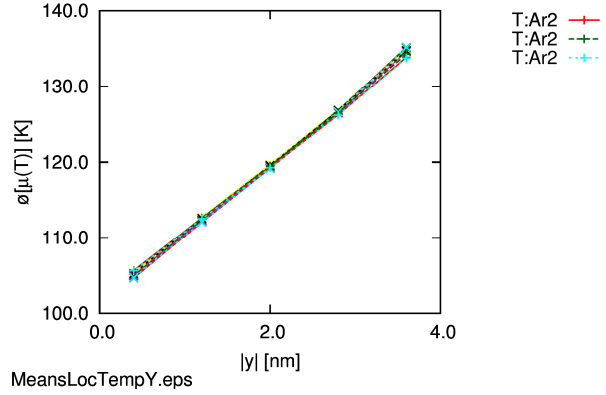
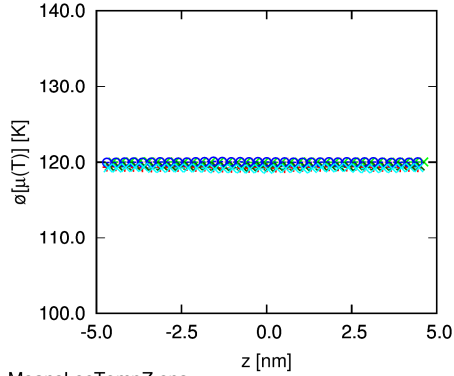
SigmaLocDenYGradZ.eps

a) Densities

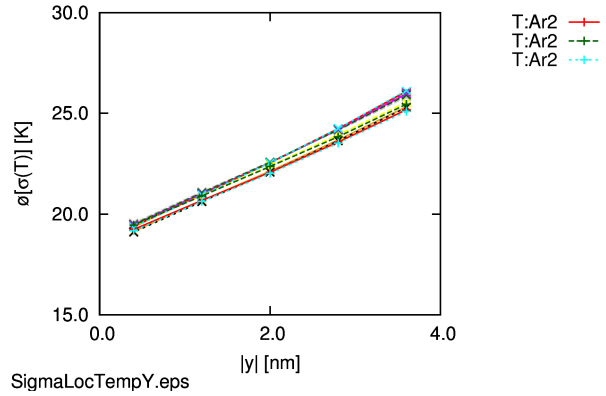
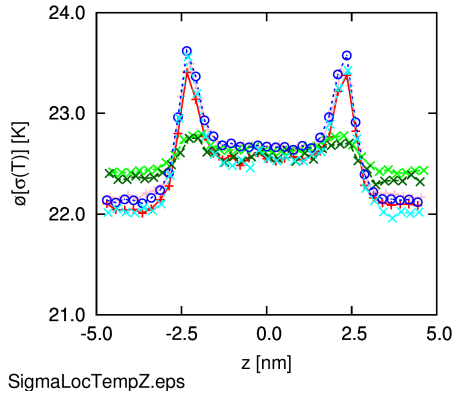


SigmaLocDenMinY.eps

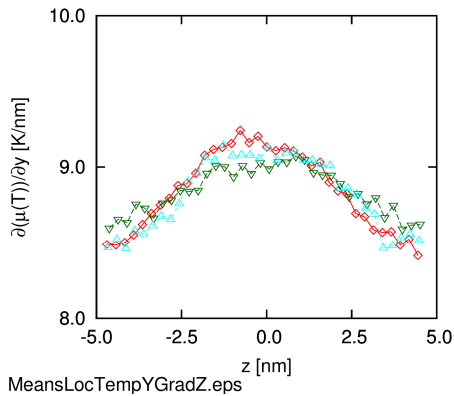
E-Ar1Ar2-0.6-1.0-3346-3524-4.74x8.00x9.40-120-ber T
 N-Ar1Ar2-0.6-1.0-3346-3524-4.74x8.00x9.40-100-140-r1 T:|y|=2.0
 E-Ar1Ar2-0.6-0.6-3346-3524-4.74x8.00x9.40-120 T
 N-Ar1Ar2-0.6-0.6-3346-3524-4.74x8.00x9.40-100-140 T:|y|=2.0
 E-Ar1Ar2-0.6-1.2-3346-3524-4.74x8.00x9.40-120 T
 N-Ar1Ar2-0.6-1.2-3346-3524-4.74x8.00x9.40-100-140 T:|y|=2.0
 N-Ar1Ar2-0.6-1.0-6795-24-4.74x8.00x9.40-100-140 T
 N-Ar1Ar2-0.6-1.0-20-7091-4.74x8.00x9.40-100-140 T
 N-Ar1Ar2-0.6-1.0-3346-3524-4.74x8.00x9.40-100-140-r1 T:Ar1
 N-Ar1Ar2-0.6-0.6-6585-250-4.74x8.00x9.40-100-140 T
 N-Ar1Ar2-0.6-0.6-251-6715-4.74x8.00x9.40-100-140 T
 N-Ar1Ar2-0.6-0.6-3346-3524-4.74x8.00x9.40-100-140 T:Ar1
 N-Ar1Ar2-0.6-1.2-6804-16-4.74x8.00x9.40-100-140 T
 N-Ar1Ar2-0.6-1.2-13-7123-4.74x8.00x9.40-100-140 T
 N-Ar1Ar2-0.6-1.2-3346-3524-4.74x8.00x9.40-100-140 T:Ar2
 T:Ar2
 T:Ar2



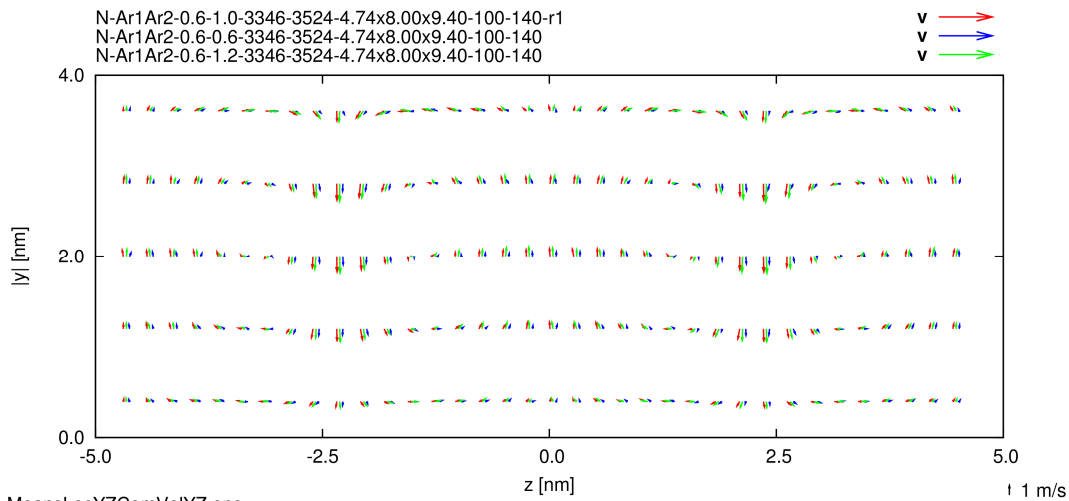
E-Ar1Ar2-0.6-1.0-3346-3524-4.74x8.00x9.40-120-ber T
 N-Ar1Ar2-0.6-1.0-3346-3524-4.74x8.00x9.40-100-140-r1 T:|y|=2.0
 E-Ar1Ar2-0.6-0.6-3346-3524-4.74x8.00x9.40-120 T
 N-Ar1Ar2-0.6-0.6-3346-3524-4.74x8.00x9.40-100-140 T:|y|=2.0
 E-Ar1Ar2-0.6-1.2-3346-3524-4.74x8.00x9.40-120 T
 N-Ar1Ar2-0.6-1.2-3346-3524-4.74x8.00x9.40-100-140 T:|y|=2.0
 N-Ar1Ar2-0.6-1.0-6795-24-4.74x8.00x9.40-100-140 T
 N-Ar1Ar2-0.6-1.0-20-7091-4.74x8.00x9.40-100-140 T
 N-Ar1Ar2-0.6-1.0-3346-3524-4.74x8.00x9.40-100-140-r1 T:Ar1
 N-Ar1Ar2-0.6-0.6-6585-250-4.74x8.00x9.40-100-140 T
 N-Ar1Ar2-0.6-0.6-251-6715-4.74x8.00x9.40-100-140 T
 N-Ar1Ar2-0.6-0.6-3346-3524-4.74x8.00x9.40-100-140 T:Ar1
 N-Ar1Ar2-0.6-1.2-6804-16-4.74x8.00x9.40-100-140 T
 N-Ar1Ar2-0.6-1.2-13-7123-4.74x8.00x9.40-100-140 T
 N-Ar1Ar2-0.6-1.2-3346-3524-4.74x8.00x9.40-100-140 T:Ar2
 T:Ar2
 T:Ar2


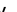



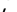








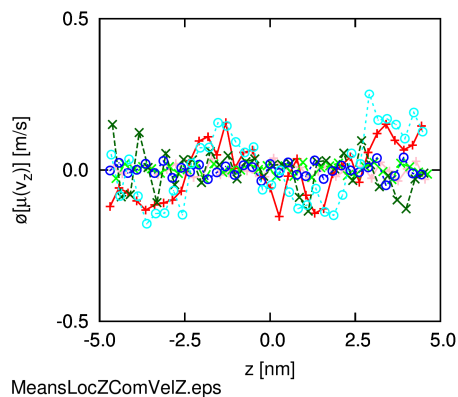
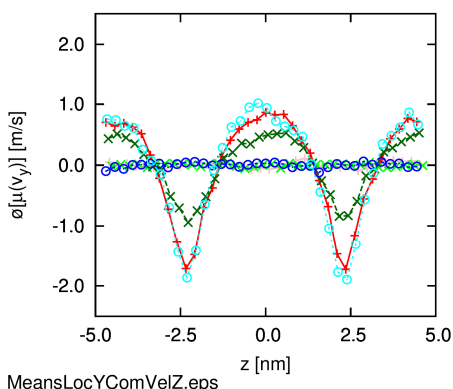
N-Ar1Ar2-0.6-1.0-3346-3524-4.74x8.00x9.40-100-140-r1 T:|
 N-Ar1Ar2-0.6-0.6-3346-3524-4.74x8.00x9.40-100-140 T:|
 N-Ar1Ar2-0.6-1.2-3346-3524-4.74x8.00x9.40-100-140 T:|


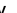



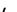








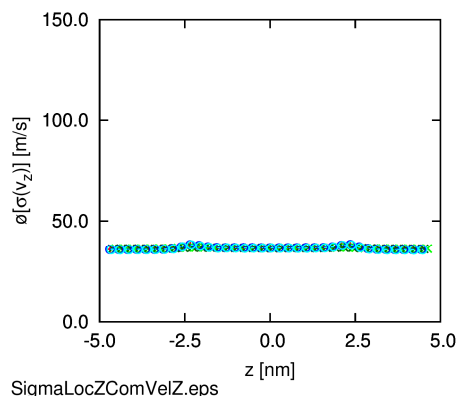
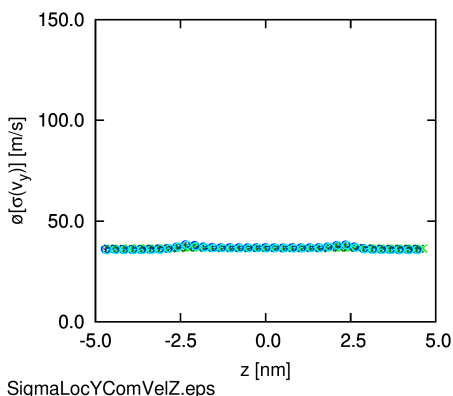
b) Temperatures



E-Ar1Ar2-0.6-1.0-3346-3524-4.74x8.00x9.40-120-ber	v_y		E-Ar1Ar2-0.6-1.0-3346-3524-4.74x8.00x9.40-120-ber	v_z	
N-Ar1Ar2-0.6-1.0-3346-3524-4.74x8.00x9.40-100-140-r1	v_y		N-Ar1Ar2-0.6-1.0-3346-3524-4.74x8.00x9.40-100-140-r1	v_z	
E-Ar1Ar2-0.6-0.6-3346-3524-4.74x8.00x9.40-120	v_y		E-Ar1Ar2-0.6-0.6-3346-3524-4.74x8.00x9.40-120	v_z	
N-Ar1Ar2-0.6-0.6-3346-3524-4.74x8.00x9.40-100-140	v_y		N-Ar1Ar2-0.6-0.6-3346-3524-4.74x8.00x9.40-100-140	v_z	
E-Ar1Ar2-0.6-1.2-3346-3524-4.74x8.00x9.40-120	v_y		E-Ar1Ar2-0.6-1.2-3346-3524-4.74x8.00x9.40-120	v_z	
N-Ar1Ar2-0.6-1.2-3346-3524-4.74x8.00x9.40-100-140	v_y		N-Ar1Ar2-0.6-1.2-3346-3524-4.74x8.00x9.40-100-140	v_z	



E-Ar1Ar2-0.6-1.0-3346-3524-4.74x8.00x9.40-120-ber	v_y		E-Ar1Ar2-0.6-1.0-3346-3524-4.74x8.00x9.40-120-ber	v_z	
N-Ar1Ar2-0.6-1.0-3346-3524-4.74x8.00x9.40-100-140-r1	v_y		N-Ar1Ar2-0.6-1.0-3346-3524-4.74x8.00x9.40-100-140-r1	v_z	
E-Ar1Ar2-0.6-0.6-3346-3524-4.74x8.00x9.40-120	v_y		E-Ar1Ar2-0.6-0.6-3346-3524-4.74x8.00x9.40-120	v_z	
N-Ar1Ar2-0.6-0.6-3346-3524-4.74x8.00x9.40-100-140	v_y		N-Ar1Ar2-0.6-0.6-3346-3524-4.74x8.00x9.40-100-140	v_z	
E-Ar1Ar2-0.6-1.2-3346-3524-4.74x8.00x9.40-120	v_y		E-Ar1Ar2-0.6-1.2-3346-3524-4.74x8.00x9.40-120	v_z	
N-Ar1Ar2-0.6-1.2-3346-3524-4.74x8.00x9.40-100-140	v_y		N-Ar1Ar2-0.6-1.2-3346-3524-4.74x8.00x9.40-100-140	v_z	

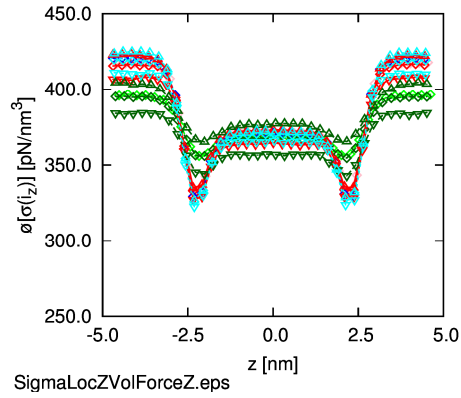
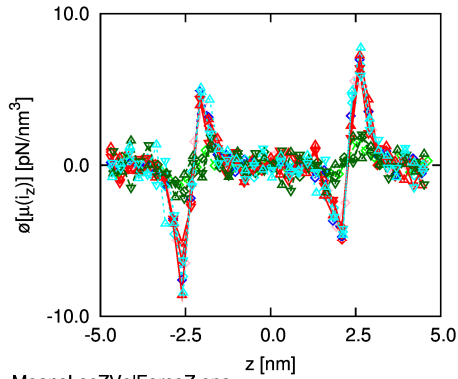


c) Com velocities

E-Ar1Ar2-0.6-1.0-3346-3524-4.74x8.00x9.40-120-ber
 N-Ar1Ar2-0.6-1.0-3346-3524-4.74x8.00x9.40-100-140-r1
 E-Ar1Ar2-0.6-0.6-3346-3524-4.74x8.00x9.40-120
 N-Ar1Ar2-0.6-0.6-3346-3524-4.74x8.00x9.40-100-140
 E-Ar1Ar2-0.6-1.2-3346-3524-4.74x8.00x9.40-120
 N-Ar1Ar2-0.6-1.2-3346-3524-4.74x8.00x9.40-100-140

l_z l_z
 l_z \uparrow l_z \uparrow
 l_z l_z
 l_z \downarrow l_z \downarrow
 l_z l_z
 l_z \uparrow l_z \uparrow

l_z l_z
 l_z \uparrow l_z \uparrow
 l_z l_z
 l_z \downarrow l_z \downarrow
 l_z l_z
 l_z \uparrow l_z \uparrow



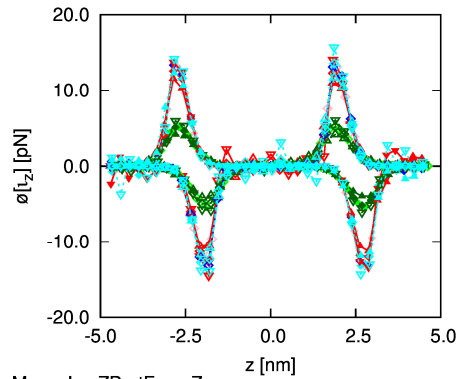
MeansLocZVolForceZ.eps

SigmaLocZVolForceZ.eps

d) Volume forces

E-Ar1Ar2-0.6-1.0-3346-3524-4.74x8.00x9.40-120-ber
 N-Ar1Ar2-0.6-1.0-3346-3524-4.74x8.00x9.40-100-140-r1
 E-Ar1Ar2-0.6-0.6-3346-3524-4.74x8.00x9.40-120
 N-Ar1Ar2-0.6-0.6-3346-3524-4.74x8.00x9.40-100-140
 E-Ar1Ar2-0.6-1.2-3346-3524-4.74x8.00x9.40-120
 N-Ar1Ar2-0.6-1.2-3346-3524-4.74x8.00x9.40-100-140

l_z ,Ar1
 l_z ,Ar1 \uparrow
 l_z ,Ar1
 l_z ,Ar1 \downarrow
 l_z ,Ar1
 l_z ,Ar1 \uparrow



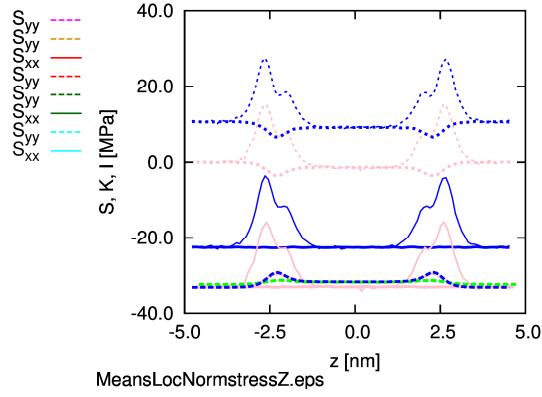
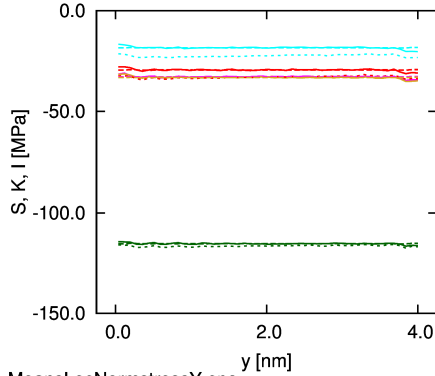
MeansLocZPartForceZ.eps

e) Particle forces

N-Ar1Ar2-0.6-1.0-6795-24-4.74x8.00x9.40-100-140
N-Ar1Ar2-0.6-1.0-20-7091-4.74x8.00x9.40-100-140
N-Ar1Ar2-0.6-1.0-3346-3524-4.74x8.00x9.40-100-140-r1
N-Ar1Ar2-0.6-0.6-3346-3524-4.74x8.00x9.40-100-140
N-Ar1Ar2-0.6-1.2-3346-3524-4.74x8.00x9.40-100-140

S_{zz} — E-Ar1Ar2-0.6-1.0-3346-3524-4.74x8.00x9.40-120-ber
 S_{zz} — E-Ar1Ar2-0.6-0.6-3346-3524-4.74x8.00x9.40-120
 S_{zz} — E-Ar1Ar2-0.6-1.2-3346-3524-4.74x8.00x9.40-120
 S_{zz} —
 S_{zz} —

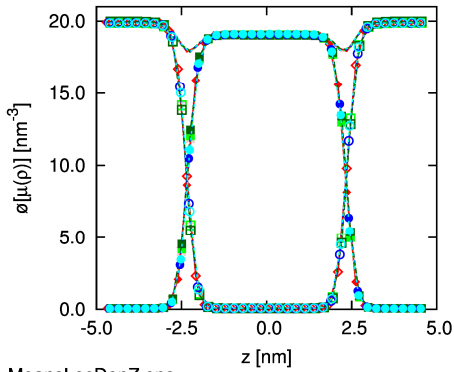
S_{zz} —
 S_{zz} —
 S_{zz} —



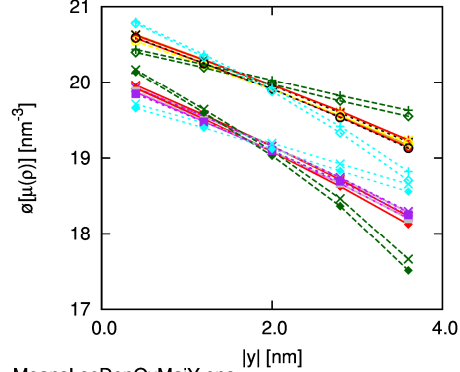
f) Normal stresses

Figure 39 Comparison of the summarised local observables in several heterophasic nonequilibrium interfacial systems with different cut-off radii
N-Ar1Ar2-0.6-1.0-3346-3524-4.74x8.00x9.40-100-140-r1,
N-Ar1Ar2-0.6-0.6-3346-3524-4.74x8.00x9.40-100-140,
and N-Ar1Ar2-0.6-1.2-3346-3524-4.74x8.00x9.40-100-140
We include also their corresponding systems in the comparison.

E-Ar1Ar2-0.6-1.0-3346-3524-4.74x8.00x9.40-120-ber ρ — N-Ar1Ar2-0.6-1.0-6795-24-4.74x8.00x9.40-100-140 ρ —
 N-Ar1Ar2-0.6-1.0-3346-3524-4.74x8.00x9.40-100-140-r1 $\rho:|y|=2.0$ — N-Ar1Ar2-0.6-1.0-20-7091-4.74x8.00x9.40-100-140 ρ —
 E-Ar1Ar3-0.6-1.0-3346-3524-4.74x8.00x9.40-120 ρ — N-Ar1Ar2-0.6-1.0-3346-3524-4.74x8.00x9.40-100-140-r1 $\rho:|y|=2.0$ —
 N-Ar1Ar3-0.6-1.0-3346-3524-4.74x8.00x9.40-100-140 $\rho:|y|=2.0$ — N-Ar1Ar3-0.6-1.0-6797-22-4.74x8.00x9.40-100-140 ρ —
 E-Ar1Ar4-0.6-1.0-3346-3524-4.74x8.00x9.40-120 ρ — N-Ar1Ar3-0.6-1.0-20-7089-4.74x8.00x9.40-100-140 ρ —
 N-Ar1Ar4-0.6-1.0-3346-3524-4.74x8.00x9.40-100-140 $\rho:|y|=2.0$ — N-Ar1Ar3-0.6-1.0-3346-3524-4.74x8.00x9.40-100-140 ρ —
 N-Ar1Ar4-0.6-1.0-6799-22-4.74x8.00x9.40-100-140 ρ —
 N-Ar1Ar4-0.6-1.0-19-7088-4.74x8.00x9.40-100-140 ρ —
 N-Ar1Ar4-0.6-1.0-3346-3524-4.74x8.00x9.40-100-140 $\rho:Ar1$ —



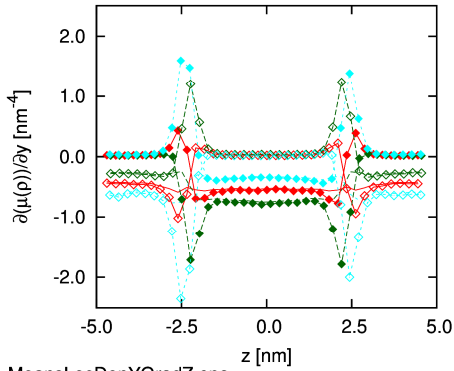
MeansLocDenZ.eps



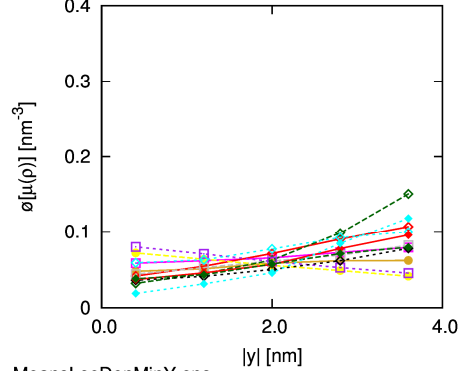
MeansLocDenOvMajY.eps

N-Ar1Ar2-0.6-1.0-3346-3524-4.74x8.00x9.40-100-140-r1 $\rho:l$ —
 N-Ar1Ar3-0.6-1.0-3346-3524-4.74x8.00x9.40-100-140 $\rho:l$ —
 N-Ar1Ar4-0.6-1.0-3346-3524-4.74x8.00x9.40-100-140 $\rho:l$ —

N-Ar1Ar2-0.6-1.0-6795-24-4.74x8.00x9.40-100-140 $\rho:Ar2$ —
 N-Ar1Ar2-0.6-1.0-20-7091-4.74x8.00x9.40-100-140 $\rho:Ar1$ —
 N-Ar1Ar2-0.6-1.0-3346-3524-4.74x8.00x9.40-100-140-r1 $\rho:Ar2:Ar1$ —
 N-Ar1Ar3-0.6-1.0-6797-22-4.74x8.00x9.40-100-140 $\rho:Ar3$ —
 N-Ar1Ar3-0.6-1.0-20-7089-4.74x8.00x9.40-100-140 $\rho:Ar1$ —
 N-Ar1Ar3-0.6-1.0-3346-3524-4.74x8.00x9.40-100-140 $\rho:Ar3:Ar1$ —
 N-Ar1Ar4-0.6-1.0-6799-22-4.74x8.00x9.40-100-140 $\rho:Ar4$ —
 N-Ar1Ar4-0.6-1.0-19-7088-4.74x8.00x9.40-100-140 $\rho:Ar1$ —
 N-Ar1Ar4-0.6-1.0-3346-3524-4.74x8.00x9.40-100-140 $\rho:Ar4:Ar1$ —

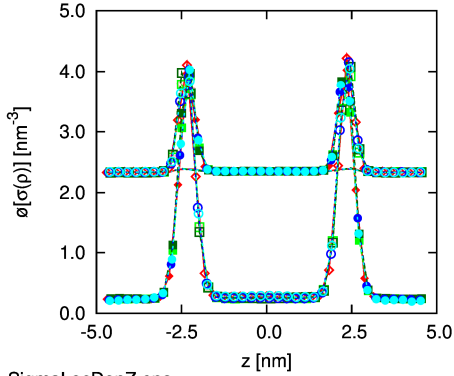


MeansLocDenYGradZ.eps

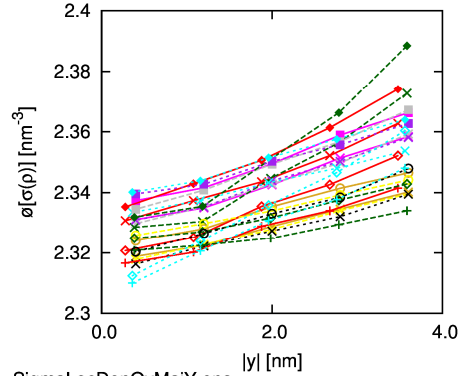


MeansLocDenMinY.eps

E-Ar1Ar2-0.6-1.0-3346-3524-4.74x8.00x9.40-120-ber ρ — N-Ar1Ar2-0.6-1.0-6795-24-4.74x8.00x9.40-100-140 ρ —
 N-Ar1Ar2-0.6-1.0-3346-3524-4.74x8.00x9.40-100-140-r1 $\rho:|y|=2.0$ — N-Ar1Ar2-0.6-1.0-20-7091-4.74x8.00x9.40-100-140 ρ —
 E-Ar1Ar3-0.6-1.0-3346-3524-4.74x8.00x9.40-120 ρ — N-Ar1Ar2-0.6-1.0-3346-3524-4.74x8.00x9.40-100-140-r1 $\rho:|y|=2.0$ —
 N-Ar1Ar3-0.6-1.0-3346-3524-4.74x8.00x9.40-100-140 $\rho:|y|=2.0$ — N-Ar1Ar3-0.6-1.0-6797-22-4.74x8.00x9.40-100-140 ρ —
 E-Ar1Ar4-0.6-1.0-3346-3524-4.74x8.00x9.40-120 ρ — N-Ar1Ar3-0.6-1.0-20-7089-4.74x8.00x9.40-100-140 ρ —
 N-Ar1Ar4-0.6-1.0-3346-3524-4.74x8.00x9.40-100-140 $\rho:|y|=2.0$ — N-Ar1Ar3-0.6-1.0-3346-3524-4.74x8.00x9.40-100-140 ρ —
 N-Ar1Ar4-0.6-1.0-6799-22-4.74x8.00x9.40-100-140 ρ —
 N-Ar1Ar4-0.6-1.0-19-7088-4.74x8.00x9.40-100-140 ρ —
 N-Ar1Ar4-0.6-1.0-3346-3524-4.74x8.00x9.40-100-140 ρ —



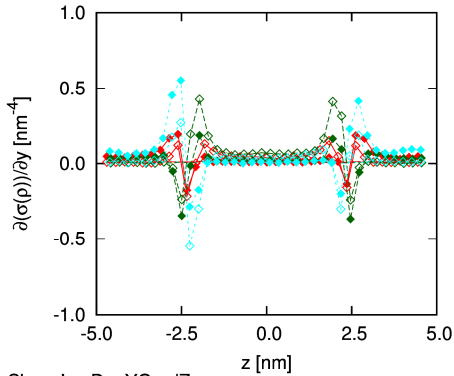
SigmaLocDenZ.eps



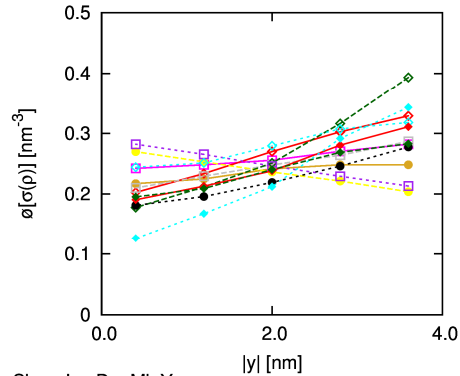
SigmaLocDenOvMajY.eps

N-Ar1Ar2-0.6-1.0-3346-3524-4.74x8.00x9.40-100-140-r1 $\rho:l$ —
 N-Ar1Ar3-0.6-1.0-3346-3524-4.74x8.00x9.40-100-140 $\rho:l$ —
 N-Ar1Ar4-0.6-1.0-3346-3524-4.74x8.00x9.40-100-140 $\rho:l$ —

N-Ar1Ar2-0.6-1.0-6795-24-4.74x8.00x9.40-100-140 ρ_{Ar2} —
 N-Ar1Ar2-0.6-1.0-20-7091-4.74x8.00x9.40-100-140 ρ_{Ar1} —
 N-Ar1Ar2-0.6-1.0-3346-3524-4.74x8.00x9.40-100-140-r1 $\rho_{Ar2}:Ar1$ —
 N-Ar1Ar3-0.6-1.0-6797-22-4.74x8.00x9.40-100-140 ρ_{Ar3} —
 N-Ar1Ar3-0.6-1.0-20-7089-4.74x8.00x9.40-100-140 ρ_{Ar1} —
 N-Ar1Ar3-0.6-1.0-3346-3524-4.74x8.00x9.40-100-140 $\rho_{Ar3}:Ar1$ —
 N-Ar1Ar4-0.6-1.0-6799-22-4.74x8.00x9.40-100-140 ρ_{Ar4} —
 N-Ar1Ar4-0.6-1.0-19-7088-4.74x8.00x9.40-100-140 ρ_{Ar1} —
 N-Ar1Ar4-0.6-1.0-3346-3524-4.74x8.00x9.40-100-140 $\rho_{Ar4}:Ar1$ —



SigmaLocDenYGradZ.eps



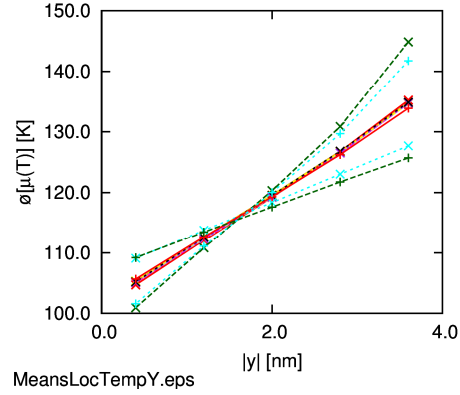
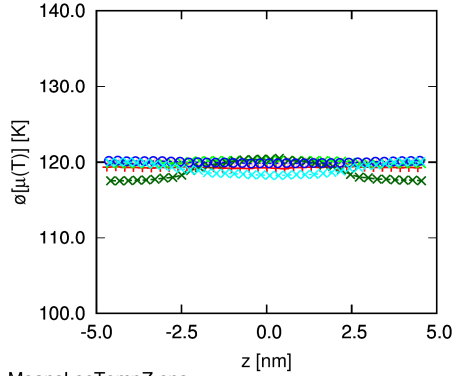
SigmaLocDenMinY.eps

a) Densities

E-Ar1Ar2-0.6-1.0-3346-3524-4.74x8.00x9.40-120-ber
 N-Ar1Ar2-0.6-1.0-3346-3524-4.74x8.00x9.40-100-140-r1 T:|y|=2.0
 E-Ar1Ar3-0.6-1.0-3346-3524-4.74x8.00x9.40-120
 N-Ar1Ar3-0.6-1.0-3346-3524-4.74x8.00x9.40-100-140 T:|y|=2.0
 E-Ar1Ar4-0.6-1.0-3346-3524-4.74x8.00x9.40-120
 N-Ar1Ar4-0.6-1.0-3346-3524-4.74x8.00x9.40-100-140 T:|y|=2.0

N-Ar1Ar2-0.6-1.0-6795-24-4.74x8.00x9.40-100-140
 N-Ar1Ar2-0.6-1.0-20-7091-4.74x8.00x9.40-100-140
 N-Ar1Ar2-0.6-1.0-3346-3524-4.74x8.00x9.40-100-140-r1
 N-Ar1Ar3-0.6-1.0-6797-22-4.74x8.00x9.40-100-140
 N-Ar1Ar3-0.6-1.0-20-7089-4.74x8.00x9.40-100-140
 N-Ar1Ar3-0.6-1.0-3346-3524-4.74x8.00x9.40-100-140
 N-Ar1Ar4-0.6-1.0-6799-22-4.74x8.00x9.40-100-140
 N-Ar1Ar4-0.6-1.0-19-7088-4.74x8.00x9.40-100-140
 N-Ar1Ar4-0.6-1.0-3346-3524-4.74x8.00x9.40-100-140

T
 T
 T:Ar1
 T
 T
 T:Ar1
 T
 T
 T
 T:Ar1
 T

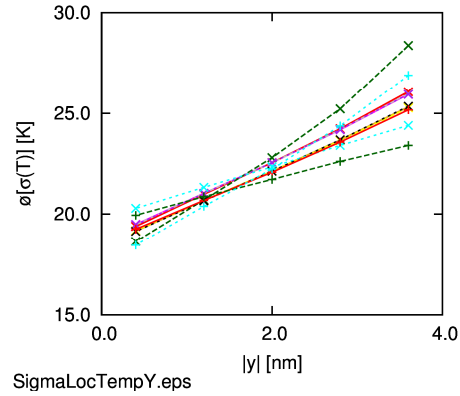
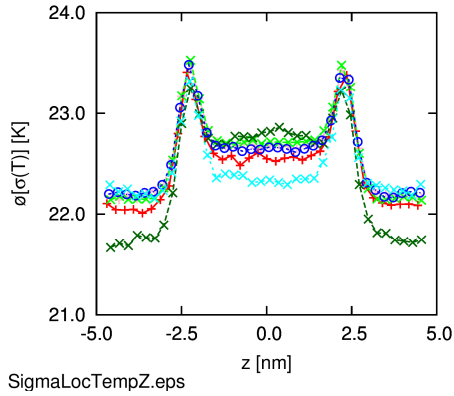


T:Ar2
 T:Ar3
 T:Ar4

E-Ar1Ar2-0.6-1.0-3346-3524-4.74x8.00x9.40-120-ber
 N-Ar1Ar2-0.6-1.0-3346-3524-4.74x8.00x9.40-100-140-r1 T:|y|=2.0
 E-Ar1Ar3-0.6-1.0-3346-3524-4.74x8.00x9.40-120
 N-Ar1Ar3-0.6-1.0-3346-3524-4.74x8.00x9.40-100-140 T:|y|=2.0
 E-Ar1Ar4-0.6-1.0-3346-3524-4.74x8.00x9.40-120
 N-Ar1Ar4-0.6-1.0-3346-3524-4.74x8.00x9.40-100-140 T:|y|=2.0

N-Ar1Ar2-0.6-1.0-6795-24-4.74x8.00x9.40-100-140
 N-Ar1Ar2-0.6-1.0-20-7091-4.74x8.00x9.40-100-140
 N-Ar1Ar2-0.6-1.0-3346-3524-4.74x8.00x9.40-100-140-r1
 N-Ar1Ar3-0.6-1.0-6797-22-4.74x8.00x9.40-100-140
 N-Ar1Ar3-0.6-1.0-20-7089-4.74x8.00x9.40-100-140
 N-Ar1Ar3-0.6-1.0-3346-3524-4.74x8.00x9.40-100-140
 N-Ar1Ar4-0.6-1.0-6799-22-4.74x8.00x9.40-100-140
 N-Ar1Ar4-0.6-1.0-19-7088-4.74x8.00x9.40-100-140
 N-Ar1Ar4-0.6-1.0-3346-3524-4.74x8.00x9.40-100-140

T
 T
 T:Ar1
 T
 T
 T:Ar1
 T
 T
 T
 T:Ar1
 T

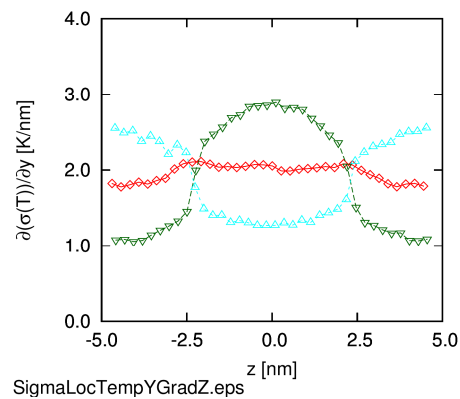
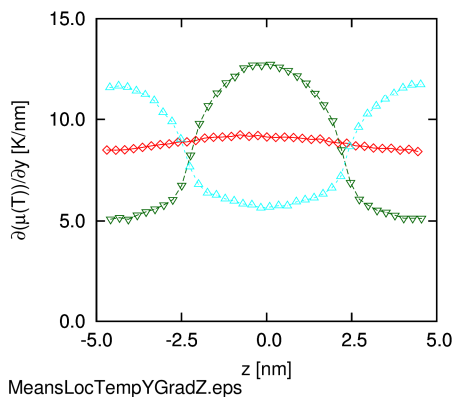


T:Ar2
 T:Ar3
 T:Ar4

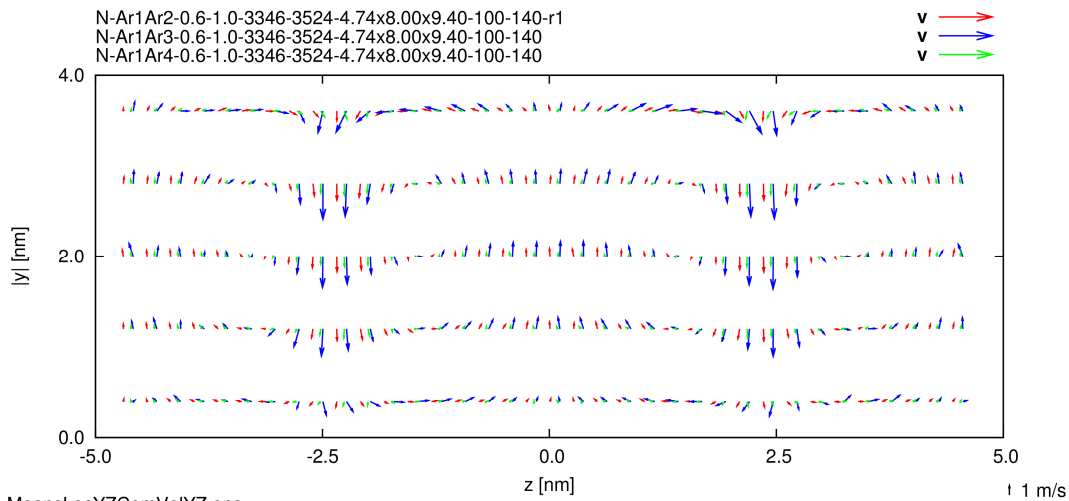
N-Ar1Ar2-0.6-1.0-3346-3524-4.74x8.00x9.40-100-140-r1
 N-Ar1Ar3-0.6-1.0-3346-3524-4.74x8.00x9.40-100-140
 N-Ar1Ar4-0.6-1.0-3346-3524-4.74x8.00x9.40-100-140

T:|
 T:|
 T:|

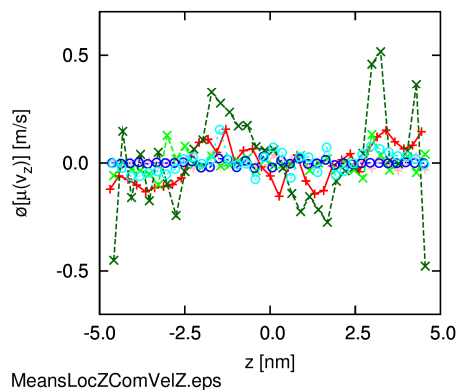
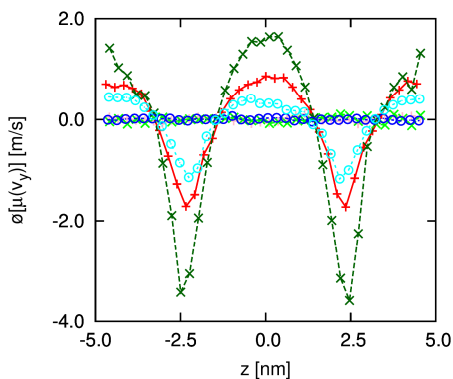
T:|
 T:|
 T:|



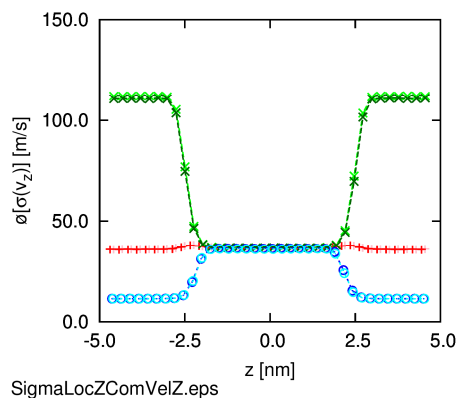
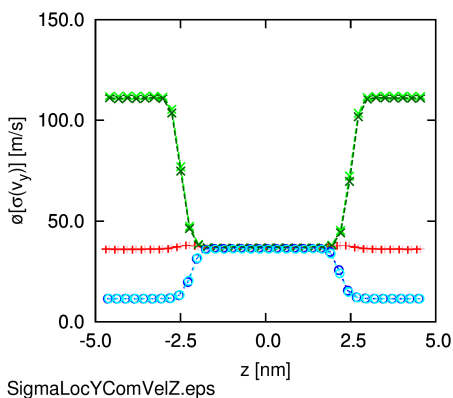
b) Temperatures



E-Ar1Ar2-0.6-1.0-3346-3524-4.74x8.00x9.40-120-ber	v_y	—	E-Ar1Ar2-0.6-1.0-3346-3524-4.74x8.00x9.40-120-ber	v_z	—
N-Ar1Ar2-0.6-1.0-3346-3524-4.74x8.00x9.40-100-140-r1	v_y	—	N-Ar1Ar2-0.6-1.0-3346-3524-4.74x8.00x9.40-100-140-r1	v_z	—
E-Ar1Ar3-0.6-1.0-3346-3524-4.74x8.00x9.40-120	v_y	—	E-Ar1Ar3-0.6-1.0-3346-3524-4.74x8.00x9.40-120	v_z	—
N-Ar1Ar3-0.6-1.0-3346-3524-4.74x8.00x9.40-100-140	v_y	—	N-Ar1Ar3-0.6-1.0-3346-3524-4.74x8.00x9.40-100-140	v_z	—
E-Ar1Ar4-0.6-1.0-3346-3524-4.74x8.00x9.40-120	v_y	—	E-Ar1Ar4-0.6-1.0-3346-3524-4.74x8.00x9.40-120	v_z	—
N-Ar1Ar4-0.6-1.0-3346-3524-4.74x8.00x9.40-100-140	v_y	—	N-Ar1Ar4-0.6-1.0-3346-3524-4.74x8.00x9.40-100-140	v_z	—



E-Ar1Ar2-0.6-1.0-3346-3524-4.74x8.00x9.40-120-ber	v_y	—	E-Ar1Ar2-0.6-1.0-3346-3524-4.74x8.00x9.40-120-ber	v_z	—
N-Ar1Ar2-0.6-1.0-3346-3524-4.74x8.00x9.40-100-140-r1	v_y	—	N-Ar1Ar2-0.6-1.0-3346-3524-4.74x8.00x9.40-100-140-r1	v_z	—
E-Ar1Ar3-0.6-1.0-3346-3524-4.74x8.00x9.40-120	v_y	—	E-Ar1Ar3-0.6-1.0-3346-3524-4.74x8.00x9.40-120	v_z	—
N-Ar1Ar3-0.6-1.0-3346-3524-4.74x8.00x9.40-100-140	v_y	—	N-Ar1Ar3-0.6-1.0-3346-3524-4.74x8.00x9.40-100-140	v_z	—
E-Ar1Ar4-0.6-1.0-3346-3524-4.74x8.00x9.40-120	v_y	—	E-Ar1Ar4-0.6-1.0-3346-3524-4.74x8.00x9.40-120	v_z	—
N-Ar1Ar4-0.6-1.0-3346-3524-4.74x8.00x9.40-100-140	v_y	—	N-Ar1Ar4-0.6-1.0-3346-3524-4.74x8.00x9.40-100-140	v_z	—

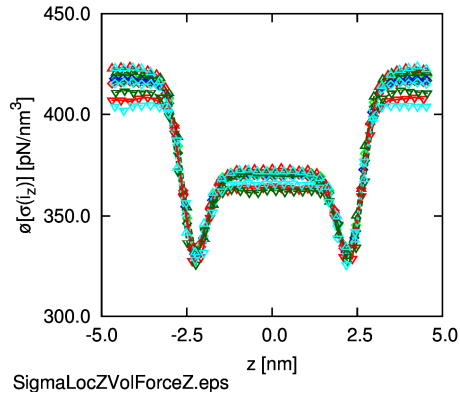
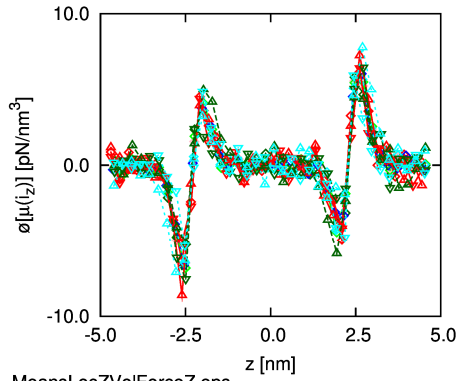


c) Com velocities

E-Ar1Ar2-0.6-1.0-3346-3524-4.74x8.00x9.40-120-ber
 N-Ar1Ar2-0.6-1.0-3346-3524-4.74x8.00x9.40-100-140-r1
 E-Ar1Ar3-0.6-1.0-3346-3524-4.74x8.00x9.40-120
 N-Ar1Ar3-0.6-1.0-3346-3524-4.74x8.00x9.40-100-140
 E-Ar1Ar4-0.6-1.0-3346-3524-4.74x8.00x9.40-120
 N-Ar1Ar4-0.6-1.0-3346-3524-4.74x8.00x9.40-100-140

i_z i_z
 i_z i_z
 i_z i_z
 i_z i_z
 i_z i_z
 i_z i_z

i_z i_z
 i_z i_z
 i_z i_z
 i_z i_z
 i_z i_z
 i_z i_z



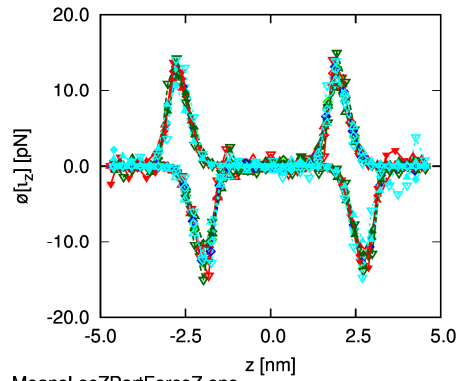
MeansLocZVolForceZ.eps

SigmaLocZVolForceZ.eps

d) Volume forces

E-Ar1Ar2-0.6-1.0-3346-3524-4.74x8.00x9.40-120-ber
 N-Ar1Ar2-0.6-1.0-3346-3524-4.74x8.00x9.40-100-140-r1
 E-Ar1Ar3-0.6-1.0-3346-3524-4.74x8.00x9.40-120
 N-Ar1Ar3-0.6-1.0-3346-3524-4.74x8.00x9.40-100-140
 E-Ar1Ar4-0.6-1.0-3346-3524-4.74x8.00x9.40-120
 N-Ar1Ar4-0.6-1.0-3346-3524-4.74x8.00x9.40-100-140

$i_z, Ar1$ $i_z, Ar1$
 $i_z, Ar1$ $i_z, Ar1$
 $i_z, Ar1$ $i_z, Ar1$
 $i_z, Ar1$ $i_z, Ar1$
 $i_z, Ar1$ $i_z, Ar1$
 $i_z, Ar1$ $i_z, Ar1$



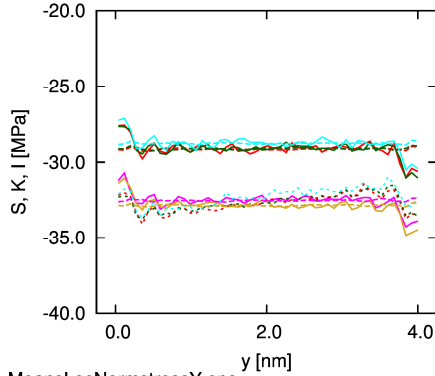
MeansLocZPartForceZ.eps

e) Particle forces

N-Ar1Ar2-0.6-1.0-6795-24-4.74x8.00x9.40-100-140
N-Ar1Ar2-0.6-1.0-20-7091-4.74x8.00x9.40-100-140
N-Ar1Ar2-0.6-1.0-3346-3524-4.74x8.00x9.40-100-140-r1
N-Ar1Ar3-0.6-1.0-3346-3524-4.74x8.00x9.40-100-140
N-Ar1Ar4-0.6-1.0-3346-3524-4.74x8.00x9.40-100-140

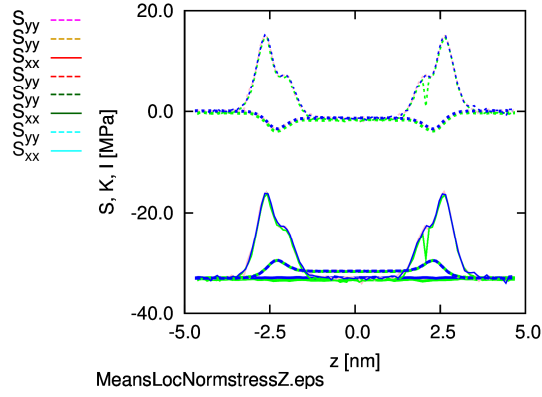
S_{zz} — E-Ar1Ar2-0.6-1.0-3346-3524-4.74x8.00x9.40-120-ber
 S_{zz} — E-Ar1Ar3-0.6-1.0-3346-3524-4.74x8.00x9.40-120
 S_{zz} — E-Ar1Ar4-0.6-1.0-3346-3524-4.74x8.00x9.40-120
 S_{zz} —
 S_{zz} —

S_{zz} —
 S_{zz} —
 S_{zz} —



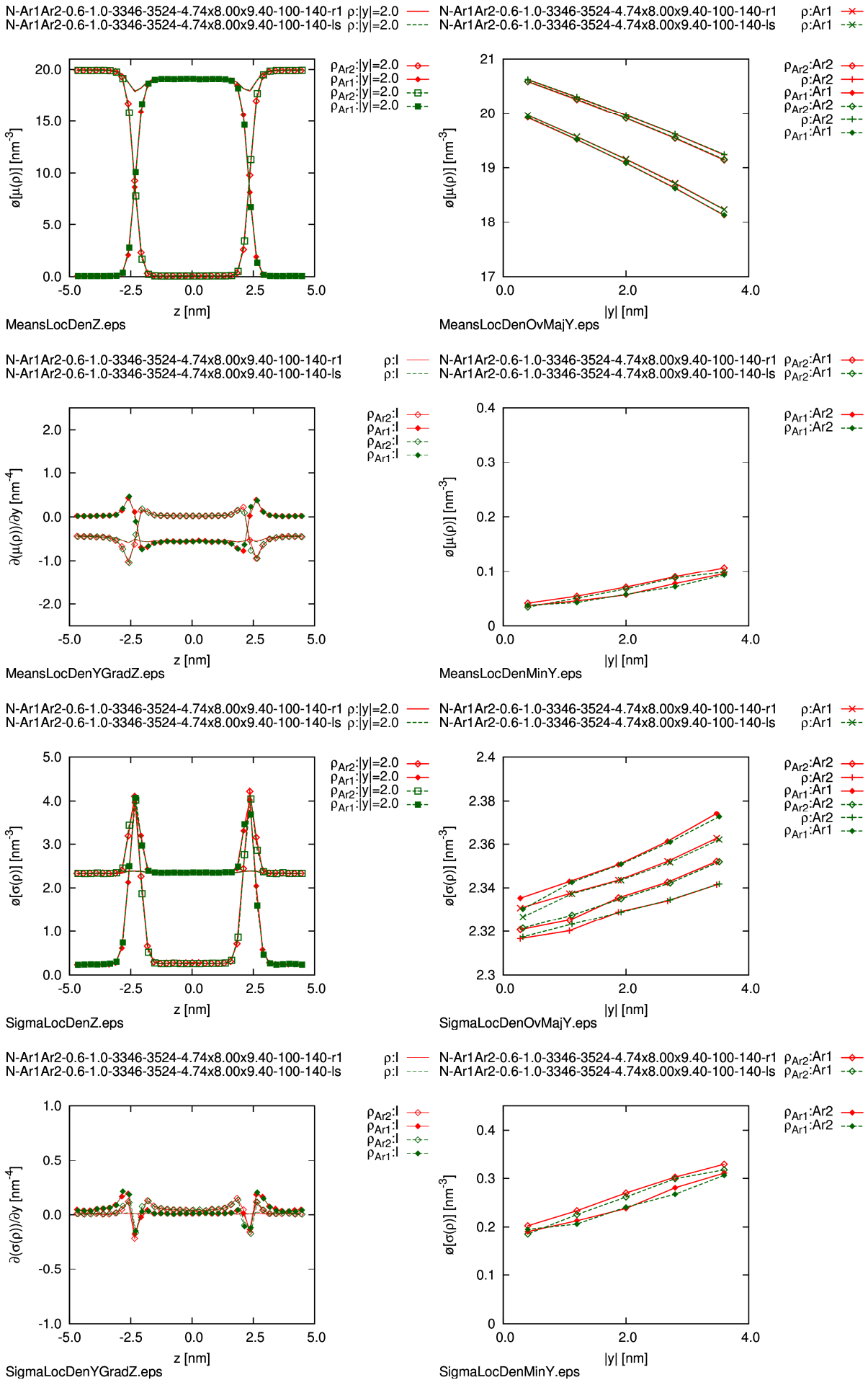
MeansLocNormstressY.eps

f) Normal stresses



MeansLocNormstressZ.eps

Figure 40 Comparison of the summarised local observables in several heterophasic nonequilibrium interfacial systems with different ArB particle masses
N-Ar1Ar2-0.6-1.0-3346-3524-4.74x8.00x9.40-100-140-r1, N-Ar1Ar3-0.6-1.0-3346-3524-4.74x8.00x9.40-100-140, and N-Ar1Ar4-0.6-1.0-3346-3524-4.74x8.00x9.40-100-140;
We include also their corresponding systems in the comparison.



a) Densities